UNIVERSITY OF THE WITWATERSRAND, JOHANNESBURG

Production and evaluation of precipitated calcium carbonate from steelmaking slag

MSc RESEARCH DISSERTATION

Prepared by

MWENGULA GENTIL KAHILU

1902723

Submitted to

School of Chemical and Metallurgical Engineering, Faculty of Engineering and the Built Environment, University of the Witwatersrand, Johannesburg, South Africa

Supervisor(s): PROF. JEAN MULOPO

16th of may 2019

DECLARATION

I declare that this dissertation is my own unaided work. It is being submitted for the Degree of Master of Science in Chemical Engineering to the University of the Witwatersrand, Johannesburg. It has not been submitted before for any degree or examination to any other university.

Signature of the candidate＿＿＿＿＿＿＿＿＿＿＿＿＿＿＿＿＿＿＿＿＿

…………………….day of …………………….year…………………….

TABLE OF CONTENTS

LIST OF FIGURES

LIST OF TABLES

ABSTRACT

This dissertation focus on the synergetic use of two of the essential wastes of modern steel manufacturing processes namely the steel slag (solid waste) and carbon dioxide (gaseous waste) in order to produce pure calcium carbonate which may be used for the neutralization of acidic mine waters. In this regards; calcium extraction from steel slag was first conducted using ammonium chloride and ammonium nitrate. Secondly precipitation of calcium carbonate from the calcium-rich leachate was assessed using carbon dioxide, and finally the calcium carbonate precipitated was evaluated for the neutralization of acidic mine waters from the Witwatersrand western basin. Both ammonium solutions selectively extract calcium from the steel slag, but the ammonium nitrate has better calcium extraction efficiency than ammonium chloride. The above was also confirmed by the number of extraction stages required to reach set extraction efficiency as determined using the Mc Cabe and Thiele Diagram method for the two different solvents. The carbonate (CO_3^{2-}) ions formation being stable in very basic solution, the use of ammonia was required in order to raise the pH of the solution after extraction above 10.3. The calcium carbonate precipitation yield at room temperature evolved as a function of volume and pressure of gaseous carbon dioxide (CO_2) injected and reached more than 80% at a pressure of 6.5 bar and a volume of 150 cm^3. The scanning electron microscopy analysis of the dry calcium carbonate precipitate obtained revealed that it is comprised mostly of fine particles of rhombohedral shapes. It is our view that the above approach may alleviate environmental management of industrial discharges from steel plants as it allows the reduction of both the solid steel slag and CO_2 emissions in the atmosphere via mineral sequestration and may eventually be a significant tool to help combat climate change. Finally, the recycle of the solvent after precipitation and associated losses were considered in order to reduce the cost implication of the overall project.

<u>ACKNOWLEDGEMENTS</u>

ABBREVIATIONS

AA   : Atomic absorption

ABC   : barium-calcium alkaline

AMD : Acid mines drainage

APMW: Alkaline paper mill waste

BF   : Blast furnace

BOF   : Basic oxygen furnace

CCS   : Carbon capture and storage

CKD   : Cement kiln dust

CTSC : Capturing, transporting and storing CO_2

EAF   : Electrical arc furnace

EDTA : Ethylene diamine tetra acetyl

GCC   : Granulate calcium carbonate

GHG   : Greenhouse gas

HSC 5.1: H = enthalpy, S = entropy and C = heat capacity, Chemistry for Windows Chemical Reaction and Equilibrium Software with Extensive Thermochemical Database Version 5.1

IISI   : International iron and steel institute

IPCC : Intergovernmental panel on climate change

L/S   : Liquid/Solid ratio

LF   : Ladle furnace

MNP : Magnetic nano-particles

PCC   : Precipitate calcium carbonate

PCI   : Pulverized coal injected

PGE   : Platinum group element

SEM   : Scanning electron microscopy

SRB   : Sulfate-reducing bacteria

ULCOS: Ultra-low carbon dioxide steelmaking

UNEP : United nations environment program

WHO : World health organization

XRD : X-ray Diffraction

XRF : X-ray Fluorescence

<u>Units</u>

Celsius : °C

Centimeter : cm

Gram : g

Joule : J

Kilowatt : kW

Liter: l

Micrometer: μm

Minutes : min

Mole/liter : M

Revolution per minute : rpm

Tone: t

CHAPTER I GENERAL INTRODUCTION

1. OVERVIEW

The reduction of production cost and the associated need for environmental management of solid, liquid and gaseous wastes remain a major problem for metallurgical industries (Norgate *et al*., 2007). Typically, 300–400 kg of slag is produced in the production of 1 tonne pig iron (hot metal) by blast furnace route which is a highly energy-intensive process and the energy required includes significant amount of electrical energy produced through coal-based thermal power plants in the case of South Africa, leading to additional solid waste generation in the form of fly ash (Bezuidenhout and Cock, 2009). Over the last few decades, intensive Research and Development (R&D) efforts have been directed towards finding cost-effective and compatible solutions for waste minimization and utilization (Lewis *et al*., 2017). Some of the recent trends in solid waste management include newer or re-engineered processes resulting in decreasing quantities of emissions, strategies to maximize current levels of waste utilization and development of high-value products (LaGrega *et al*., 2010). Also, the synergistic treatment of solid wastes from different industries to produce value-added products is also finding preference over the treatment of single waste streams. On the other hand; the iron and steel industry is one of the most energy-intensive industrial sectors and the largest emitter of CO_2 emissions. In 2015, it accounted for about 20% of global industrial energy use and 30% of energy and process CO_2 emissions from industry (Krausmann *et al*., 2017).

There exists different potential strategies for the reduction of CO_2 in the atmosphere:(i) reducing the amount of CO_2 via process energy integration; ii) capturing and storing CO_2 innovative, available and cost-effective carbon capture and storage (CCS) technologies; (iii) switching to less carbon-intensive fuels; and (iv) increasing the use of renewable energy (Friedrich and Trois, 2013; Morfeldt *et al*., 2015).

In recent years extending CCS technology incorporating "utilization" has been considered as a viable option for reducing CO_2 emissions sustainably (Sas *et al*., 2015; Eloneva *et al*., 2009). The utilization routes of the captured CO_2 include enhanced fuel recovery (i.e., EOR and EGR), refrigerant, inerting agents, fire suppression, plastics, and mineralization as carbonates (i.e., precipitation calcium carbonates and construction materials).

CO_2 mineralization as carbonates is termed as accelerated carbonation technology (Pan *et al*., 2018). Accelerated carbonation (chemical adsorption) may be a feasible and attractive alternative method for the mitigation of CO_2 emissions in the coming decades because it involves storing CO_2 as carbonate precipitation, which is environmentally benign (Gerdemann *et al*., 2007; Eloneva *et al*., 2008; Chang *et al.,* 2017). Moreover, carbonation is an exothermal reaction, so energy consumption and costs may be reduced by its inherent properties (Chiang *et al*., 2017).

Steelmaking slags are alkaline and appear to be potential raw materials for CO_2 sequestration by accelerated carbonation because they are generally rich in metal oxides including calcium, magnesium, aluminium, iron, and manganese oxide (Pan.*et al*., 2012). Accelerated carbonation has been primarily investigated through:

 i) The direct aqueous route where carbonation occurs in a single process step using a dry, moist or aqueous environment (Huijgen *et al*., 2005). The resulting carbonated material consists of the precipitated carbonate and residual components of the initially solid material (e.g. residual silica, iron oxides and unreacted minerals). While this technology can achieve a high degree of carbonation in acceptable time periods, the additional processing requirements i.e. requiring energy-intensive crushing/milling, mixing, pressurization, water treatment, still prove too expensive for large-scale implementation as a CO_2 sequestration solution (Mattila *et al*., 2012; Bodénan *et al.*, 2014).

ii) the indirect route, where the reactive alkaline element (Ca, Mg, or both) is first extracted from the feedstock, and subsequently reacted in a separate stage with CO_2 to form carbonates (Olajire, 2013). Additional attractive features of indirect mineral carbonation, besides the production of relatively pure carbonate products with potentially high market value, is its ability to overcome the mobility of the alkaline elements from the solids which is a significant limitation of direct carbonation for achieving high conversion rates and CO_2 uptake; but also the inherent elimination of the carbonate passivating layer that blocks access to the unreacted particle core in direct carbonation (Olajire, 2013). Further research is required on identifying and testing suitable leaching agents, which ideally should have high extraction efficiency, but at the same time should have less affinity for the alkaline-earth elements than the carbonate ion to allow for more efficient precipitation of carbonates in the second carbonation stage (Adams, 2005; Bao *et al.*, 2010; Mo *et al.*, 2016).

In South Africa ArcelorMittal Steel (the biggest steel producer in the country) generates about 4 million tons of by-products each year, including 7 million tons of waste BOF slag (0.6 ton of waste per ton of steel produced) (Strunz, 2018). The recycling of basic oxygen furnace (BOF) slag has made significant progress in past years with much of the material being utilized as construction aggregate and in road applications (Takeshi *et al.*, 2018). However, the recycling of BOF slag still faces many technical, economic, and environmental challenges (Setién *et al.*, 2009; Arribas *et al.*, 2015):

• The high levels of free lime in the BOF slag affect its performance and limit its widespread applications for road and concrete production.

• In-plant recycling of the by-products has achieved limited success because of its phosphorus content.

As a result, large amounts of waste BOF slag have been stockpiled at various sites across South Africa (about 300000 tons/year BOF slag at the Gauteng plant and ~250000 tons BOF

slag /year at the New Castle plant) (Mulopo *et al.*, 2012). Moreover; the National Environmental Management of Waste Act (NEMAW) 59 of 2008 in South Africa places a strong emphasis on waste management according to the waste hierarchy as shown in Figure 1 (Strydom and King, 2009). Cleaner production is the most preferred waste management route and is a guiding principle for many companies nationally, especially in the development of new processes and new operations (Strydom and King, 2009; Mulopo *et al.*, 2012). For existing operations, there will always be waste material being produced, and the associated impacts surrounding it are handling and final disposal. Recovery, reuse and recycle (collectively referred to here as beneficiation) becomes an attractive option for companies interested in reducing their environmental footprint, waste management costs and conversion of waste into resources (Gerdemann *et al.*, 2007; Eloneva *et al.*, 2008).
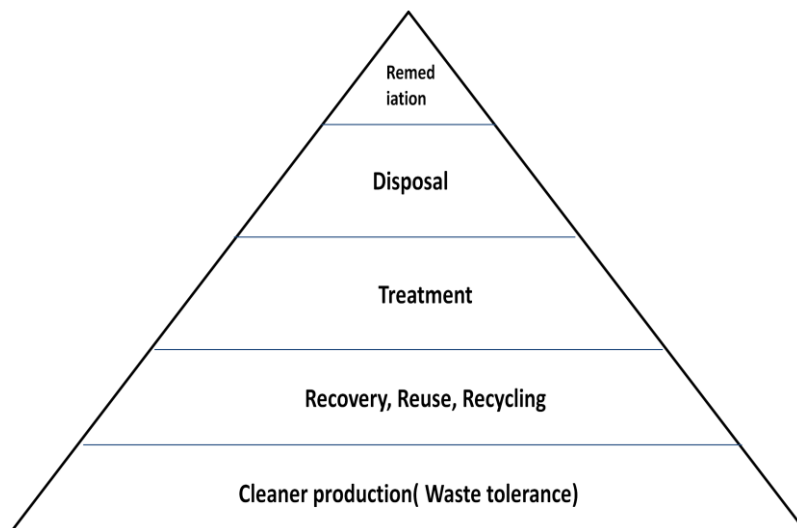
Figure 1: Waste management hierarchy

It is, therefore, the objective of this research to assess the treatment of local steel slag for the production of precipitated calcium carbonate via a two steps route:

a) Optimization of calcium extraction from steelmaking slag using a low-cost route

b) The subsequent precipitation of high-grade calcium carbonate using carbon dioxide

The idea is to investigate the potential of not only materials recovery but also the reduction of carbon dioxide emission into the atmosphere. Furthermore, the calcium carbonate produced will be assessed for neutralization of acid mine drainage from West Rand gold mines.

2. PROBLEM STATEMENT

During steel production in a Basic Oxygen Furnace (BOF), for every ton of crude steel produced, about 100–600 kg of slag is generated in the form of waste by ArcelorMittal Steel South Africa. The BOF slag produced is rich in calcium oxide (CaO) and is currently stockpiled at various sites across the country (Mulopo *et al*., 2012). Generally; the steel slag producers are rapidly running out of landfill space even though in some extent blast furnace slags and steel slags are used in road construction, cement plants, rock wool manufacturing, and fertilization as co-products with high added value (Bobicki *et al*., 2012). Moreover, legislative requirements for landfill disposal methods such as the National Environmental Management Act (NEMA) 59 of 2008 have become more stringent concerning solid waste management resulting in the need to have alternative waste management approaches(Strydom and King, 2009; Anderson, 2013).

On the other hand, CO_2 emissions are about 1.8 t / t of steel produced, accounting for 6.7% of total global emissions as for every ton of steel about 780 kilograms of coal are needed (Mæstad, 2000; Kundak *et al*., 2009).

Three primary options have been globally considered in order to tackle CO_2 emissions by the steel industry (Friedrich & Trois, 2013; Morfeldt *et al*., 2015):

o Capture the CO_2 and store it or reuse it.

o electrolyze molten iron ore at various temperature levels.

o Replace the gas mixture in the direct reduction of iron with hydrogen obtained from water electrolysis so that the reduction of iron ore generates only water as a by-product.

However, the last two options can be only free of all CO_2 emissions if the electricity used is itself free of all emissions (Olajire, 2013). In this regards; ex-situ mineral carbonation offers a unique opportunity for proper disposal or recycling of solid waste materials. It allows reactions between CO_2 and various industrial by-products or waste materials, i.e., coal fly ash, steel and stainless-steel slags, cement and lime kiln dust to produce carbonate products such as $CaCO_3$ (Eloneva *et al*., 2008). The calcium carbonate produced can be used in various applications such as adhesives, sealants, food and pharmaceuticals, paints, coatings, paper, cement, and construction materials (Gerdemann et al., 2007; Eloneva *et al*., 2008; Chang *et al*., 2017).

It was reported that the global calcium carbonate market in 2016 was about 98 million tons, and further growth is expected (Chang *et al*., 2017). In South Africa, the utilized method to produce calcium carbonate is the crushed limestone process. This process is not flexible in that it cannot be directly applied to calcium-containing solid waste and address environmental problems associated with solid waste handling. Moreover, it does not have the product quality flexibility which could be associated with precipitated calcium carbonate generated from ex-situ mineral carbonation of industrial by-products or waste materials, which can be utilized for specialized industrial applications (Erdogan and Eken, 2017). The precipitated $CaCO_3$ has many industrial applications depending on its physicochemical characteristics such as particle size, shape, density, color, brightness, and other properties. It is also known that those characteristics are significantly governed by the polymorphs of $CaCO_3$, which are themselves driven by process synthesis factors including pH, temperature, concentration, and the ratio of carbonate and calcium ions, additives, stirring, reaction time, etc. (Sanna *et al*., 2014; Chang *et al*., 2017).

However, the challenge is that ex-situ mineral carbonation involves energy-intensive processes during the preparation of the solid reactants, including leaching, grinding and/or activation. The recycling of additives and catalysts and therefore process optimization is still required for cost reduction (Sanna *et al*., 2014; Rigopoulos *et al*., 2018). This is the background of this research.

3. RESEARCH OBJECTIVES

The research objective is to investigate the recovery of precipitated calcium carbonate using steel slag collected from Arcello-Mittal via a two stages process namely a) calcium extraction from the slag matrix and b) carbonation of the calcium-rich leachate for precipitated calcium carbonate production, with the following specifics objectives:

- Determine optimum condition for the calcium extraction from the solid slag matrix using different reagents and for CO_2 driven calcium carbonate precipitation with or without selected catalysts.

- Analyze the quality of calcium carbonate produced compared to commercial calcium carbonate.

- Assess the effectiveness of acid mine drainage neutralization using the produced $CaCO_3$.

CHAPTER II LITERATURE REVIEW

1. INTRODUCTION

Recent researches have proven that climate degradation is an environmental problem mostly due to the effects of human activities (Portier *et al.,* 2017). Some gases, generated by human activities, can retain radiation emitted by the earth heated by sunlight such as carbon dioxide (CO_2), water vapour (H_2O), methane (CH_4), nitrous oxide (N_2O). These gases are termed greenhouse gases (Rahman *et al.*, 2017). The greenhouse effect is the phenomenon that occurs when part of the sunlight received by the earth is converted into heat and the gases in the troposphere (lower part of the atmosphere about ~10 to 15 km thick) absorb this energy and trap it near the surface of the earth thereby causing warming (Leeson *et al.*, 2017).

In recent years, the carbon dioxide content in the atmosphere has globally increased significantly and may have a considerable impact on global warming if more severe measures are not considered (Karve, 2018). It is envisaged that carbon dioxide emissions will continue to increase in the next few decades because of the lifetime of carbon dioxide in the troposphere which is about 50 to 200 years (Martens et al., 2017). Industrial activities such as fossil fuels, steel manufacturing and transportation have mainly contributed to the amount of carbon dioxide about 22% of the total concentration contained in the atmosphere (Martens *et al.*, 2017).

Several studies have been conducted recently in order to reduce industrial carbon dioxide emissions but for the most parts, these studies remain limited concerning the efficiency and cost of energy required (Rahman *et al.*, 2017).

The development of mineral carbonation though at a primary stage represents one of the most suitable methods for the capture and storage of carbon dioxide although no real proposal for its application on an industrial scale has been considered yet (Ahmad *et al*., 2017).

2. REVIEW OF TECHNOLOGIES TO REDUCE CARBON DIOXIDE EMISSIONS

2.1 Introduction

Despite the challenges to eliminate industrial CO_2 emissions, many processes (in combination or isolation) may be considered in order to reduce industrial CO_2 emissions such as (Friedrich and Trois, 2013; Morfeldt *et al*., 2015):

- The reduction of energy consumption.

- The substitution of fossil energies by renewable energies.

- The capture and storage or reuse of CO_2 emitted by human activities.

The first and second steps would require a change in technologies and therefore a significant time of implementation and huge expenses (Percival *et al*., 2017). CO_2 capture is a great practical way of reducing CO_2 emissions and would help reduce 19% of total global CO_2 emissions by 2050 (Rahman *et al*., 2017). CO_2 capture and storage have sparked interest in developing technologies for concentrating and storing CO_2 emitted by production plants such as coal-fired power plants, cement plants and steelmaking plants, which are all large industrial emitters (Reddy *et al*., 2017). Some of these technologies are on industrial demonstrations scales such as pre-combustion capture and CO_2 injection in the underground (Rahman *et al*., 2017).

2.2 Carbon dioxide Capture

Through CSC (Capture and Storage CO_2 technique) CO_2 is first captured before being transported and stored in predestined geological sites. There are three CO_2 main capture methods namely (Kanniche *et al.*, 2010; Rahman *et al.*, 2017; Cherbański *et al.*, 2018):

- Pre-combustion capture in which the initial fuel (gas, coal, oil, and biomass) is transformed in a mixture of $H_2 + CO_2$ is first extracted and the hydrogen is then burned to produce water, which is returned to the atmosphere.

- Oxy-combustion capture where only oxygen or an oxide mass is used to produce nitrogen-free smoke

- Post-combustion capture where CO_2 is directly captured in the smoke at the exit of the combustion or industrial plant and is separated from other gases by an amine process.

Comparison of these carbon capture methods has been the subject of several research projects (Figueroa *et al.*, 2008; Yang *et al.*, 2008; Leeson *et al.*, 2017), which have shown that at this point in time post-combustion capture is probably more ready for industrial applications as it is overall less expensive from an energy and investment point of view.

2.3 Carbon dioxide storage

The destination of carbon dioxide after capture is a critical aspect of the overall strategy aiming to reduce CO_2 emissions. As mentioned above, the CSC technique proposes several ways of storing carbon dioxide, for secure and long-term storage (Voormeij *et al.*, 2004; Samadi *et al.*, 2018):

- Acids reservoirs of liquid or gaseous hydrocarbons

- Deep saline aquifers

- Unused coal veins.

Despite the large capacity and availability of the underground reservoirs, questions remain on the long-term stability and the social acceptability of the geological storage of carbon dioxide (Xu *et al*., 2017). It has been shown that carbon dioxide can seep through the subsoil to acidify the metals that will result in chemical modification of deep aquifers, which in turn can influence the qualities of the shallow aquifers (Xu *et al*., 2017). Moreover, the high-pressure injection of CO_2 not only requires additional cost for energy consumption but can also cause cracking of aquifers, which may require geological storage of carbon dioxide to be regulated (Samadi *et al*., 2018).

The captured CO_2 can be used in the following areas: bactericides, refrigeration, fire extinguishers, food preservation, water treatment, Enhanced Oil Recovery (EOR), as a drink additive, the synthesis of urea, industrial photosynthesis, greenhouse, mineral carbonation etc. (Zheng *et al*., 2017)

Mineral carbonation is, therefore, the most promising method of capturing and storing carbon dioxide (Olajire, 2013), though there are still challenges for its industrial application (Pan *et al*., 2018). Carbonation consists of a reaction of CO_2 dioxide with a mineral (magnesium or calcium, usually a natural silicate) to form a chemically stable solid carbonate in which the CO_2 would be trapped. Mineral carbonation occurs only under certain conditions that are absent in geological stocks and reservoirs, which prevents it from developing naturally (Olajire, 2013; Eikeland *et al*., 2015). Recent researches have focused on the study of the different parameters of mineral carbonation and the source of potential CO_2 and minerals that can be treated by this process (Mæstad, 2000; Olajire, 2013; Leeson *et al.*, 2017).

Table 1 below provides a comparison of CO_2 storage methods without capture cost (Bobicki *et al*., 2012). Table 1 shows the benefits of mineral carbonation method from the point of view of efficiency vis-a-vis the geological storage excluding the fact that geological storage

may incur additional energy penalty for landfill and transport and further costs such as the cost of monitoring the injection areas and the integrity of the reservoirs.

TABLE 1: COMPARISON OF CO_2 STORAGE METHODS WITHOUT CAPTURE COST
(Bobicki et al., 2012)

CO_2 storage method	Advantages	Disadvantages	Cost (US$/t CO_2 stored)
Geologic sequestration	➢ Feasible on a large scale ➢ Substantial storage capacity known ➢ Extensive experience	➢ Monitoring necessary ➢ Leakage possible ➢ Energy-intensive ➢ High cost	0.5-8.0 (storage) 0.1 -0.3 (monitoring)
Ocean carbon sequestration	➢ Large storage capacity	➢ Temporary storage ➢ Potential harmful effects on aquatic microbes and biota ➢ Energy-intensive ➢ High production cost	6-31 (pipeline) 12-16 (tanker)
Industrial use	➢ CO_2 incorporated into valuable products	➢ Limited storage capacity ➢ Storage time short	
Mineral carbon sequestration	➢ Only known form of permanent storage ➢ Minerals required available in quantities capable of binding all fossil-fuel bound carbon ➢ Carbonation products environmentally benign	➢ Mineral pretreatment required ➢ Energy required ➢ Realization cost	50 -100

2.4 Mineral carbonation techniques

Mineral carbonation is a reaction between carbon dioxide and certain minerals of the earth to form mineral carbonates. It is a slow reaction but which can be accelerated by the modification of specific fundamental parameters such as (Bobicki *et al*., 2012; Liu *et al*., 2017):

- The temperature increasing is inversely proportional to the solubility of CO_2

- The pressure which increases proportionally with the solubility of carbon dioxide

- A large amount of dissolved substances which decreases the solubility of carbon dioxide.

There are two main types of carbonation namely:

- Direct carbonation

Here the carbonation occurs in an aqueous medium where the precipitation happens concurrently to the dissolution of the ions of the solid mineral. Direct carbonation can be carried out in two forms:

a) Direct carbonation gas / solid

Direct gas/solid carbonation is the most basic method of carbonation and is carried out at specified temperatures and pressures (Bobicki *et al*., 2012; Liu *et al*., 2017, Liu *et al*., 2018). The reaction of gaseous carbon dioxide with a metal oxide can produce superheated steam. The realization of this process requires pre-processing of the mineral as well as the use of high pressures and temperatures to accelerate the reaction (Liu *et al*., 2018). Direct gas/solid carbonation remains generally slow (Lackner *et al*.,1997; Azdarpour *et al*., 2014) and is unpractical for calcium and magnesium silicates, although it is at least feasible for oxides and hydroxides often found in industrial waste residues mainly CaO and MgO for chemical treatment (Metz *et al*., 2005; Azapour *et al*., 2014; Azdarpour, 2015, Criado *et al*., 2018).

$$(Mg,Ca)_xSi_yO_{x+2y.}\, zH_2O + xCO_2 \longrightarrow x(Mg,Ca)CO_3 + ySiO_2(s) + zH_2O \qquad (1)$$
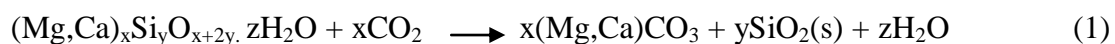
b) Direct Aqueous carbonation

Indirect aqueous mineral carbonation, CO_2 reacts with the alkaline mineral which is in an aqueous suspension form (Bodénan *et al.*, 2014, Rahmani, 2018). First, the bicarbonate and the proton H^+ are formed, which liberate the alkaline metal ion, which then reacts with the bicarbonate to form an alkali carbonate precipitate (Chakraborty *et al.*, 2018). To improve the speed of the reaction, it is imperative to work under high pressure and temperature conditions (Mun *et al.*, 2017). Some studies have suggested the use of activators to improve the rate of the reaction (Bobicki *et al.*, 2012; Junin *et al.*, 2014; Azdarpour, 2015). Direct aqueous mineral carbonation has several advantages over the direct gas/solid carbonation because it offers the option of improving the carbonation capacity by increasing the rate of the reaction and the possibility to use additives (Rahmani, 2018):

$$CO_2 + H_2O \longrightarrow H_2CO_3 \longrightarrow H^+ + HCO_3^- \tag{2}$$

$$(Mg, Ca)_2SiO_4 + 4H^+ \longrightarrow 2(Mg, Ca)^{2+} + SiO_2 + 2H_2O \tag{3}$$

$$(Mg, Ca)^{2+} + HCO_3^- \longrightarrow (Mg, Ca)CO_3 + H^+ \tag{4}$$

$$(Mg, Ca)_2SiO_4 + 2CO_2 + 2H_2O \longrightarrow 2(Mg, Ca)CO_3 + SiO_2 + 2H_2O \tag{5}$$
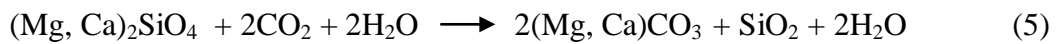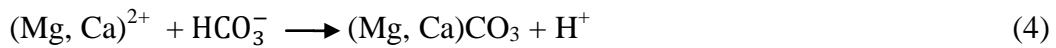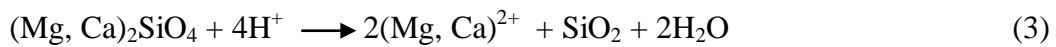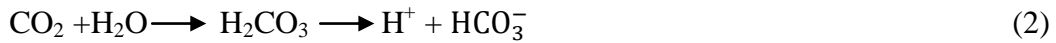
- Indirect carbonation

The indirect mineral carbonation process is generally carried out in several stages. It consists first of an extraction stage where the reactive element is extracted before it undergoes a reaction with the CO_2 (Olajire 2013). The advantage of this process is that it allows the production of pure carbonates because the reactive element is free of impurities such as silica and iron during the carbonation stage (Bobicki *et al.*, 2012). Several extraction methods have been considered (Olajire 2013 and Rahmani 2018).

There are two techniques of indirect carbonation that are:

- The indirect carbonation solid/gas which unlike direct solid/gas carbonation could be more efficient for the selective extraction of the mineral and carbonation at high pressure and temperature.

- The indirect aqueous carbonation consists of two sub-stages namely the solubilisation of carbon dioxide and the precipitation of carbonate in an aqueous medium. It offers the potential of separate optimization of the two successive steps and the possibility to increase the efficiency of carbonation compared to the other methods mentioned above by acting on the parameters of the two stages (Eloneva *et al*., 2008; Bobicki *et al*., 2012).

The first stage is the extraction of the reactive component of the complex mineral using a suitable solvent (water, acid, ammonium salt, etc.).

$$MO(s) + 2RX\ (aq) + H_2O\ (l) \longrightarrow MX_2\ (aq) + 2ROH\ (aq) \qquad (6)$$

$$(M)_2SiO_4(s)\ + 4RX\ (aq) + 2H_2O\ (l) \longrightarrow 2MX_2\ (aq) + SiO_2(s)\ + 4ROH\ (aq)\ (7)$$
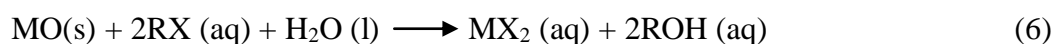
RX is the solvent and M the providential metal for carbonation. The second stage is the reaction of the reactive components (in two steps) with carbon dioxide to form a precipitate.

$$2ROH(aq) + CO_2(g) \longrightarrow R_2CO_3(aq) + H_2O(l) \qquad (8)$$

$$R_2CO_3(aq) +\ MX_2(aq) \longrightarrow MCO_3(s) +\ 2RX\ (aq) \qquad (9)$$
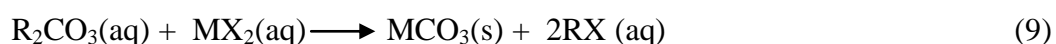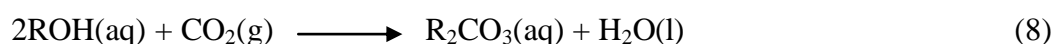
The main parameters to optimize during carbonation are:

- The amount of CO_2 introduced into the reaction medium

- The pressure

- The pH; at high pH the carbon dioxide is easily captured as gas dissolution follows the Henry's law:

$$CO_2\ (aq) = K_o * PCO_2 \qquad (1)$$

Where PCO$_2$ is the partial pressure of CO_2 in the gas phase, K_o is the coefficient of solubility of CO_2. This implies that pressurized CO_2 gas in a liquid is hydrated as carbonic acid according to the reaction (Fassbender *et al*., 2018).

$$CO_2 + H_2O \rightleftharpoons H_2CO_3 \text{ (carbonic acid)} \tag{10}$$

$$H_2CO_3 + H_2O \rightleftharpoons H_3O^+ + HCO_3^- \tag{11}$$

$$HCO_3^- + H_3O^+ \rightleftharpoons CO_3^{2-} + H_2O + 2H^+ \tag{12}$$
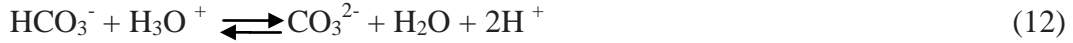
At high pH, carbonic acid behaves (Droste *et al*., 2018) like a weak diacid and dissociates in two phases according to the reactions below;

$$H_2CO_3 + OH^- \rightleftharpoons HCO_3^- + H_2O \tag{13}$$

$$HCO_3^- + OH^- \rightleftharpoons CO_3^{2-} + H_2O \tag{14}$$

At equilibrium, the two acidities have different predominance regions at 20 ° C.

- For: pH> 10.3 the CO_3^{2-} ion predominates.

- For: 6.4 <pH <10, 3 the HCO_3^- ion predominates. (Ampholyte).

- For: pH <6.3, the H_2CO_3 ion predominates.

Olajire, (2013) showed that in situ carbonation is less limited than ex situ carbonation because it involves direct injection of CO_2 into the mineral site. It, therefore, solves the transport problem and can generate the heat necessary to accelerate the reaction. However; the challenges of in situ carbonation lie in the properties and composition of the mineral (Oelkers *et al*., 2008), the availability of the necessary reagents (Brady *et al*., 1997), and the control of the reactions which is associated to the probability of forming toxic co-products that may be difficult to manage on site (Luhmann *et al*., 2017). Olajire (2013) further showed that indirect carbonation might be beneficial than direct carbonation concerning the purity of the product, the effectiveness of the reactions and appears to be more promising regarding practical realization (Liu *et al*., 2017).

However, the limited knowledge of the physical and physicochemical properties does not permit extrapolation to large-scale. The efficient and acceptable mineral carbonation regarding avoided CO_2 and cost-effectiveness still lack in this method (Olajire, 2013).

2.5 Source of metal

Calcium and magnesium are highly available carbonate-reactive compounds within the earth's crust that form insoluble and more thermodynamically stable carbonates (Koukouzas *et al*., 2018). Except in natural materials, calcium and magnesium are also found in mining and industrial residues such as steel slag, brines, fly ash (Ghouleh *et al*., 2017). Mafic and ultramafic rocks are natural materials containing magnesium. Silicon and iron are succevely mafic and ultramafic rocks. Projects on the possibility of carbonation of listed mining residues have been carried out using geographic information systems (Bonfils *et al*., 2012). Despite the advantages of carbonation of natural materials regarding their reactivity, the problem lies in the fact that only sites close to a CO_2 emitting point are considered fit for the application of mineral carbonation due to transport costs (Bobicki *et al*., 2012). The actual quantification and exact chemical composition of these residues also remain unreliable and in some cases these residues are recycled, and therefore their availability may become a problem (Bobicki *et al*., 2012; Olajire, 2013)

Solid residues consisting of calcium and magnesium are called alkaline residues they are generally found in industrial waste and have several advantages for carbonation in terms of reactivity, compared to natural minerals and mining residues (Bobicki *et al*., 2012). The carbonation of alkaline wastes contributes to the preservation of natural materials and eliminates the costs related to environmental constraints, mining exploitation operation and waste management (Wang *et al*., 2018).

In some cases, the grinding of solid residues may also not be necessary because they are sometimes constituted by particles of suitable size for mineral carbonation (Gerdemann *et al*., 2007).

As wastes, they are therefore less expensive and very available in industrial areas close to sources of carbon dioxide emissions (Mun *et al.*, 2017). The availability of alkaline waste is low in quantity compared to other materials listed above, but they have the advantage of being more reactive because of their compositions and offer a possibility of co-treatment with other industrial by-products (Koukouzas *et al.*, 2018). This considerably reduces the cost of transport (in situ carbonation). Their high reactivity allows them to undergo efficient carbonation without the need for a pre-treatment stage and to have by-products that are less dangerous for the environment, therefore, increasing their economic value (Olajire, 2013).

Alkaline wastes including steel slag, ash waste and alkaline papermaking wastes were investigated for mineral carbonation (Bobicki *et al.*, 2012). The ability of mineral sequestration of CO_2 by these wastes varies and depends mainly on the chemical composition (calcium and/or magnesium content) and the mineral type on which they are present (oxide, hydroxyl and/or silicate) (Mun *et al.*, 2017). The comparison of the efficiency of carbonation of these different forms of alkaline waste remains a challenge because the different studies do not provide a clear summary but rather dwell on the application of the technique (Bobicki *et al.*, 2012; Mun *et al.*, 2017).

Moreover, the results gathered are provided in terms of CO_2 sequestration by mass of alkali residue used or regarding carbonate produced (Gunning *et al.*, 2010; Huijgen *et al.*, 2005; Eloneva *et al.*, 2008). It is difficult to link the different wastes from the carbonation applicability because they present a great contrast about the capacity of sequestration, availability and quantity generated. Data on the life cycle and evolution are also not very available and are quite different for each waste (Bobicki *et al.*, 2012). Therefore it may be more appropriate to describe the main alkaline wastes that are found in industrial settings, the processes that generate each of them and the different ways in which they undergo mineral carbonation to better elucidate the context.

- Cement waste

The product used in the manufacture of concrete is mainly composed of limestone, silica, alumina, and iron oxides (Mun *et al.*, 2017). These materials are combined at high temperature (1400°C) to form a compound called clinker which after cooling is mixed with gypsum (Mun *et al.*, 2017; Zhang *et al.*, 2017). World cement production is estimated to date at 4 Gt per year. The cement industry is one of the largest emitters of CO_2 at about 5% of global emissions (Ong *et al.*, 2018) mainly emitted during calcinations and fossil fuel combustion. The cement industry also produces a large amount of dust which is estimated at 15-20 tonnes per 100 tonnes of cement produced (Zhang *et al.*, 2017), that dust is made up by fine unburned particles and partially burned raw materials. It is a potentially dangerous waste because it irritates the skin, eyes and respiratory tract by its caustic nature.

Cement waste is similar to the cement kiln dust (CKD), which is a by-product of the recycling of aggregates or concrete of demolished buildings. Cement waste represents a potential raw material for carbonation because its annual global production is estimated at 3 Gt (Cadavid, 2017). Cement waste consists of 20 to 60% of CaO (Bobicki *et al.*, 2012). It is found in large quantities in fine particle form and is therefore suitable for mineral carbonation. The carbonate produced is stable, less dangerous and can be reused in the manufacture of cement or elsewhere (Bobicki *et al.*, 2012; Mun *et al.*, 2017).

In addition to sequestering CO_2 and allowing recycling, carbonation of cement waste mitigates the potential risk of CKD-related irritation (Chiang *et al.*, 2017). Few results of experimental tests on the carbonation of cement waste are available. Gunning *et al.*, (2010) has studied the carbonation of cement wastes, and it was found that it is possible to produce $CaCO_3$ with a purity of 98% at a lower cost than the carbonate available on the market.

Carbonation of cement waste from the major producing countries would sequester nearly 61 Mt CO_2 per year, which represents 0.2% of global emissions generated by fuel combustion

(Lopez *et al*., 2018; Jewell *et al*., 2018). The mineral carbonation technique is therefore appropriate for cement wastes and presents a high potential for resource recovery because they are available in large quantities and reactive for this procedure (Uibu *et al*., 2017).

- Ash waste

Industrial combustion produces several categories of ash residues such as coal fly ash, bituminous shale ash and municipal ash (Rendek *et al*., 2006; Perez-lopez *et al*., 2009). Ashes contain CaO in different proportion. The carbon sequestration capacity of the residual ash is low compared with other alkaline wastes, but it has the advantage of being very fine and is produced in large quantity near sources of CO_2 emissions (Uibu *et al*., 2017). There is, therefore, a potential raw material for CO_2 sequestration. The sequestration capacity depends on the CaO content and the mineral form (Bobicki *et al*., 2012).

- Municipal solid incinerator ash

The amount of municipal solid waste is increasing and becoming a major environmental problem (Wei *et al.,* 2017). Incineration is the primary method used especially when it is difficult to recycle or reuse (Li *et al*., 2016). Incineration can significantly reduce the mass of waste (60-90%) and allows the reduction of organic matter, disinfection and the possibility of energy recovery (Wang *et al*., 2010).

Incineration produces residues and gaseous effluents containing CO_2 (12% vol). Solid residues from incineration are subdivided into two types of waste: ashes and air pollution control residues (Sanna, 2015). The solid residues from the incineration are rich in calcium oxide (Perez-lopez *et al*., 2009).

The ash is a mixture of ceramics, slag, metals, glass, other non-combustible materials and unburned organic products (Bobicki *et al*., 2012). Incineration ashes may contain heavy metals, and because of their high content of lime, soluble salt and chlorine compounds they become dangerous, they can be used in several ways after pre-treatment (Bertos *et al*., 2004).

To stabilise ash, carbonation may be a suitable method as it reduces the mobility of heavy metals and captures the CO_2 produced by incineration. The large amount of CaO, the proximity to the source of CO_2 production and the availability in the form of fine particles make ash incineration a suitable raw material for carbonation (Bobicki *et al*., 2012).

- Oil shale ashes

Oil shale is a fine grain carbon fossil fuel estimated globally at about 2.8 billion barrels (Han *et al*., 2014). The CO_2 emissions and ash production generated by the combustion of schist oils are very high compared to natural gas and coal (Uibu *et al*., 2015). The content of free lime depends on the combustion technology used; the ashes produced are alkaline and contain polycyclic aromatic unburned, heavy metals and phenols (Han *et al*., 2014). Oil shale ash has a very fine particle size and can be used to mitigate the CO_2 emissions of the site where it is produced. Although; the quantity available is low compared to other alkaline wastes the content of free lime still presents a great capacity of CO_2 sequestration (Grunewald *et al*., 2016).

- Coal fly ash

40% of electricity is supplied worldwide by coal combustion (Montes-Hernandez *et al*., 2009). Part of the coal fly ash (16%) is used in the manufacture of cement and concrete; the rest is taken to landfills (Aprianti, 2017). The growth in global energy demand has simultaneously increased the amount of coal fly ash generated by coal combustion and has created a serious problem of tailings disposal (Soog *et al*., 2006).

Coal fly ash is found to be toxic because it contains concentrated flue gas contaminant. Therefore the reuse of the fly ash may be a better way to manage the tailings rather than eliminate them (Li *et al*., 2018).

A large amount of CO_2 generated by the production of electricity from coal and the free lime content of the ash produced during the combustion could make them suitable for mineral carbonation (Bobicki *et al*., 2012, Uibu *et al*., 2015).

However, the overall potential for CO_2 sequestration is weak compared to other alkaline wastes and studies have shown that they cannot be used alone to significantly reduce CO_2 emissions (Montes-Hernandez *et al*., 2009).

- Mining and mineral processing wastes

Mining and mineral processing wastes are already mined and crushed into fine particles, they are preferable as a raw material for mineral carbonation more than mineral residues (Larachi *et al*., 2010). Mine tailings suitable for mineral carbonation come from some deposits (Olajire, 2013) such as copper deposits, PGE (platinum group element) and asbestos contained in dunite, serpentine and gabbronorite, and also diamondiferous kimberlite pipes and podiform chromite deposits (Power *et al*., 2009). The treatment of bauxite (red mud) for the production of alumina produces a residue suitable for mineral sequestration (Bobicki *et al*., 2012). During the carbonation of these residues, the CO_2 is retained which improves at the same time the properties of the waste to facilitate their later uses or their secure stockpiling (Olajire, 2013).

In situ carbonation of mining and mineral processing wastes would conveniently reduce CO_2 emissions (Hitch *et al.*, 2010) and allow strict regulation. The quantity of mine wastes produced at the sites is in most cases more significant than the amount of greenhouse gases emitted by the treatment operations. This would make it possible to sequester external emissions to the sites. The use of these wastes for the external sequestration would thus have an added economic value (Bobicki, 2014).

- Asbestos residues

The primary type of asbestos used is chrysotile (Sufriadin *et al*., 2018). 20 t of asbestos residues are generated for every ton of asbestos produced, and the annual world production of asbestos is estimated at 4Mt. This means that about 80Mt of asbestos waste is generated every year in the world (Bobicki, 2014).

These residues are dangerous because they contain residual asbestos and it is envisaged that the carbonation of these residues could alleviate their dangerous nature and make them ideal for mineral sequestration due to their high MgO content and the fact that they have already undergone size reduction (Bobicki, 2014). The mineral sequestration of these residues would allow the elimination of hazardous waste and the reduction of CO_2 emissions (Goldberg *et al*., 2001; Kumar *et al*., 2016).

- Nickel residue

Laterites are used as the main source of nickel (Mudd, 2010, Elshkaki *et al*., 2017). Large quantities of residues are generated during the processing of nickel ores, which have a high MgO content, which would allow for mineral carbonation and the technique could provide a cost-effective economic contribution to nickel ore processing (Hitch *et al*., 2010). Work on the carbonation of nickel residues has been carried out by Teir et al., (2009); and Li *et al*., (2018).

- Red mud

The production of alumina from bauxite (Bayer process) involves the digestion of the ore in caustic liquor of sodium hydroxide, it is generated two flows namely the alumina liquor and a slurry product called red mud (Cusack *et al*., 2018). The red mud has very high alkalinity and contains several elements (Han *et al*., 2017). The annual global production of red mud is about 70 million tonnes (Braga *et al*., 2018). Management of red mud is a serious environmental problem for animal and plant life because of its caustic nature (Braga *et al*., 2018).

The mineral carbonation of red mud would reduce the toxicity, reduce the storage of these alkaline materials and reduce CO_2 emissions. Red mud can also be used in various other applications (plastic fillers, soil almonds, cement, bricks) (Cai *et al*., 2018; Sutar *et al*., 2014). The red mud plant built by Alcoa at Kwinana (Australia) sequestered 70,000 tonnes of CO_2 generated by an ammonia plant nearby (Bobicki, 2014; Clark *et al*., 2015).

The high alkalinity due to the presence of NaOH and other elements promotes the formation of Na_2CO_3 and $NaHCO_3$ during the mineral carbonation of red muds which are soluble products and therefore are less stable for permanent storage (Cusack *et al*., 2018).

Red mud carbonation studies conducted by Johnston *et al*., (2015), and Dilmore *et al.,*(2017) focused on the applicability of the carbonation and red mud neutralization demonstration. They deduced that using brine for the neutralization of red mud and the sequestration of CO_2 provides more carbon-efficient storage.

- Alkaline paper mill waste

In the Kraft pulp process, the wood chips containing sodium sulphide are prepared in a caustic solution for 2 hours and at 170 ° C, to separate the dissolved lignin from the cellulose fibres (Gierer, 1980, Perez-Lopez *et al*., 2008). Several forms of waste rich in portlandite are generated by the formation of caustic liquor (Perez-Lopez *et al*., 2008). These wastes are called alkaline paper mill waste (APMW), and are generally discharged. The high CaO content makes these wastes a possible material for mineral carbonation. $CaCO_3$ can be produced trough reaction of these APMW with CO_2 emitted by pulp mills (boiler and lime kiln) (Nurmesniemi *et al*., 2008; Perez-Lopez *et al*., 2008). Research on the carbonation of APMW is limited. Pérez-López, (2008) was able to study the carbonation of APMW and concluded that APMW is a suitable material for mineral carbonation because the sequestration capacity is high and the powder of $CaCO_3$ produced is selective for neutralization of acid mine drainage.

- Steelmaking slags

The most common type of slag in the world is slag from iron processing (Afanga, 2014). They are defined as the iron-free slag obtained by chemical reactions during the melting of metals in the iron and steel industry (Habashi, 2017).

Steel slags, which are by-products of steel production processes (Afanga, 2014), are a widely available class of industrial waste materials that can potentially be used for mineral carbonation resulting in the reduction in basicity (pH), swelling stabilization, and reduction of heavy metals leaching (Eloneva *et al*., 2008).

Currently, the treatment and disposal of these slags represent a costly burden on steel plants (Habashi, 2017). Steel slags high CO_2 uptake capacities, coupled to the large onsite CO_2 emissions of steelworks, offers opportunities for carbon capture. Slags are generated at different levels of steelmaking process by reactions of impurities (mainly silica) with lime (Eloneva *et al*., 2010).

There are four principal kinds of steelmaking slags depending on the process from which they have produced, i.e. Blast furnace, basic oxygen furnace, electrical arc furnace and ladle furnace (Chiang *et al*., 2017). Integrated carbon steel production consists of iron-making in the blast furnace, steelmaking in the basic oxygen furnace and continuous casting of steel billets, slabs and blooms (De Beer *et al*., 1998; Yi *et al*., 2012). For over a century, with iron and steel industry booming worldwide, a vast amount of slag has been produced as an inevitable by-product of the steelmaking process (Li *et al*., 2009; Chitaka *et al*., 2018). While valuable applications have been found for BF slag, mostly in the construction sector such as in cement manufacturing and as a cement replacement in concrete, much of BOF slag production, estimated at 60-120 kg/t steel presently, still ends up in landfill sites (Setién *et al*., 2009; Arribas *et al*., 2015; Georgakopoulos *et al*., 2017).

2.6 Carbonation of steelmaking slags

Global estimations of the annual amount of steelmaking slag produced range from 315 Mt to 420 Mt (Eloneva and Teir, 2008). In South Africa, the steelmaking industry generates about 4 million tons of by-products each year, including 600 000 tons of BOF slag waste (Mulopo *et al*., 2012). In the blast furnace, hematite (Fe_2O_3) ore is fed into the top of the furnace along with limestone (calcium carbonate) and coke (carbon) (Figure 2). The purpose of a blast furnace is to chemically reduce and physically convert iron oxides into liquid iron called "hot metal" as shown in Figure 2. Hot air is 'blasted' through the base of the furnace and generates the high temperatures required in the furnace. The iron is runoff from the bottom of the blast furnace into moulds to form ingots of cast iron. Cast iron is very brittle since it contains 3-4% carbon and so it is converted to steel.

Scrap steel can also be added to the mixture. The heat of the furnace changes the limestone into calcium oxide and carbon dioxide. The calcium oxide then reacts with the silicon oxide impurities in the iron to produce calcium silicate (slag) which is skimmed off the top of the molten iron. Different types of slag result from the various furnaces used (Piatak *et al*.2015, Bodsworth, 2018). In addition to slag produced in the primary stage of steelmaking, slags are also produced in secondary steel refining operations (Chiang *et al*., 2017).

The utilization of blast furnace slag, from the steel industry, is relatively well known for many applications in road construction, i.e. use as aggregates for the base layers, as aggregates for hydraulic concretes, hot asphalt or hydraulic binder (Özbay *et al*., 2016; Takeshi *et al*., 2018). Unlike blast furnaces slags are volumetrically stable and easy to use in their construction applications, steel plant conversion slag and steel mill electric furnace slag contain in varying proportions unhydrated free lime (CaO) (Setién *et al*., 2009).

That may cause volumetric instability (expansion) and require appropriate tests and quality controls, to ensure their proper use in construction (Setién *et al*., 2009; Arribas *et al*., 2015; Chiang et al., 2017).

It is often essential that each slag depending on its type, treatment and origin, be thoroughly evaluated for each intended use, about significant property variances that may be solicited and the specific performance requirements for the intended uses (Chiang *et al*., 2017).

The uses of these slags are very diverse and extend to various fields, but they more often face economic and environmental considerations (Liu *et al*., 2017). The quantity of slag produced depends on the quality of the raw material and type of kiln used but is usually about 10 to 15% of the amount of steel produced (Li *et al*., 2009; Chitaka *et al*., 2018).

TABLE 2: TYPICAL COMPOSITION OF STEEL SLAG (Afanga, 2014; Chitaka *et al*., 2018)

TYPICAL COMPOSITIONS OF STEEL DAIRY (% mass)									
Type of dairy	FeO/Fe_2O_3	MnO	SiO_2	Al_2O_3	CaO	MgO	P_2O_5	Cr_2O_3	S
Blast furnace	-	0.1-0.5	33-39	9-13	39-42	6-9	-	-	1.2-1.4
Electric arc furnace	15- 35	< 10	10 - 20	< 10	30-40	< 10	< 2	< 2	<0.25
Converter	15- 35	3-10	9 13	0.5-3	42 - 52	1-8	1.5 4	~ 2	~0.25

- Main steelmaking reactions and flow sheet

The primary reaction in the elaboration of steel and iron is the reduction that can be represented by the following three steps (Afanga, 2014);

$$T > 320°C \qquad 3Fe_2O_3 + CO \longrightarrow 2\,Fe_3O_4 + CO_2 \qquad (15)$$

$$620°C < T < 950°C \quad Fe_3O_4 + CO \longrightarrow 3\,FeO + CO_2 \qquad (16)$$

$$1100°C \qquad FeO + CO \longrightarrow Fe + CO_2 \qquad (17)$$

Iron reduction

$$CO_2 + C \rightleftharpoons 2CO \qquad (18) \Longrightarrow \textbf{Bouduard}$$

$$FeO\ (l) + C \longrightarrow Fe\ (l) + CO \qquad (19)$$

$$Fe\ (l) + C \longrightarrow Cast \qquad (20)$$

Conversion
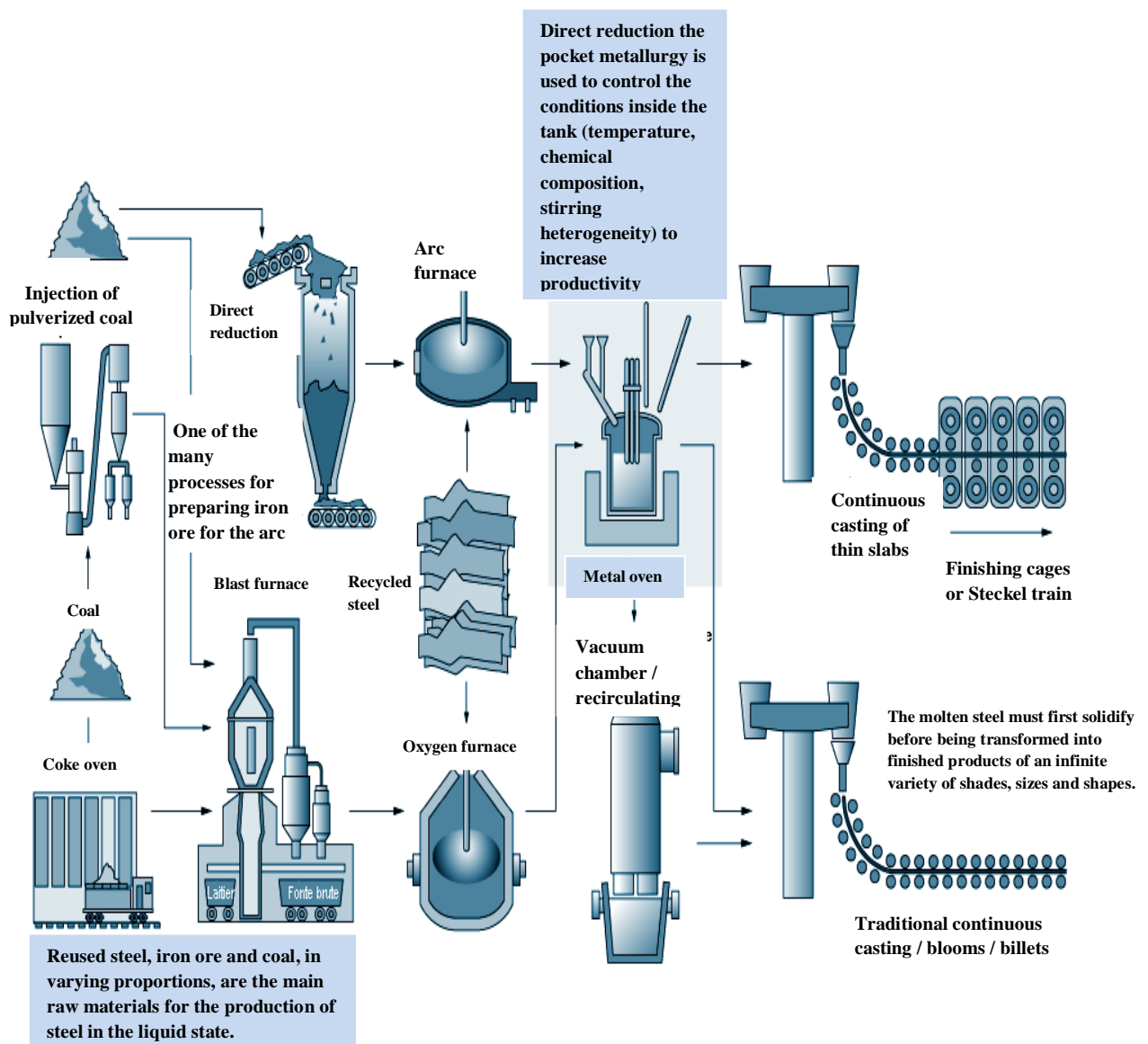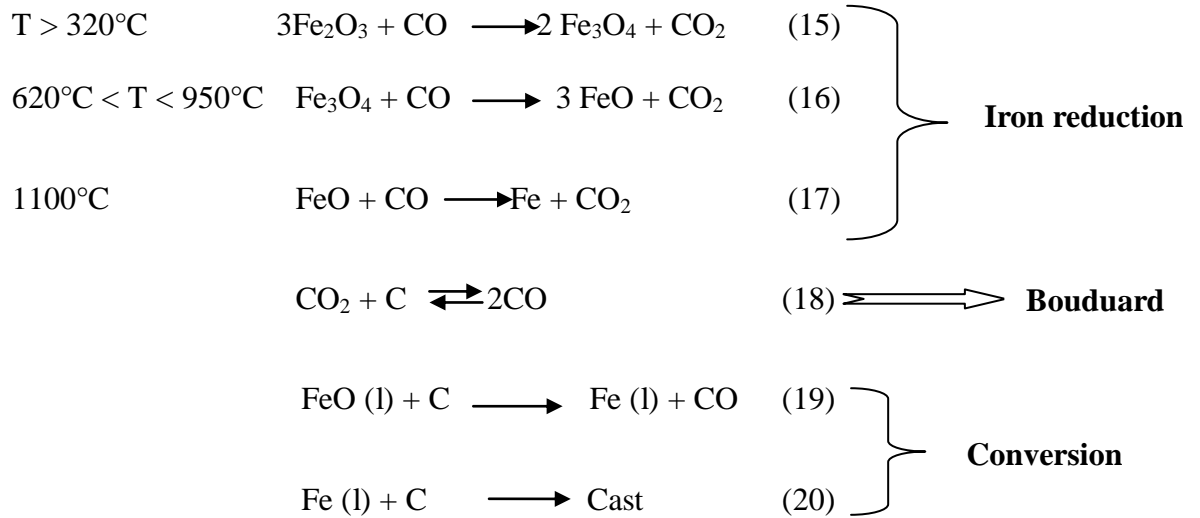
Figure 2: Manufacture of iron and steel Flowsheet (Source: American iron and steel 1995, Ruth, M. 1995)

- Carbon dioxide from the steelmaking industry

During the manufacturing process of iron and steel, the production of carbon dioxide is inevitable (Kundak *et al*., 2009). During the reduction of iron ore (iron oxide) carbon, in the form of coal or coke, is used as a reducing agent and the latter acts with oxygen to firstly form carbon monoxide and subsequently carbon dioxide (Kundak *et al*., 2009; Xu *et al*., 2017).

Each ton of steel produced in the iron and steel industry corresponds to about 2 tons of carbon dioxide emitted (Mæstad, 2000; Kundak *et al*., 2009; Chen *et al*., 2018). The steel industry is the world's largest emitter of CO_2 because it contributes more than 30% of emissions (Kundak *et al*., 2009). The steel industry accounts for about 7% of anthropogenic emissions of CO_2. When mining and transportation of iron ore are included, the share may be as high as 10% (Leeson *et al*., 2017).

The CO_2 emissions associated with iron and steel production differ across countries and regions, depending on how much energy is used and the CO_2 intensity of that energy (Ukwattage *et al*., 2015; Cabral *et al*., 2017). About 75% of the global CO_2 emissions from steel production are related to the use of coke and coal in iron making (Liu *et al*., 2017). Other notable emission sources are the use of electric power for scrap melting and the use of natural gas in the production of direct reduced iron (Leeson *et al*., 2017) as shown in Figure 3.

Several studies have been carried out to find technological methods to reduce these CO_2 emissions such as the use of biomass instead of coal, the capture and sequestration of CO_2 in saline aquifers or the recycling of top gas (Liu *et al*., 2017).
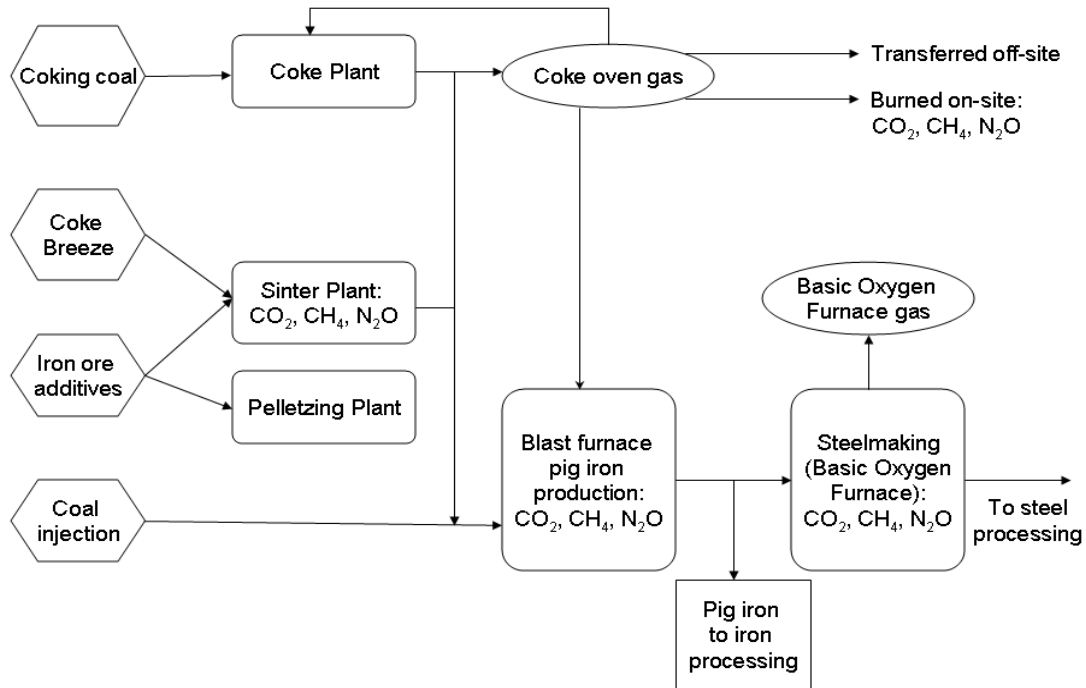
Figure 3: The main GHG emission sources associated with iron and steel production (Leeson *et al*., 2017)

3. PRODUCTION OF CALCIUM CARBONATE FROM STEEL SLAG

Calcium carbonate is a solid compound consisting of calcium associated with carbonate ions whose chemical formula is $CaCO_3$ (Santos *et al*., 2014). It is found in nature mainly in the form of calcite and aragonite in limestone rocks, or the form of limestone (Al Omari *et al*., 2016, Cheng *et al*., 2018). It is also found in the form of dolomite and the main constituent of coral shells, snails and marine animals (Cheng *et al*., 2018). The shapes of limestone rocks or minerals may have similar characteristics. They are differentiated by chemical analysis, X-ray diffraction and electron microscopy to derive the physicochemical characteristics (Rey *et al*., 2017):

- Calcite of general formula $CaCO_3$ which contains a high content of limestone and occurs under the hexagonal and rhombohedral crystalline system.

- The dolomite of formula $CaCO_3MgCO_3$, which occurs in a hexagonal crystalline system, in the general case in the form of rhombohedral crystals with curved dimensions. It is often of white or pink colour.

- Aragonite is stable and occurs at low temperatures near the surface deposits in orthorhombic crystalline form.

- The ankerite of formula $Ca_2MgFe (CO_3)$ which occurs in the hexagonal system in the form of rhombohedral crystals. It is white, pink or grey.

Calcium carbonate is a white tasteless, odourless, chemically and physically stable solid of the empirical formula $CaCO_3$ with very low solubility in water 0, 013 g/l (at 25 °C) and a basic character pK_a 9. Its melting temperature is 825°C and its density varies between 2.7 and 2.9 g/cm^3 (Santos *et al.*, 2014).

World production of calcium carbonate from pure natural limestone and calcium carbonate precipitate is estimated at 100 million tonnes per year (Al Omari *et al.*, 2016). These products are called calcium carbonates of chemical qualities. Calcium carbonate is produced synthetically by;

- precipitation of the lime using carbon dioxide (CO_2) following the reaction:

$$Ca (OH)_2 + CO_2 \longrightarrow CaCO_3 + H_2O \tag{21}$$

- precipitation from sodium carbonate according to the reaction:

$$Ca (OH)_2 + Na_2CO_3 \longrightarrow CaCO_3 + 2 Na^+ + 2 OH^- \tag{22}$$
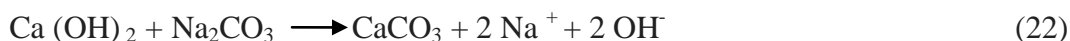
- direct and/or indirect carbonation of mineral residues containing calcium in the form of oxide, hydroxide or silicate as shown in the preceding paragraphs.

The basic character of the calcium carbonate makes it possible for acidic species neutralization what can make them suitable for acid mines drainages (AMD) management (Kefeni *et al.*, 2017).

Natural pre-treated and synthetic calcium carbonates are in economic competition in the paper industry due to charge in the paper industry and coating material (Said et al., 2013; Gane *et al*., 2009).

The synthetic product, therefore, has a higher purity than the natural one, but the quantity produced is small. Figure 4 shows an industrial example of calcium carbonate precipitate production flowsheet (Gane *et al*., 2009, Said, 2017).
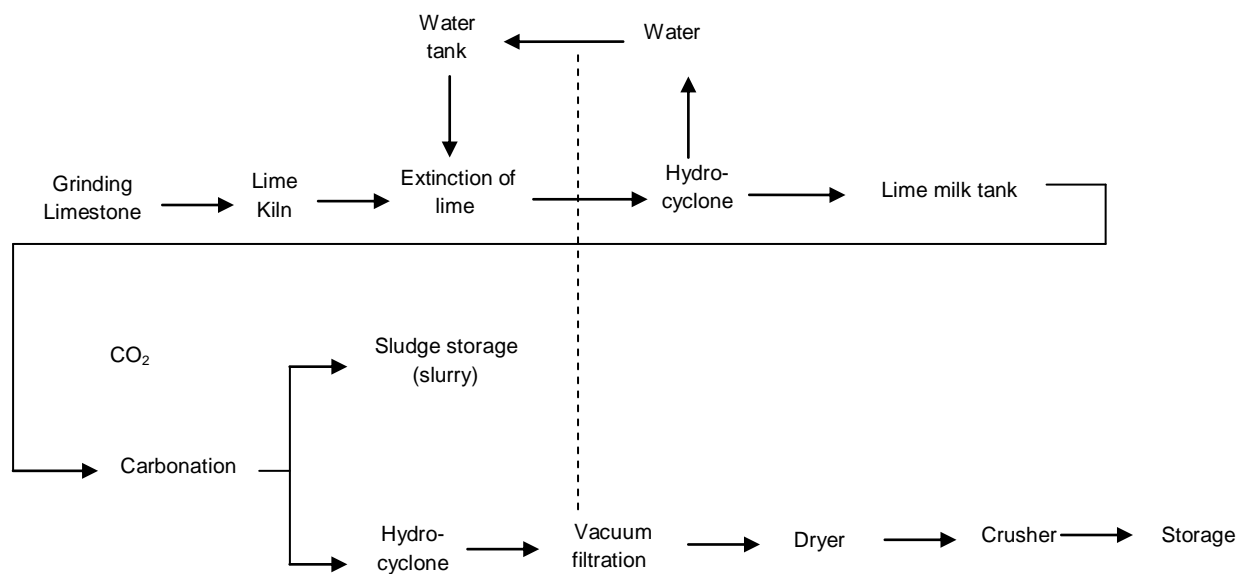
Figure 4: Precipitation of calcium carbonate Process (Gane et al., 2009)

In Figure 4 the raw material can be replaced by the alkaline wastes previously described (steel slag, cement waste, etc.) and pass directly to the carbonation (direct or indirect) without necessarily using the other stages of material preparation.

The production of calcium carbonate from the steel slag has also been considered by previous workers. For instance, Kakizawa *et al*. (2001) used acetic acid as a solvent to extract calcium from the slag and produce calcium carbonate by fixing the carbon dioxide on the formed calcium acetate. Their study showed that the use of acetic acid to produce calcium carbonate still requires the additional use of sodium hydroxide.

The concentration of acid affected the amount of calcium and dissolved impurities. The amount of dissolved calcium increased with acid concentration. Impurities such as iron and silicon as well as other elements such as manganese, magnesium, vanadium and aluminium were also dissolved at high acid concentration and this ultimately affected the purity of calcium carbonate produced.

They further showed that the temperature did not have a significant influence on the extraction but that time had a very significant effect as a longer extraction period possibly allowed the formation of silicone gel that facilitated the removal of silica by mechanical action. The purity and the amount of calcium carbonate formed do not depend on the concentration of carbon dioxide, so it follows that for the precipitation of calcium carbonate the source of carbon dioxide could be the flue gas. However, a low concentration of gas CO_2 affects the pH stabilization time of a solution; this could be offset using large gas flows.

Furthermore, during the precipitation of calcium carbonate from calcium acetate, acetic acid regenerated and hindered a new formation of the precipitate by lowering the pH of the solution (Teiret *et al*., 2007). This led to the use of more sodium hydroxide which reacts with calcium acetate and produces calcium hydroxide and sodium acetate (Eloneva *et al*., 2008).

The feasibility of producing calcium carbonate from steel slag using acetic acid has been proven but its application remains elusive due to the additional use of sodium hydroxide, which makes it very expensive (Kakizawa *et al*., 2001; Eloneva *et al*., 2009; Hall *et al*., 2014). It is therefore one of the objectives of this study to assess different solvents for efficient CO_2 driven calcium carbonate precipitation with or without selected catalysts and the potential for regeneration and reuse.

Although various solvents have been tested, recent studies have shown that ammonium salts dissolve calcium more selectively and effectively as they avoid the problem of acid formation during precipitation (Eloneva *et al.*, 2008; Eloneva *et al.*, 2012; Olajire, 2013; Mattila *et al.*, 2014).

The effect of slag particles size and the effect of the solid/liquid ratio (slag/solvent) on calcium extraction were also studied. The results report that particle size has a noticeable effect on calcium extraction from the slag and the finer the grain size, the larger is the grain contact surface with the solvent and higher is the transfer rate of the metal ion and therefore higher is the efficiency of extraction (Eloneva *et al.*, 2009).

To improve the extraction efficiency, the ratio between liquid/solid generally increased implying increased capital and operation cost (Eloneva *et al.*, 2009; Said *et al.*, 2013). Ammonium nitrate has been identified as the most effective saline solution as a solvent for calcium (Eloneva *et al.*, 2009). It was further found that the calcium carbonate produced using ammonium salts as a solvent had a rhombohedral shape and that the extraction yield of calcium could reach 70% and the precipitate could be pure up to 99.8%. However, the regeneration of the ammonium salts used was still a challenge (Adams, 2005; Bao *et al.*, 2010; Mo *et al.*, 2016). To produce a pure precipitate of carbonate, it may be better to use indirect carbonation (Bobicki, 2014) and this is the route we will follow in this project. The high calcium content of steelmaking slags makes them useful as raw materials to produce calcium carbonate and thus allows safe and beneficial storage of carbon dioxide in a solid compound without risk of escape (Said *et al.*, 2016). Carbonation makes it possible to fix the carbon dioxide on the oxides of calcium or magnesium contained in silicate-based materials to produce carbonates (Eloneva *et al.*, 2009; Olajire, 2013).

4. ACID MINES DRAINAGE TREATMENT USING CALCIUM CARBONATE

Active or abandoned mines and mineralogical activities produce waters with generally low pH and high concentrations of toxic and polluting metals for the ecosystem (Galhardi *et al*., 2016; Kefeni *et al*., 2017). The increase in the flow of waters due to mining promotes the dissolution of sulphide minerals by oxidation in water and the presence of microorganisms (Yu *et al*., 2016; Kefeni *et al*., 2017; Jallath *et al*., 2018). This dissolution allows the release of the acidity of exclusively ferrous minerals (pyrite).

The attack of other minerals by this acidity causes the liberation of the latter in solution which constitutes a serious environmental problem (Kefeni *et al*., 2017). The treatment methods and the prevention of AMD generation have been considered extensively (Ali *et al*., 2015; Luptáková *et al*., 2018; Balci *et al*., 2018). The possibility of recovering resources such as ferric hydroxide, rare metals, ferrite, sulphur and sulphuric acid and their economic values have also been the subject of several discussions (Modabberi *et al*., 2013).

Studies have shown that the recovery and reuse of resources would preserve the environment and reduce the pollution caused by acid mine drainage (Galhardi *et al*., 2016; Kefeni *et al*., 2017). Acid mine drainages are challenging to control once produced; the processing cost of these AMD is high and its impacts very profound on the environment (Galhardi *et al*., 2016; Ndlovu, 2017).

The oxidation reactions of pyrite under different conditions are presented below, (Vasquez *et al*., 2016, Evangelou, 2018);

$$FeS_2 + 7/2O_2 + H_2O \longrightarrow Fe^{2+} + 2SO_4^{2-} + 2H^+ \tag{23}$$
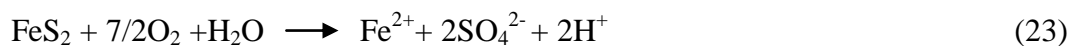
Oxidation of pyrite under molecular oxygen in the presence of excess water at neutral pH.

$$Fe^{2+} + 1/4O_2 + H^+ \longrightarrow Fe^{3+} + 1/2H_2O \tag{24}$$

$$Fe^{3+} + 3H_2O \longrightarrow Fe(OH)_3 + 3H^+ \tag{25}$$

$$2FeS_2 + 17/2O_2 + 5\ H_2O \longrightarrow 2Fe\ (OH)_3 + 4\ SO_4^{2-} + 4H^+ \qquad (26)$$
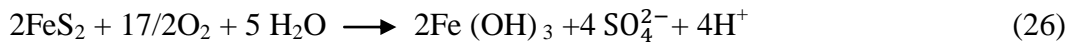
Global reaction of oxidation of pyrite

$$FeS_2 + 14Fe^{3+} + 8H_2O \longrightarrow 15Fe^{2+} + 2\ SO_4^{2-} + 16H^+ \qquad (27)$$
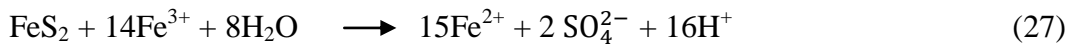
Complete oxidation of pyrite with ferric ions acting as an oxidizing agent that is faster than the first reaction (Pierre Louis *et al*., 2015).

$$FeS_2 + 15/4O_2 + 1/2H_2O \longrightarrow Fe^{3+} + 2\ SO_4^{2-} + H^+ \qquad (28)$$
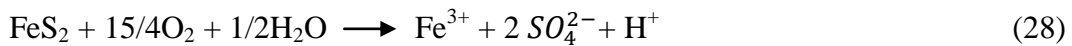
Complete oxidation of pyrite in the presence of water content (Chen *et al*., 2015).

Iron (II) dissolved in AMD reacts with dissolved oxygen and forms precipitates of iron oxide (yellow boy) that can prevent breathing of living organisms when it seeps into waters and can destroy aquatic life and many microorganisms by drastically lowering pH (Agrawal *et al*., 2009; Han *et al*. 2015). The contact of AMD with different types of ore facilitates the solubilization of toxic metals. The level of pollution due to AMD's depends on their compositions and their pH which varies according to the production site (Hedrich *et al*., 2014). The investigations led by Kefeni *et al.* (2018) shows that in South Africa the Fe (II) content is high but that the AMD compositions depend mostly on where they are produced.

The process of treating AMDs with several dissolved metals is too complex and expensive, but the abandonment of AMDs in nature has severe and long-lasting consequences on the terrestrial and aquatic environment (Nancucheo *et al*., 2017). It is therefore vital to prevent the generation of AMD, but if they are already produced, it is imperative to treat them (Vaněk *et al*., 2013; Kefeni *et al*., 2017; Nancucheo *et al*., 2017). Recently the focus in AMD treatment has been on the sequential removal of metals and other toxic pollutants. However, only a limited number of AMD treatment techniques can be deemed economically affordable (Judd *et al*., 2015).

Neutralization, stabilization and elimination of pollutants through chemical, physical and biological processes is the fundamental principle for many AMD treatment methods (Luptakova et al., 2012; Tolonen *et al*., 2014).

Some recent methods of treating AMD are passive biological treatment with sulfate-reducing bacteria (SRB), magnetic nanoparticles (MNP), treatment with the materials available in the environment (bentonite, lignite, zeolite, etc.) (Luptakova *et al*., 2012). However, the traditional neutralization method remains prevalent.

4.1 Prevention of AMD generation

The protection of sulphide minerals from the air, water and bacteria avoids the production of AMD's and protects the environment (Moult *et al*., 2014). The techniques that can enable this prevention are;

- Backfilling of tailings and soils, quarry aggregate and grinding, sandy materials, cement and other binders that minimizes acid formation (Benzaazoua *et al*., 2013).

- Dry cover, water cover, oxygen-consuming blanket used as oxygen barriers (Amos *et al*., 2015), industrial alkaline by-products have been used recently in several applications to cover rock wastes and residues. Studies have been carried out to prove the effectiveness of the soil mix and mud cover technique and have been shown to be successful (Demers *et al*., 2017). Water prevents the oxygen from reaching the sulphide minerals because it has a low solubility and a very low diffusion coefficient than in the air (Amos *et al*., 2015; Demers *et al*., 2017). Organic materials are less used because they have a minimal life. Oxygen contact with residues reactive materials can be prevented by the elimination of subaquatic residues (Amos *et al*., 2015; Nancucheo *et al*., 2017).

4.2 AMD Treatment

The treatment of AMD is subdivided into two main techniques which are the active and passive cleanings. Active treatments use metal precipitation with alkaline chemical reagents as well as ion exchange techniques (Fu *et al*., 2011) and membranes (Kefeni *et al*., 2017).

The most commonly used active cleaning method is the neutralization of AMD with the aid of industrial alkaline products, calcium hydroxide ($Ca(OH)_2$) and calcium carbonate ($CaCO_3$), which favors precipitation of metals in the form of hydroxides and sulphate sludges in calcium sulphate form ($CaSO_4.2H_2O$) (Tolonen *et al*., 2014).

Among the active treatment methods, there is also the barium-calcium alkaline desalting (ABC) which is recent in which the metals and the sulphate are reduced below the toxic level (Kefeni *et al*., 2017).

In ABC technique, the metals and the chemical products are recovered with a low sludge removal (Mulopo, 2015). In recent years passive treatment has been widely used for the treatment of AMD (Yadav *et al*., 2015). It consists on biological treatment with wetlands constructed between a chemical treatment with limestone drains and bioreactors reducing water sulphate (Tolonen *et al*., 2014), passive treatment can also be based on the construction of a permeable reactive barrier that uses a chemical or biological process (Escobar *et al.*, 2016). This treatment technique is more appropriate for applications in abandoned mines because it is less expensive and easier to maintain. The choice of the technique depends on the ability of the system to produce alkalinity and the efficiency of metal removal (Zhu *et al*., 2017). In order to reduce the cost of AMD treatment, researchers are focusing on the development of a low-cost technique that would use industrial waste by-products, available natural materials and organic substrates (Kefeni *et al*., 2017).

The disadvantage of the traditional treatment of AMD by lime or limestone is that it requires ample space to get rid of waste and presents risks of contamination of the environment with toxic leachate metals (Tolonen *et al.*, 2014). Therefore studies on the application of the magnetic nano-particles MNP method have shown that it facilitates the recovery of these magnetic nano-particles which makes the technique more profitable and the environment healthier for a long duration (Kefeni *et al.*, 2017).

The absence of experimental data thus makes it impossible to make a clear comparison between the conventional (neutralization, precipitation) and modern (MNP, membrane) processing techniques of AMD (Fu *et al.*, 2011; Tolonen *et al.*, 2014). It is currently based on the profitability and the quality of the final products.

Preference is given to techniques that can reduce the amount of waste and provide a better recovery and resource reuse option which makes them profitable. However, for the moment none of the techniques has been proven to be effective (Santos *et al.*, 2017).

Further research on AMD prevention and control techniques based on options such as recovery and reuse of wastes and possible combination of treatment methods will ensure environmental protection (Agrawal *et al.*, 2009; Hedrich *et al.*, 2014; Amos *et al.*, 2015; Kefeni *et al.*, 2017). The use of calcium carbonate produced from steelmaking slag is therefore possible for the treatment of acid mining drainages and neutralization of AMD using calcium carbonate remains one of the most straightforward methods (Kefeni *et al.*, 2017).

CHAPTER III EXPERIMENTAL PROCEDURE: MATERIALS, CHEMICAL ANALYSIS AND METHODS

1. MATERIALS

1.1 Slag preparation

A sample of the BOF slags from ArcelorMittal was collected and subjected to a particles size analysis. Sampling was done using a rotating pot splitter which allowed several samples at equivalent proportions. Samples were weighed and then dried in an oven at 130°C for 3 hours to determine the moisture. Then four of these dry samples were divided into 25g each for subsequent experiments.

1.2 Reagents

- 20 liters of distilled water prepared in the mineral processing laboratory of the School of Chemical and Metallurgical Engineering at the University of the Witwatersrand

- 1 Kg of ammonium nitrate (Merck. PTY.LTD NH_4NO_3 M=80.04g/mol) from Sigma Aldrich.

- 2.5 liters of ammonia 25 %(NH_4OH, gold line (CP) M=35.05) from Acechem South Africa with the following specifications:

- Assay (NH_3) 25%

- Chloride (Cl) 0.0001 %

- Iron (Fe) 0.000 1%

- Sulphate (SO4) 0.001%

- 2.5 liters of EDTA(di –sodium salt) from Sigma Aldrich with the composition of 0.2N+/- 0.5%

- Technical carbon dioxide gas cylinder under pressure (CO_2, 31.3 kg/17m^3) from AFROX

- 1Kg ammonium chloride (Merck. PTY.LTD NH_4Cl (M=53.49g/mol) from Sigma

TABLE 3: CHEMICAL PROPERTIES OF NH₄NO₃ USED

Elements	Value
acidimetric calculated on dried substance	≥ 99.0%
Assay	≥ 95.0%
insoluble matter	≤ 0.005%
pH-value	4.5-6
chloride	≤ 0.0003%
Phosphate	≤0.0005%
Sulphate	≤0.002%
Calcium	≤0.0005%
Heavy metal	≤ 0.003%
Iron Fe	≤0.0002%
Water	≤0.01%
Residue on ignition	3.0 – 5.0%

Table 4: CHEMICAL PROPERTIES OF NH$_4$Cl USED

Elements	Value
Assay (argentometric)	$\geq 99.8\%$
Assay (argentometric; calculated on dried substance)	$99.0 - 100.5$
insoluble matter	$\leq 0.005\%$
pH-value	4.5-5.5
chloride	$\leq 0.0003\%$
Nitrate (NO$_3$)	$\leq 0.0005\%$
Phosphate (PO$_4$)	$\leq 0.0002\%$
Sulphate (SO$_4$)	$\leq 0.002\%$
Heavy metal (as Pb)	$\leq 0.0005\%$

1.3 Equipment

- Sampling and chemical and particles size distribution

Sampling was done with a rotary splitter Eriez of 10 pots rotating with variable speeds regulator. Then four samples were weighed on a Mettler Toledo scale and dried in the Labotec oven.

Using the splitter, four aliquots were taken from each sample and subsequently pulverized and prepared for the chemical analysis. The dried slags were subjected to a particles size analysis using Macsalab Electronic sieve shaker. The mesh sizes were in the range from 4000 to 75 µm arranged in descending order from top to bottom during 3 hours each. The holding proportions of each sieve are weighed and pulverized before chemical analysis.

- Extraction

The ammonium salt solutions were prepared in different concentrations by diluting the corresponding mass with distilled water in volumetric flasks of 500 ml each. Steel slag - solvent mixture of different ratios were prepared in a 500 ml beaker. The beaker was placed in a Precisterm Selecta (0-220°C) water bath maintained at a constant temperature of 25°C. An overhead Labotec (HEIDOLPH) mechanical stirrer was used for stirring (rate: 400 rpm). The temperature was taken with a thermometer after a short time interval (3 minutes). The pH evolution during reaction was measured with a Starter 3100 pH meter (OHAUS). The extraction equipment is shown in Figures 5 and 6 below.

Figure 5: Extraction experiment using water bath and electrical stirrer.
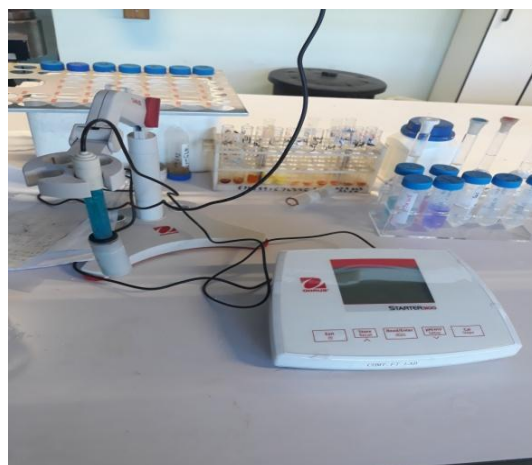
Figure 6: pH experimental measurement

The pH meter was calibrated as follows;

- Once the instrument is on, the probe was placed in the pH 7 standard and the Cal/Slope button was pressed. The sample was agitated while reading.

- Between every reading the electrode was rinsed with deionised water using a wash bottle and waste beaker and dab dry gently, before placing in the next calibration standard/sample.

- The operation was repeated 4 times using the others pH standards (pH4 and pH10)

- After calibration was completed, control solution was read.

NB: when the control sample did not fall in the acceptable pH range, the calibration was repeated.

- To read a sample, the pH probe was immersed in the sample and the Read/enter button was pressed while agitating the probe. The pH reading was recorded, the electrode rinsed with deionised water, dab dry and immersed into the next sample

- The control sample was checked after every 10 readings and calibration was done if the control did not fall into an acceptable pH range.

After a determined time, a sample of the reaction mixture was collected and filtered off using a 47 mm filter paper (pore size: 0.45 μm) well placed in a funnel, and the filtrate was collected in a 250 ml flask and later distributed in test tubes for chemical analysis.

- Carbonation

The carbonation was carried out in a 100 ml autoclave reactor placed in a CO_2 gas circulation setup. The carbon dioxide under pressure in a gas cylinder was fed into the reactor using a metal pipe, which first passes through a flow meter calibrated from 0 to 150 cm^3.

The mounting of the carbonation equipment used is shown in Figures 7 and 8 below;

Figure 7: Gas tanks of carbon dioxide under pressure surmounted by a regulator

Figure 8: Experimental gas / liquid reactor autoclave connected to flow meter

Precipitates obtained are filtered using a 47 mm filter paper (pore size: 0.45 µm) placed in a funnel subtended by a 250 ml graduated flask. The filtrates were distributed into test tubes for chemical analysis, and the precipitate is placed in a porcelain dish and dried in an oven at 150° C for 150 minutes.

2. EXPERIMENTAL PROTOCOL

Moisture was determined according to the formula:

$$\%H = \left(\frac{P_h - P_s}{P_h}\right) * 100 \tag{2}$$

Where; P_h is the wet weight of the sample and P_s the dry weight of the sample and H the moisture in %. Subsequently, a particle size analysis was conducted using macsalab siever to determine the particle size distribution of the samples and calculate the P80 which is the size of the sieve on which passes more than 80% of the load using the following formula:

$$P_x = 1 - Exp\left(-\frac{dx}{dm}\right)^a \tag{3}$$

Where: P_x is the proportion passing trough x size, dx/dm, *a* and m is the distribution parameters

2.1 Extraction experiments

While extracting a metal, it is imperative to establish the characteristics (chemical composition, pH, temperature) of the solvent. The critical parameters of the extraction are, therefore:

- The pH
- The liquid/solid ratio
- The concentration of the solvent
- The selectivity of the solution used for calcium extraction

The extraction experiments were carried out using two ammonium solutions namely ammonium chloride and ammonium nitrate whose characteristics are defined above.

Different L/S ratios were tested to determine the optimum parameters for efficient extraction with the two different solvents. The equilibrium isotherms were determined and used for plotting the McCabe and Thiele diagrams for the determination of the number of extraction stages for different working lines. A 25 g sample was dissolved into 2 M, 2.5 M and 3 M NH_4NO_3 and NH_4Cl respectively and at different L/S ratios, i.e. 3/2, 2/1, 5/2, 3/1, 5/1, 7/1, 10/1, 20/1 and 50/1. The various filtrates were then collected in tubes for chemical analysis. The residues of the extraction were also analyzed to determine their constitution (calcium content and mineral form) for their subsequent uses or disposal. The measurement of the pH variation concerning the L/S ratio, solvent concentration, particles size and the extraction time were the study parameters for the extraction operations. It has been assumed that grinding the slag before extraction would require additional energy consumption as highlighted by various previous studies on this subject (Rahmani *et al*., 2018).

It was assumed in this work that the extraction in several stages of untreated slag may be a less expensive step and could facilitate the solid-liquid separation. The construction of the McCabe and Thiele diagram was used to determine the number of stages required for extraction. The general model of McCabe and Thiele diagram construction was described on Figure 10 which is combination of experimental values explaining the variation of extracted element in different phases (liquid and solid). The principle of extraction is based on the distribution of the solute between the two phases as a function of its affinity for one or other (Amania *et al*., 2000). Extraction is in most cases less expensive and allows recovering of metal without the requirement of a prior concentration of the mineral to be treated (Habashi *et al*., 2017). There is therefore a distribution of the metal species in the two phases in equilibrium which is reached when the ions do not pass from one phase to the other. When equilibrium is reached the two phases are separated.

This could be summarized as follow:

-       Extraction of ion from the matrix composed of several other elements by mixing it with an appropriate solvent

-       Phase separation (solid / liquid).The solution contains the extracted metal and the solid is depleted.

The extraction can be done in several identical stages. A high concentration of the solvent promotes the extraction but the solubility of the metal in this solvent limits the expansion of its extraction (Habashi *et al*., 2017). The pH is also a parameter which increases the extraction of metal while it is necessary to work at a pH below the pH of chemical decomposition of solute by water (hydrolysis). The pH is a function of the concentration of the solvent mixed with the solid contained in the metal (Amania *et al*., 2000; Habashi *et al*., 2017). The extraction is a surface reaction and therefore takes place at the liquid/solid interface, which leads to the use of a large dispersion of the solid in the liquid to ensure efficient extraction. The contact of these two phases is carried out in a suitable reactor (beaker, Erlen meyer or balloon in the laboratory, mixer settler for the factories) (Amania *et al*., 2000). The distribution of the solute between the two phases is characterized by the extraction coefficient (E) from which we can draw a curve (M^{n+}) solvent = f $[(M^{n+})]$ residue $(M^{n+}$ is metal ion), which is called "equilibrium isotherm" and shows the different values of the extraction coefficient graphically (Rane *et al*., 2006). The equilibrium isotherm is established in a graph giving the concentration of the solute in the solvent as a function of that in the balance at equilibrium.

During the laboratory tests, the isotherm is obtained from the different L/S ratio until the equilibrium is reached for each of them for defined parameters such as the temperature and the concentration of the solvent. The general configuration of the extraction circuit depends on operational costs and investment in capital (Otto *et al*., 1991).

The plot of the Mc Cabe and Thiele diagram is therefore a mathematical concept that would not only determines the number of extraction stages but also uses for the establishment of certain technical keys values of the extraction process such as the limiting concentration of the solute in the starting solvent (Rane *et al*., 2006). Indeed, this plot is based on the variation of the proportion of the element to be extracted in the filtrate (y) and in the residue (x) which varies according to the L/S ratio between the solvent and the solid containing the element to extract. The equilibrium isotherm which is a curve generated by this variation $y = f (x)$ therefore has the origin defined by the proportion in element to be extracted in the solvent ($y_{n + 1}$) and $x_1 = 0$ for n; the number of extraction stage, because at the beginning of the operation the residue is not yet formed (Lee *et al*., 2000).

All the points of the curve therefore represent an equilibrium (there is no longer any exchange between the solid phase and the liquid phase) extraction at a L/S ratio fixed. These points also determine a proportion of the solute in the liquid phase relative to that remaining in the extraction residue (Lee *et al*., 2000; Rane *et al*., 2006). On the other hand, the line passing through the points expressing the beginning and the end of the extraction and having the slope of the S/L ratio is called the working line because it passes through the operating set points which provide the proportions of the solute in the solvent and in the residue before and after extraction (Mathias *et al*., 2009).

The combination of the two graphs allows the trace of the diagram called McCabe and Thiele diagram, which makes it possible to determine the number of extraction stages necessary to reach the extraction set point with a solvent of defined concentration, a fixed S/L ratio who is the slope of the working line and a solute concentration in the starting solvent (Lee *et al*., 2000; Mathias *et al*., 2009). The variation of one of the defined parameters thus causes a transformation in the representative plot of the diagram.

For example when the proportion of element to be extracted in the starting solvent is no longer equal to zero as it is the case when a recycling solvent is used, the origin of the equilibrium isotherm changes and consequently the slope of the straight line changes for the same operating instruction which would also cause a number of extraction stages different for certain cases (Rane *et al*., 2006; Mathias *et al*., 2009).

It follows that the proportion of solute in the starting solvent influences the progress of the extraction operation. The increase of the latter could reach a value from which the working line would hardly correspond with the equilibrium isotherm, which would therefore make it impossible to plot the McCabe and Thiele diagram because no combination would be possible between the equilibrium isotherm and the working line to determine the number of extraction stages required (Mathias *et al*., 2009). This would physically mean that there will be no extraction with a starting solvent containing that value of solute; the equilibrium is already established between the proportions of the element extract in the two phases, the liquid phase is saturated with solute. The illustrations of all the above could be provided by the graphs below finally to better elucidate the concept; in the process of extracting an element from a solid phase to a liquid phase, isolating a step on which an equilibrium is established, this follows;

- S and L are the mass (or volume) flow rates of slag and solvent
- R and E are the mass flows (or volume) of extraction residues and the rich filtrate
- The calcium portions in are expressed by the mass ratio X_S (slag sample), X_R (in the residue), Y_L (in the feed solvent liquid) and Y_E (in the filtrate).
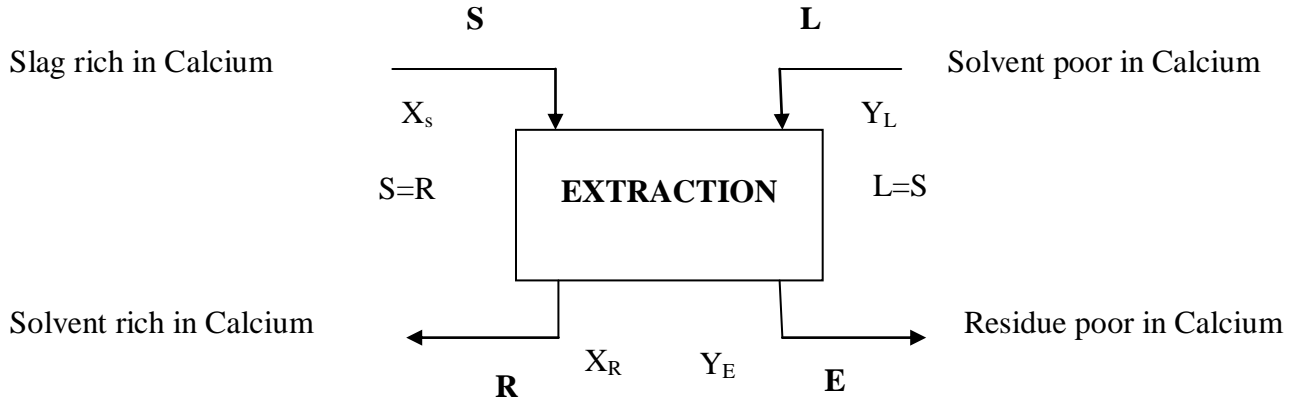
Figure 9: masse balance representation on extraction stage in equilibrium

The mass balance equations are as follows:

- Slag sample / Liquid solvent balances S = R and L = E

- Calcium mass balance:

$$SX_s + LY_L = RX_R + EY_E \qquad (4)$$

$$S(X_S - X_R) = L(Y_E - Y_L) \qquad (5)$$

$$\frac{S}{L} = \frac{(Y_E - Y_L)}{(X_S - X_R)} \qquad (6)$$

$$Y_E = \frac{S}{L}(X_s) - \frac{S}{L}(X_R) + Y_L \qquad (7)$$

Equation 7 above shows that at equilibrium X_R and Y_E follows the equation of a straight line passing through the point (X_S, Y_L) after n extraction stage. Starting from the initial point $(X_o$ and $Y_{n+1})$ this equation becomes;

$$SX_0 + LY_{n+1} = SX_n + LY_n \qquad (8)$$

$$\frac{S}{L} = \frac{(Y_n - Y_{n+1})}{(X_0 - X_n)} \qquad (9)$$

The line passing through the points (X_o, Y_n) and (X_n, Y_{n+1}), Equation (8) can, therefore, be written as:

$$Y_{n+1} - Y_n = \frac{S}{L}(X_n - X_0) \qquad (10)$$

50

The number of extraction stages can be better defined by other studies using analytical methods such as those proposed by Ritcey and Ashbrook, (1984), which prove to be more accurate than the graphical method which allows us to have an insight into the extraction process. The first extraction residue undergoes other extractions under the same conditions and this extraction results in a residue deficient in calcium and a more or less rich filtrate, which was mixed with the first filtrate to be sent to the carbonation stage.

Equation (10) represents the working line and, as stated above, the equilibrium isotherm is an experimentally obtained curve expressing the proportion of the element to be extracted in the liquid phase relative to that in the solid phase. Depending on the S/L ratio, the combination of the two graphs represents the McCabe Thiele diagram shown in Figures 10- 12;

The points M and P are the two points of the working line that slope for the S/L ratio and represent the beginning and the end of the extraction operation.
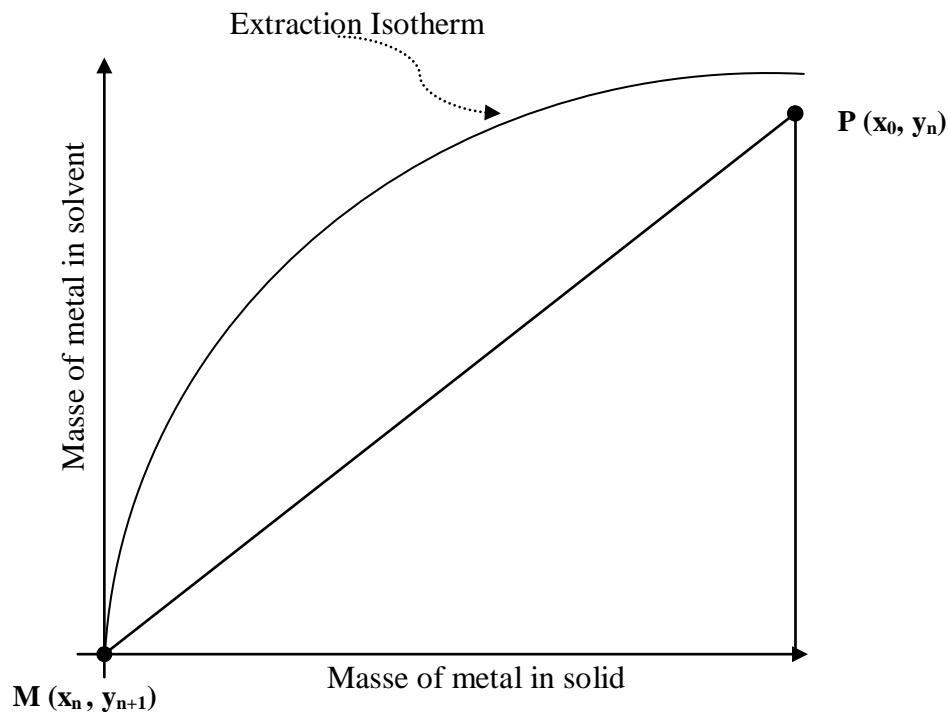
Figure 10: Plot of McCabe thiele diagram

It is therefore easier under these conditions to determine the number of extraction stages by graphing as follows;

• take a vertical straight line from the proportion of solute in the solid diet;

• at the point P, as shown in Figure 3 below, carry a horizontal to the equilibrium isotherm. It corresponds to the first extraction stage. Then, at the point of contact N, a vertical is lowered to the working line;

• go down stairs until you do not fall on the right of work.
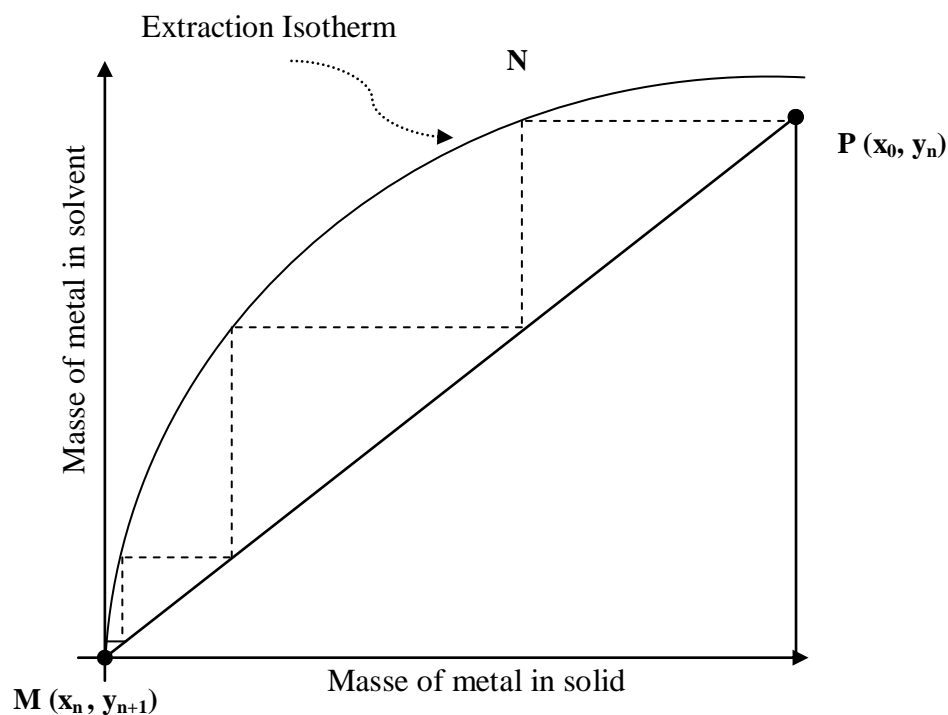
Figure 11: Determination of extraction stage number using McCabe Thiele diagram

In the case where the solvent already contains a large portion of solute; the diagram becomes;

The practical consideration of these applications makes it possible to use the plot of the McCabe and Thiele diagram for the determination of the number of extraction stages and also the limit quantity of solute in the recycled solvent.
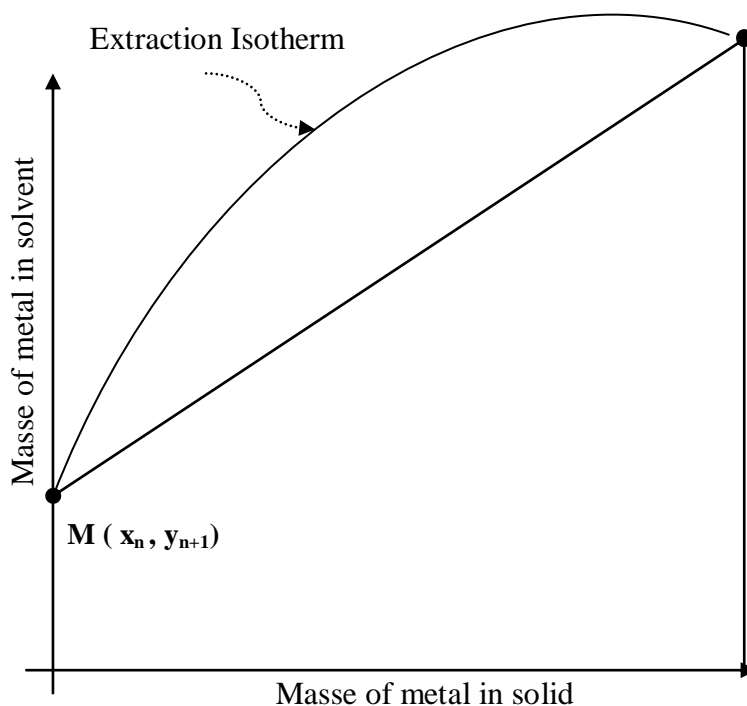
Figure 12: Presentation of McCabe Thiele diagram of
extraction when solvent is saturated

Reading of the diagram above (Figure 12) shows that there is a value of the amount of solute in the starting solvent for which the maximum point of the working line of the extraction P $(x_0; y_n)$ passing by the point $M(x_n, y_{n+1})$ which is the operating instruction for a determined Solid/Liquid ratio (slope of the line) is found at the intersection of the working line and the equilibrium isotherm, at this point and above it cannot be possible to lead any horizontal for an extraction stage(Mathias *et al*., 2009). It is therefore the limit from which there will be no further extraction possible, the solvent is saturated with solute. The experimental equilibrium isotherm was determined and used to plot the McCabe and Thiele diagrams for determination of the number of extraction stages for a defined working line. The first extraction residue undergoes other extractions under the same conditions and this extraction results in a residue deficient in calcium and a more or less rich filtrate, which was mixed with the first filtrate to be sent to the carbonation stage. The measurement of the pH variation concerning the L/S ratio, solvent concentration, particles size and the extraction time were the study parameters for the extraction operations.

2.2 Precipitation experiment

25 ml of calcium-rich filtrate from the extraction stage was mixed with 10 ml of 25% NH_4OH (pH 12.9) solution in order to raise the pH to 10.4. The raising of pH was performed with the NH_4OH solution placed in a graduated burette progressively drained into the calcium-rich solution until a pH of 10.4 was reached on the calibrated pH meter which corresponded to 10 ml reading on graduated burette. The resulting mixture was placed in a 100 ml autoclave reactor, where carbon dioxide gas at a constant and defined flow rate was injected with or not the addition of Ethylene Diamine Tetra-acetyl (EDTA 0.1M) for CO_2 absorption as a amine solution. The CO_2 gas pressure was used for agitation and was regulated by an adjustment module placed on the bottle, which, was varied from 1 to 6.5 bars to obtain an optimum precipitation yield. The precipitation time was varied from 5 minutes to 3 hours. The precipitate thus obtained was filtered, dried, weighted and analyzed (SEM and XRF analyzer) and used for AMD neutralisation. The full experimental protocol is shown in Figure 13.

2.3 AMD Treatment

The neutralization experiment was conducted by using 0.5 g of calcium carbonate produced which reacted with 450 g of acid mine drainage from Witwatersrand western basin for a measured interval of time (90 minutes). After each reaction the pH and the acidity of the AMD solution was reported to assume the effectiveness of the neutralization using the produced calcium carbonate compare to commercial calcium carbonate.
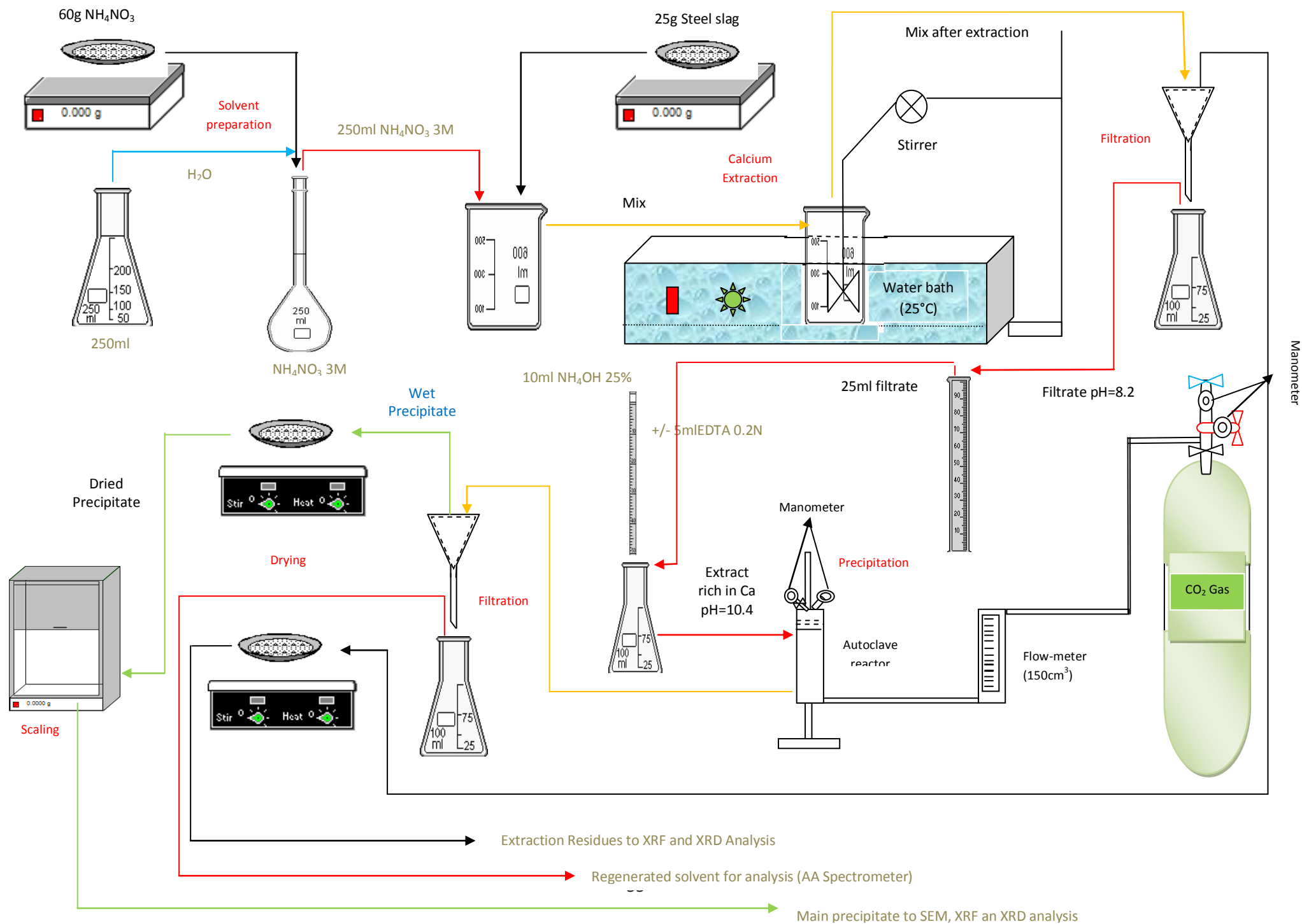
Figure 13: Experimental methodology

3. REACTIONS AND CALCULATION FORMULAS FOR EXTRACTION AND CARBONATION EXPIRIMENTS

3.1 Reactions

Dissolution of calcium:

$$CaO(s) + 2H^+ (aq) \xrightarrow{K_1} Ca^{2+} (aq) + H_2O (l) \tag{29}$$
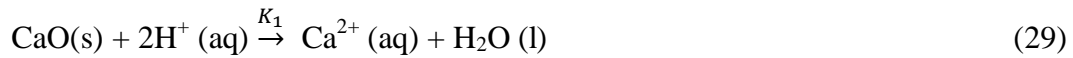
Protonation balances of solvent components:

$$NH_4^+ \underset{K_2}{\overset{K_2}{\rightleftarrows}} NH_3 (aq) + H^+ (aq) \tag{30}$$

$$HX (aq) \underset{K_3}{\overset{K_3}{\rightleftarrows}} H^+ (aq) + X^- (aq) \tag{31}$$

$$H_2O (l) \xrightarrow{K_w} H^+(aq) + OH^-(aq) \tag{32}$$

Precipitation of calcium:

$$Ca^{2+} (aq) + CO_3^{2-} \underset{K_4}{\overset{K_4}{\rightleftarrows}} CaCO_3(s) \tag{33}$$

$$Ca^{2+} (aq) + HCO_3^- \underset{K_5}{\overset{K_5}{\rightleftarrows}} CaCO_3(s) + H^+ (aq) \tag{34}$$
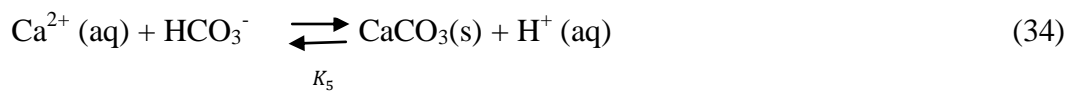
Reactions of carbon dioxide:

$$CO_2 (g) \underset{K_6}{\overset{K_6}{\rightleftarrows}} CO_2 (aq) \tag{35}$$

$$CO_2 (aq) + H_2O (l) \underset{K_7}{\overset{K_7}{\rightleftarrows}} HCO_3^-(aq) + H^+ (aq) \tag{36}$$

$$HCO_3^-(aq) \underset{K_8}{\overset{K_8}{\rightleftarrows}} CO_3^{2-}(aq) + H^+(aq) \tag{37}$$

$$CO_2 \text{ (g)} + OH^-\text{(aq)} \underset{K_9}{\overset{K_9}{\rightleftharpoons}} HCO_3^-\text{(aq)} \tag{38}$$
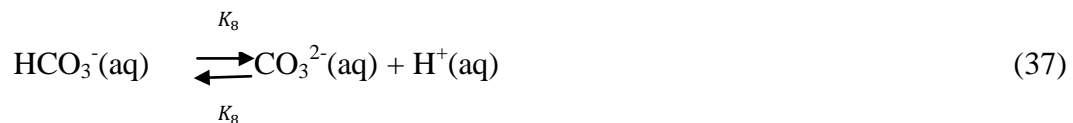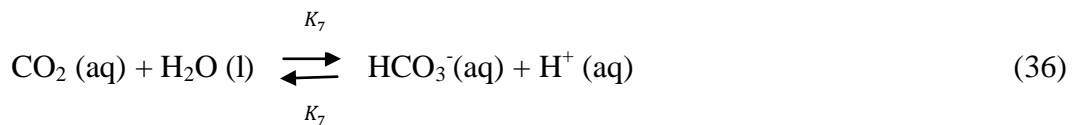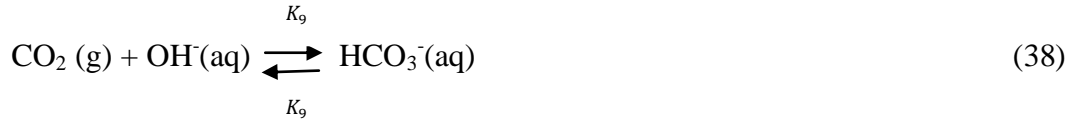
The steel converter slags mainly contain calcium oxide that is why during the extraction experiments the origin of the dissolved calcium could not be distinguished. So, all the calcium has been treated as calcium oxide in the modeling work. During calcium extraction between ammonium chloride and nitrate can be made on the basis of the protonation the corresponding acids (acidic hydrochloric acid, nitric acid represented by HX) as shown in reaction (31).

3.2 Kinetic analysis

The carbonation kinetic calculation was based on the model studied by Mattila *et al.*, (2012) which considers that the dissolved calcium is in oxide form. Starting from this reaction mechanism the calculation of the rates of dissolution of calcium and carbonation was carried out according to the Arrhenius law (11) via the following equations;

$$K_i = K_{mean,i} * exp^{\left(-\frac{E_{a,mean,i}}{R}*\left(\frac{1}{T}-\frac{1}{T_{mean}}\right)\right)} \tag{11}$$

$$K_i^- = \frac{K_i}{K_{eq,i}} \tag{12}$$

$$\frac{d[CaO_{(S)}]}{dt} = -g * K_1 * [CaO_{(S)}] * [H^+]^2 \tag{13}$$

$$\frac{d[H^+]}{dt} = -2 * K_1 * [CaO_{(S)}] * [H^+]^2 + K_2 * [NH_4^+] - \frac{K_2}{K_{2(T)}} * [NH_3] * [H^+] + K_3 * [HX] - \frac{K_3}{K_{3(T)}} * [H^+] *$$

$$[X^-] + K_5 * [Ca^{2+}] * [HCO_3^-] - \frac{K_5}{K_{5(T)}} * [H^+] + K_7 * [CO_2] - \frac{K_7}{K_{7(T)}} * [HCO_3^-] * [H^+] + K_8 *$$

$$[HCO_3^-] - \frac{K_8}{K_{8(T)}} * [CO_3^{2-}] * [H^+] \tag{14}$$

$$\frac{d[NH_4^+]}{dt} = -K_2 * [NH_4^+] + \frac{K_2}{K_{2(T)}} * [NH_3] * [H^+] \tag{15}$$

$$\frac{d[NH_3]}{dt} = +K_2 * [NH_4^+] - \frac{K_2}{K_{2(T)}} * [NH_3] * [H^+] \tag{16}$$

$$\frac{d[X^-]}{dt} = +K_3 * [HX] - \frac{K_3}{K_{3(T)}} * [H^+] * [X^-] \tag{17}$$

$$\frac{d[HX]}{dt} = -K_3 * [HX] + \frac{K_3}{K_{3(T)}} * [H^+] * [X^-] \tag{18}$$

$$\frac{d[CO_3^{2-}]}{dt} = -K_4 * [Ca^{2+}] * [CO_3^{2-}] + \frac{K_4}{K_{4(T)}} + K_8 * [HCO_3^-] - \frac{K_8}{K_{8(T)}} * [CO_3^{2-}] * [H^+] \tag{19}$$

$$\frac{d[HCO_3^-]}{dt} = -K_5 * [Ca^{2+}] * [HCO_3^-] - \frac{K_5}{K_{5(T)}} * [H^+] + K_7 * [CO_2] - \frac{K_7}{K_{7(T)}} * [HCO_3^-] * [H^+] - K_8 *$$

$$[HCO_3^-] + \frac{K_8}{K_{8(T)}} * [CO_3^{2-}] * [H^+] + K_9 * [CO_2] * [OH^-] - \frac{K_9}{K_{9(T)}} * [HCO_3^-] \tag{20}$$

$$\frac{d[CO_{2(aq)}]}{dt} = +K_6 * [CO_{2(g)}] - \frac{K_6}{K_{6(T)}} * [CO_{2(aq)}] - K_7 * [CO_{2(aq)}] + \frac{K_7}{K_{7(T)}} * [HCO_3^-] * [H^+] \tag{21}$$

$$\frac{d[CO_{2(g)}]}{dt} = 0 \tag{22}$$

$$[H^+] * [OH^-] = K_w \tag{23}$$

The reversible dissolution of the calcium in the ammonium salt has been divided into reactions (30) and (31) whereas the absorption of CO_2 is represented by reaction (35) and (38). The equilibrium constant (k_{eq}) and the heat (enthalpy) of the reactions were estimated using HSC Chemistry 5.11 (Hannu-Petteri *et al.*, 2012). In HSC chemistry the activity constants are considered equal to 1, and the activities are represented directly by the concentration ($a_i = c_i$).

By comparing the precipitation reactions (33) and (34), we find that only the bicarbonate ions play an important decisive role essential in the equilibrium reaction (35).

Starting from equationss (29) - (38) by modifying the concentrations of compounds as a function of time, the process described by equations (13 to 23) above in which the reaction rate coefficient is calculated using equation (11) according to the modified Arrhenius law(Hannu-Petteri *et al.*, 2012). Unlike the original Arrhenius equation, the kinetic parameters are adapted to the

temperature range. The constant equilibrium k_{eq} for reaction (Table17) was used to calculate the inverse reaction rate coefficient according to Equation (12). The parameter g in equation (13) has been included to adapt the particle size of the slag particles to the rate of calcium extraction. For the physical absorption of CO_2 (22) the parameters K_{mean} and E_{mean} should be interpreted respectively as pre-exponential factor and apparent activation energy. Equation (22) was deduced taking into account the fact that the concentration of the gas in the reaction remains constant.

However, one should be careful that this is not the case at the beginning of the reaction when the gas is introduced into the liquid, or it diffuses gradually, resulting in the rapid mass transfer of carbon dioxide into the solution. As shown in Equation (23), the autoprotolysis reaction of water is always in equilibrium.

3.3 Calcium extraction and carbonation yield

The calcium extraction yield was calculated by relating the calcium contained in the filtrate to the total calcium contained in the primary steel slag sample. The equation (24) was used to calculate the conversion yield of Ca to $CaCO_3$, and it was assumed that only the calcium contained in the post-extraction solution was carbonated and that there was no loss:

$$\%Ca = \frac{\text{Ca content in the filtrate} * \text{mass of the filtrate}}{\text{Ca content in slag} * \text{mass of slag}} \text{x100} \qquad (24)$$

$$\%Ca \text{ converted} = \frac{\text{Ca content in precipite} * \text{mass of precipitate}}{\text{Ca content in slag} * \text{mass of slag}} \text{x100} \qquad (25)$$

The amount of carbon dioxide captured by this reaction is determined as follows:

$$\text{CO}_2 \text{ sequestration} = \sum_i^n \frac{(p_{co2\ in} - p_{co2\ out})Q\Delta t}{MTR} \tag{26}$$

In this equation P_{CO2} in and P_{CO2} out, denotes the mean value of P_{CO2} (atm) at the input and the output, respectively, Q and Δt are the flow rate (min^{-1}) and the time interval (min), respectively, R gives the gas constant (0.082057 L.atm.mol^{-1}K^{-1}), M and T are the mass of precipitate (g) and the temperature (K), respectively.

The carbonation yield was calculated using the following formula:

$$\text{Carbonation yield} = \frac{\text{Mass CaCO}_3 \text{ precipitate} * 100}{\text{Concentration [Ca]} * \text{Volume filtrat} * 40} * 100 \tag{27}$$

3.4 Energy needed

The calcium extraction yield may be increased by grinding the coarse particles contained in the first steel slag to increase the contact area of the particle with the ammonium solution. The grinding energy required may be estimated using the Bond's formula as follows:

$$W = 0.01W_1 \left(\frac{1}{\sqrt{d_1}} - \frac{1}{\sqrt{d_0}} \right) \tag{28}$$

Where: W represents the energy required to reduce a particle of dimension d_0 to dimension d_1 and W_1 the experimental work index of the steel slag in Kwh/t. In our case, the work index was 12.2 (Doering international, 2015). By adding to equation (24) the over grinding due to crushing of the particles that have already reached the optimal dimension for calcium extraction which was experimentally found to be 125 µm, then the equation becomes:

$$W = 0.01W_1 \left(\frac{1}{\sqrt{d_1}} - \frac{1}{\sqrt{d_0}} \right) + \sum W_s \tag{29}$$

Where W_s represents the over grinding energy of fine and ultrafine particles.

4. CHEMICAL ANALYSIS

The chemical composition of the solid samples (untreated slag, different particle size fractions, extraction residues and precipitate) was determined out using the X-Ray fluorescence (XRF) to determine the contents of each constitutive chemical element of the samples analyzed.

The chemical elements contained in the extraction and precipitation filtrates were determined using the atomic absorption spectrophotometer (Agilent AA 100). The precipitates obtained were analyzed by scanning electron microscopy (SEM) to determine the morphology and the atomic composition of the various constituent elements. The solution regenerated was analyzed by absorption spectrophotometer AA in order to determine its calcium content.

CHAPTER IV RESULTS AND DISCUSSIONS

1. MINERAL CHARACTERIZATION OF THE SLAG

TABLE 5: CHEMICAL COMPOSITION OF THE MAJOR ELEMENTS OF THE STEEL SLAG OBTAINED BY XRF ANALYSER

Element	% Content
SiO_2	17.29
Al_2O_3	3.72
Fe_2O_3	2.26
FeO	18.26
MnO	0.89
MgO	6.32
CaO	37.68
Na_2O	0.01
K_2O	0.04
TiO_2	1.96
P_2O_5	0.22
Cr_2O_3	0.42
NiO	0.01

Analysis of the table above showing the results of the XRF analyzer, it is clearly detected that calcium is the dominant constituent in the sample of steel slag with a content of 37.68 in the form of calcium oxide followed by iron and silicon which are in the form of FeO, Fe_2O_3 and SiO_2 with respective contents of 18.26, 2.26 and 17.29. The high calcium contained of the steel slag sample allows testing experiment of calcium extraction.

TABLE 6: PARTICLE SIZE DISTRIBUTION OF STEEL SLAG PARTICLES

Dimension (µm)	Mass refusal (g)	% Refusal	% Cumulated passing
4000	0	0.00	100
2800	0.6	0.06	99.94
2000	79.61	8.06	91.88
1400	89.69	9.08	82.80
1180	41.4	4.19	78.60
850	73.18	7.41	71.19
600	81.92	8.29	62.90
425	58.7	5.94	56.96
300	81.36	8.24	48.72
212	77.34	7.83	40.89
180	48.41	4.90	35.99
150	40.61	4.11	31.87
125	45.07	4.56	27.31
106	44	4.46	22.85
+75	64.51	6.53	16.32
-75	161.2	16.32	0

Particles size distribution presented in Table 6 above has shown that the sample is composed by many different size of particle. Except for on 4000 µm sieve size, there are refusals on all other sieves sizes. It is therefore important to find the more representative size which will give a general overview of sample size. The P80 represent the size of the sieve which allows passing of 80 % of the bulk materiel and was calculated by using the Equation (3). This size has well defined the represented sample and has been used for calculation of energy for grinding. The particle size distribution permitted also to set the calcium distribution on different range.
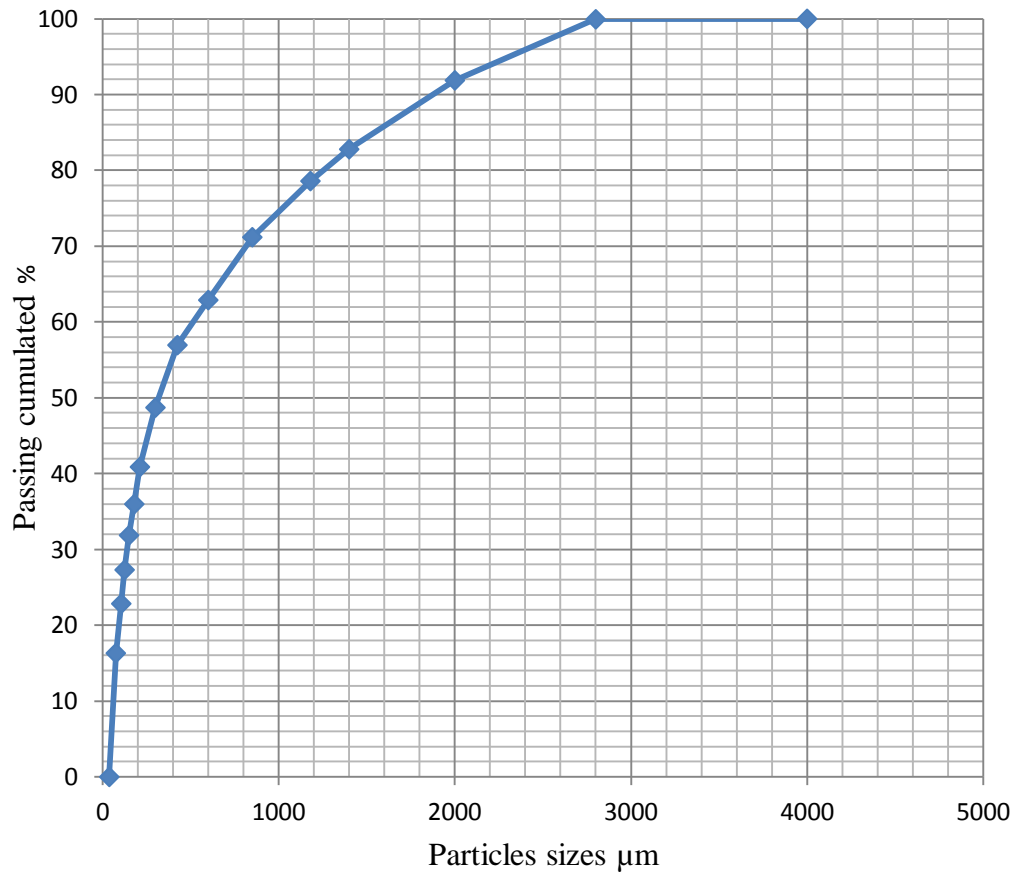
Figure 14: Particle size distribution curve of steel slag particles

The particle size distribution of steel slag was represented in Table 6 and shown on the graph in Figure14 above. The P80 calculated was 1247.22 µm, and the distribution of calcium into two distinct ranges of particle size fractions is further shown in Tables 7, 8 and 9 given by XRF analysis.

TABLE 7: CHEMICAL COMPOSITION OF THE MAJOR ELEMENTS OF
STEEL SLAG PARTICLES HAVING A SIZE BETWEEN 125 AND 300 μm

Element	SiO_2	Al_2O_3	Fe_2O_3	FeO	MnO	MgO	CaO	Na_2O	K_2O	TiO_2	P_2O_5	Cr_2O_3
(%)	17.16	3.65	1.6	12.92	0.86	6.3	40.66	0.01	0.03	1.53	0.23	0.34

TABLE 8: CHEMICAL COMPOSITION OF THE MAJOR ELEMENTS OF
STEEL SLAG PARTICLES HAVING A SIZE SMALLER THAN 125 μm

Element	SiO_2	Al_2O_3	Fe_2O_3	FeO	MnO	MgO	CaO	Na_2O	K_2O	TiO_2	P_2O_5	Cr_2O_3
(%)	13	3.19	1.23	9.92	0.79	8.99	39.8	0.01	0.01	1.01	0.19	0.29

The dry steel slag sample contains 37.68% CaO (26.91% calcium) 2.26% Fe_2O_3, 18.26% FeO

(15.78% Fe) and 17.29% SiO_2 (8.06% of silicon). Other elements such as magnesium (3.81%)

and manganese (0.68%) are present but at low levels.

The distribution of calcium in the slag is described in Table 9 below:

TABLE 9: CALCIUM DISTRIBUTION IN DIFFERENT PARTICLE SIZE
RANGES OF THE STEEL SLAG

Particles size range	CaO (%)	Ca (%)
X= main slag	37.68	26.91
X >300 μm	18.12	12.94
125 μm < X<300 μm	8.70	6.21
X<125 μm	10.86	7.75

X: particle size.

The moisture content of the fresh slag sample was determined by the ratio of the mass of the dry

sample obtained after 3 hours of drying in an oven at 150 °C to the mass of the fresh sample

using Equation (1). The average mass of the fresh sample and dried sample was 1245 g and 1232

g respectively.

The moisture of the slag was, therefore:

$$\%H = \frac{1245 - 1232}{1245} * 100 = 1.04\%$$

The results in Table 9 had shown a large amount of calcium in the particles having a size less than 300 μm.

2. CALCIUM EXTRACTION FROM BOF STEEL SLAG

The results in Table 10 show that calcium extraction efficiency was more than 70% when the L/S ratio was more than 30 for NH_4NO_3 and NH_4Cl extracting solution with a concentration of 3M as also shown in Figure 15. These results imply large equipment for extraction, which may be expensive for industrial applications. We further investigated the effect of particles size and extraction stages number for an efficient extraction at lower L/S ratio in order to have a calcium extraction economically feasible at industrial level. However calcium extraction experiments of the steel slag were carried out on an ungrinded received sample (- 4000 + 38μm). The size is an essential parameter if residues would be used such as aggregate in construction. The results obtained by spectrophotometer (AA-100) analysis of extraction filtrates showed that a large amount of calcium was extracted using 3M concentration for both solvents (Table 10). The results showed in Figure 15 that calcium is more extracted when using NH_4NO_3 than NH_4Cl solution.

TABLE 10: CALCIUM EXTRACTION FROM STEEL SLAG EFFICIENCY AS FUNCTION OF SOLVENT CONCENTRATION AND LIQUID /SOLID RATIO

Ratio L/S(ml/g)	Solvent concentration (mole/l)	Calcium extracted using NH_4NO_3 (g)	Calcium extracted using NH_4Cl (g)	Calcium extracted yield using NH_4NO_3 (%)	Calcium extracted yield using NH_4Cl (%)
75/50	2	0.020	0.018	0.295	0.260
100/50		0.029	0.024	0.426	0.361
125/50		0.036	0.034	0.540	0.510
150/50		0.044	0.040	0.649	0.592
75/50	2.5	0.023	0.020	0.335	0.300
100/50		0.030	0.027	0.452	0.404
125/50		0.039	0.035	0.581	0.520
150/50		0.048	0.043	0.721	0.639
75/50	3	0.025	0.022	0.372	0.326
100/50		0.034	0.031	0.511	0.454
125/50		0.048	0.040	0.716	0.601
150/50		0.082	0.073	1.217	1.084
125/25		2.150	1.446	32.000	21.518
175/25		3.158	2.756	46.990	41.016
250/25		3.927	3.475	58.430	51.711
200/10		1.829	1.618	68.254	60.373
250/5		1.140	1.077	85.037	76.642
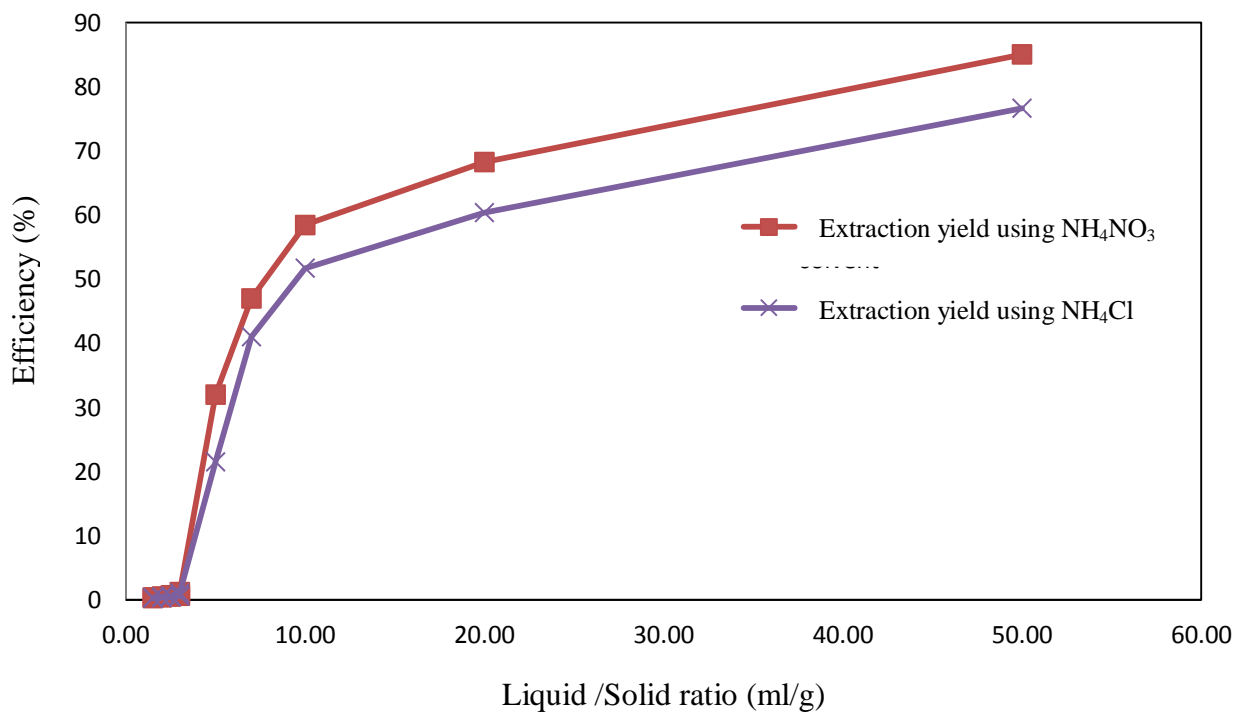
Figure 15: Calcium extraction efficiency from steel slag versus L/S ratio using 3M concentration of solvent

TABLE 11: VARIATION OF CALCIUM EXTRACTION YIELD AND pH FROM BOF STEEL SLAG AS FUNCTION OF TIME AND SOLVENT

Time (Min)	NH_4NO_3(3M)			NH_4Cl(3M)		
	Mass Ca extract (g)	%Ca	pH	Mass Ca extract (g)	%Ca	pH
0	0	0	0	0	0	0
5	4.63	68.83	8.93	3.29	60.99	8.29
10	4.48	66.65	8.86	3.18	58.84	7.68
15	4.40	65.52	8.78	3.21	59.47	7.32
25	4.39	65.39	8.75	3.04	56.28	6.49
40	4.45	66.24	8.48	3.13	57.88	5.98
60	4.64	69.01	8.2	3.24	60.06	5.88

The results of the Table11 show that not only high calcium extraction yields were achieved after 5minutes, but also at higher reaction time other impurities precipitated in hydroxide form favors by the basic pH in of the solution, it follows that the impurities such as iron which is found in large quantities in the sample of steel slag precipitated as hydroxide after their oxidation when the reaction continues in this basic medium because the analysis extraction solutions after 5 min show a large amount of iron compared to those obtained after 60 min reaction. Results also show that calcium extraction reached a plateau at 60 minutes and that extraction with ammonium nitrate was more efficient than ammonium chloride.
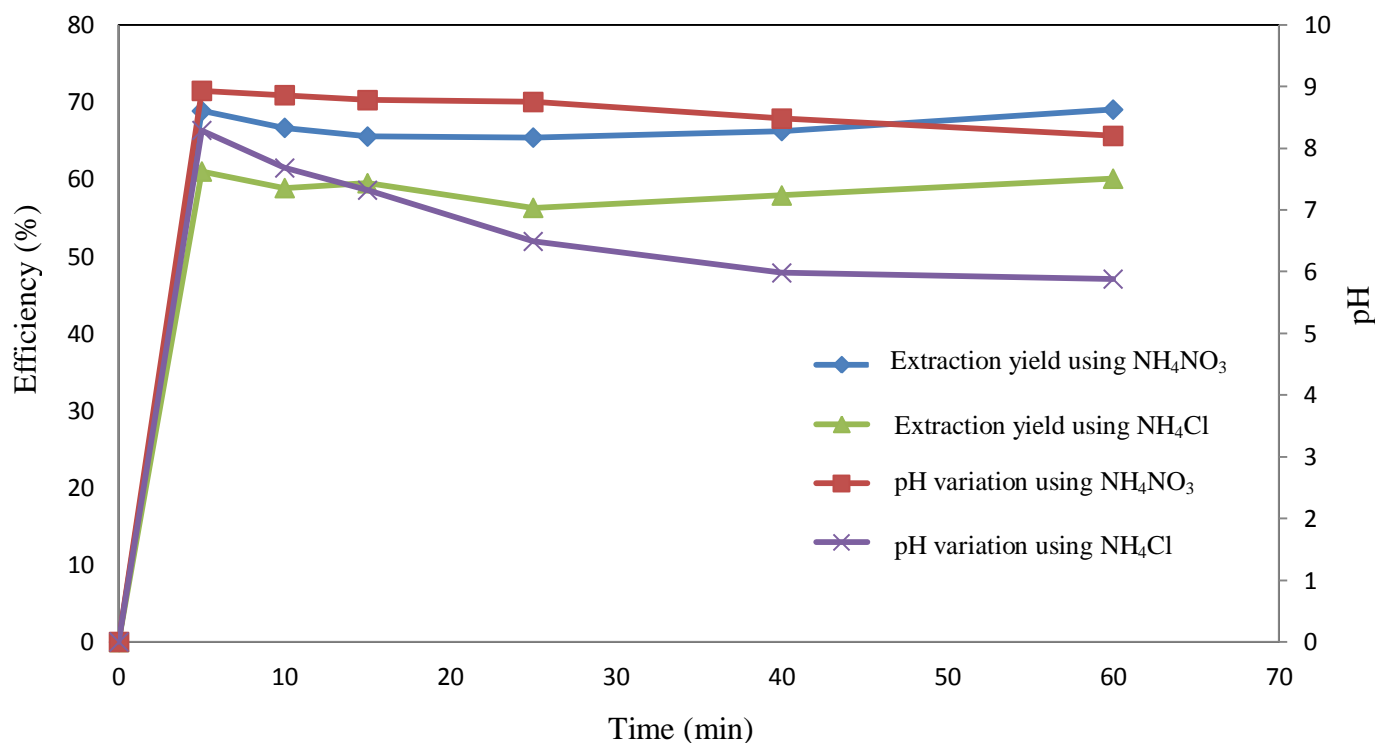
Figure 16: Extraction yield versus time and pH

TABLE 12: CALCIUM EXTRACTION FROM STEEL SLAG EFFICIENCY AS FUNCTION OF PARTICLES SIZE USING L/S RATIO OF 10

Steel slag Particle size (X)	Mass calcium extracted using NH_4NO_3 solvent (g)	Mass calcium extracted using NH_4Cl solvent (g)	Extraction efficiency using NH_4NO_3 solvent (%)	Extraction efficiency using NH_4Cl solvent (%)
X<75 µm	4.99	4.79	87.97	82.68
X<125 µm	4.85	4.48	85.35	78.87
[125µm, 300 µm]	3.63	3.4	62.52	58.62
X>300 µm	1.48	1.28	58.77	50.79

The results in Table 12 above show that 85% extraction efficiency was reached with particles of slag smaller than 125 µm and L/S ratio of 10. It may be therefore necessary to grind the steel slag to a size less than or equal to 125 μm to achieve an extraction yield higher than 85% using a L/S ratio of 10 for 60 min at 25°C with NH_4NO_3 or NH_4Cl solvents with a concentration of 3 mol/l (Figure 17).
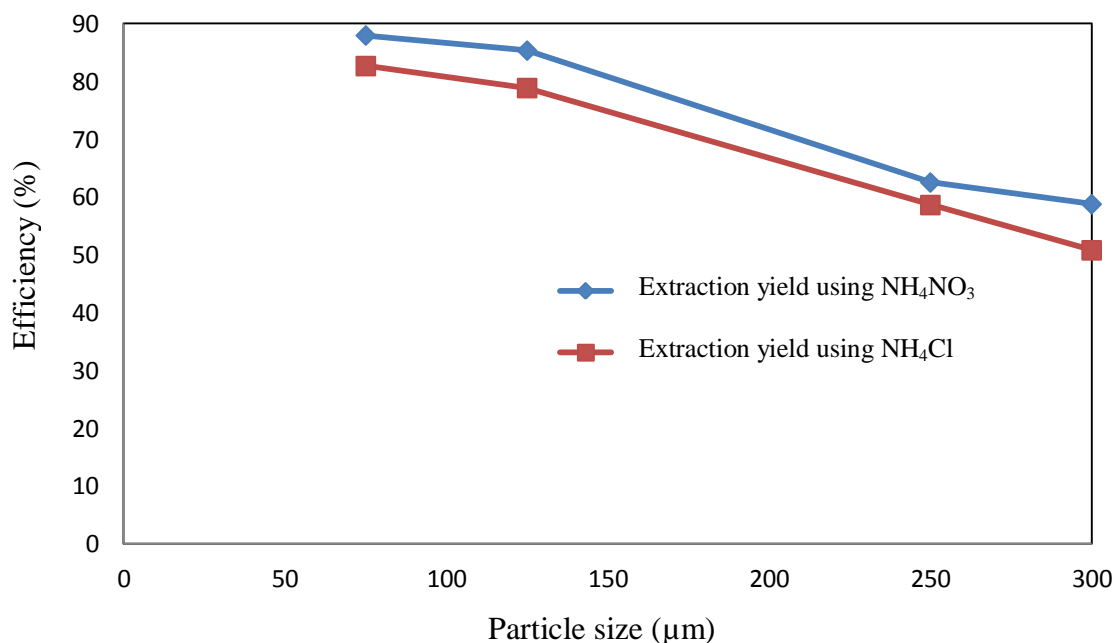
Figure 17: Calcium extraction efficiency from steel slag versus particle size

TABLE 13: CHEMICAL COMPOSITION OF STEEL SLAG RESIDUS FROM EXTRACTION

Sample	SiO_2 (%)	Al_2O_3 (%)	Fe_2O_3 (%)	MnO (%)	MgO (%)	CaO (%)	Na_2O (%)	K_2O (%)	TiO_2 (%)	P_2O_5 (%)	Cr_2O_3 (%)	NiO (%)
L/S=5/1 Ungrinded steel slag	21.81	5.91	34.43	1.5	9.71	22.55	0	0.03	3.12	0.53	0.62	0.02
L/S=10/1 Ungrinded steel slag	25.72	7.17	33.34	1.32	10.25	18.17	0	0.02	2.73	0.45	0.64	0.02
Steel slag size >125µm	21.49	6.82	37.67	1.92	9.61	15.04	0.69	0.01	3.06	1.35	0.59	0.02
Steel slag size <125µm	20.12	6.68	46.22	1.83	13.53	7.96	0.54	0.02	2.36	0.29	0.43	0

XRF analysis of calcium extraction residues are provided in Table 13. Calcium extraction data for different liquid/solid ratios were used to draw the equilibrium isotherm and the operational line using Equation (10) above. The values of x_n and y_n, which are respectively the amount of calcium in the extraction residue and the solvent at the end of extraction, were determined. The McCabe and Thiele diagram was then constructed by considering; i) the solvent used is pure (does not contain calcium $y_{n+1} = 0$) (Figure 15-18); ii) the solvent used is a regenerated solution that contains at least 15% of calcium ($y_{n+1} \geq 1$) compared to calcium contained in the solid, and where x_0 represents the calcium content in the primary sample before the beginning of extraction (Figure 22-26). The McCabe and Thiele diagram was then used to determine the number of stages required for a given extraction. The lowest L/S ratio for extracting at least 50% of calcium was determined to 10/1.

The number of extraction stages using 3M NH_4NO_3 at different L/S ratios ranging from 10/1 to 50/1 (corresponding to working slopes of 0.1 to 0.02) were determined to be 2 for a L/S ratio of 10/1 (Figure 18) and 1 for a ratio of 50/1 (Figure19).

Whereas the number of extraction stages remained constant at 2 for both L/S ratio of 10/1 and 50/1 when using NH_4Cl as the extracting solution as shown in Figures 20 and 21. The above results corroborate the fact that the use of NH_4NO_3 as calcium extracting solution may contribute to reducing the number of extraction stages required. The points (x_a, y_a) and (x_b, y_b) in Figures indicate the calcium contents in the two phases at each extraction step (first stage =A, second stage=B). The examination of (x_a, y_a) and (x_b, y_b) coordinates show that the use of two extraction stages produces a residue containing less than 4% of calcium and the filtrates of first extraction stage using NH_4NO_3 contain more calcium than when using NH_4Cl.
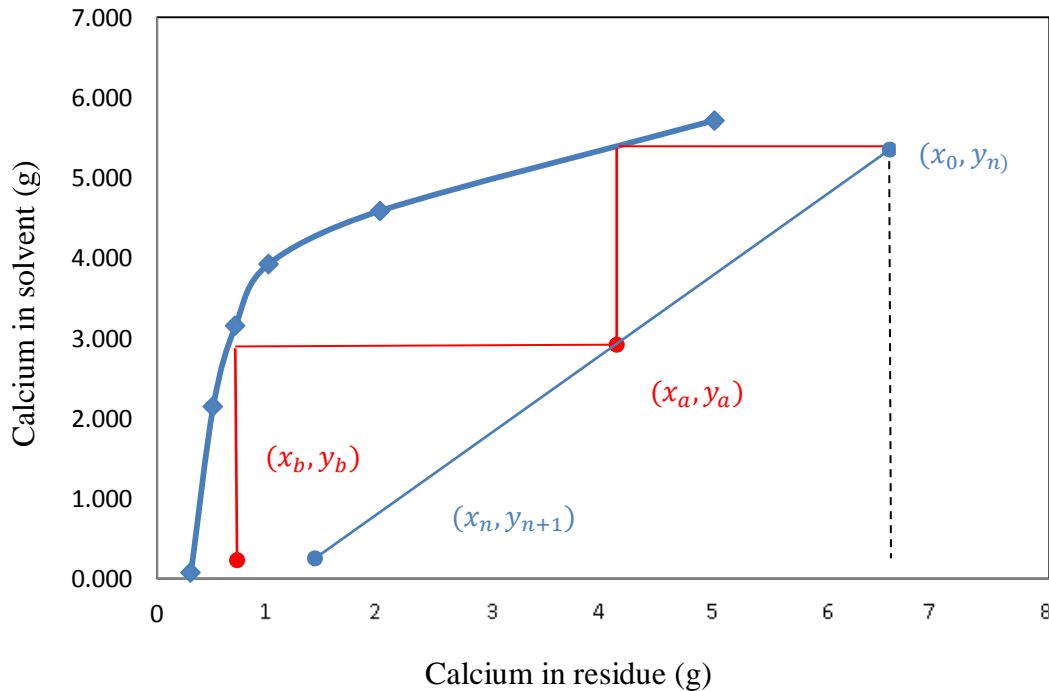
Figure 18: Mc Cabe and Thiele diagram of calcium extraction using 3 M NH_4NO_3 s and a steel slag-solvent ratio (L/S) of 10/1
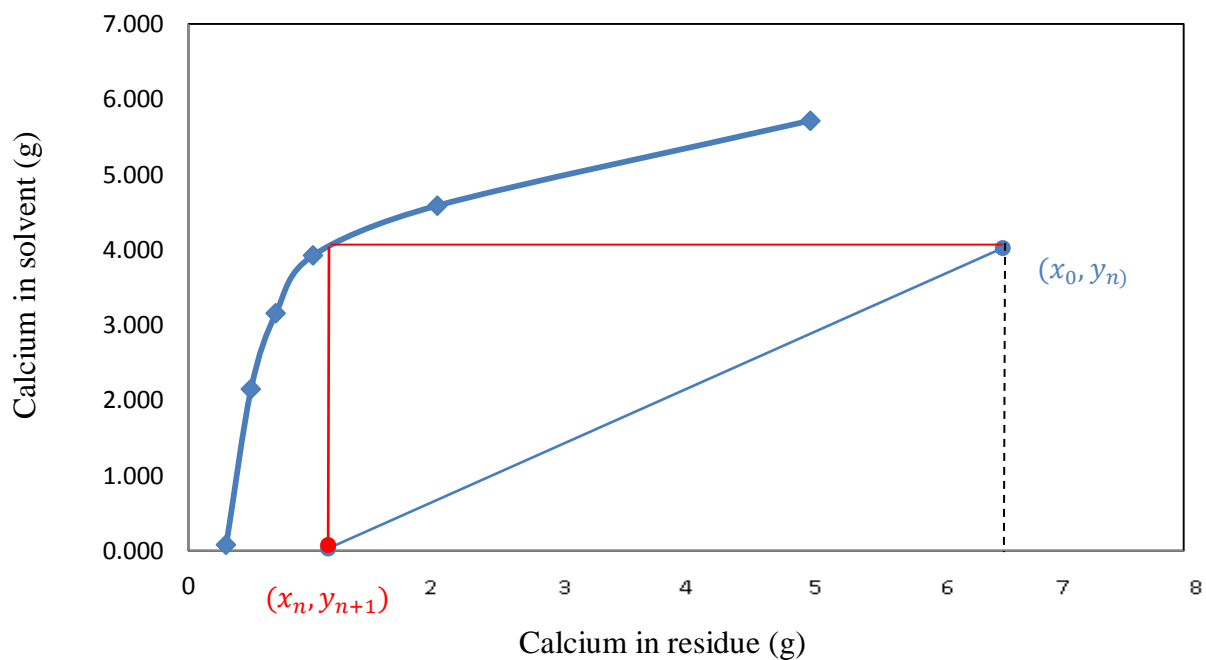
Figure 19: Mc Cabe and Thiele diagram of calcium extraction using 3 M NH_4NO_3 s and a steel slag-solvent ratio (L/S) of 50/1
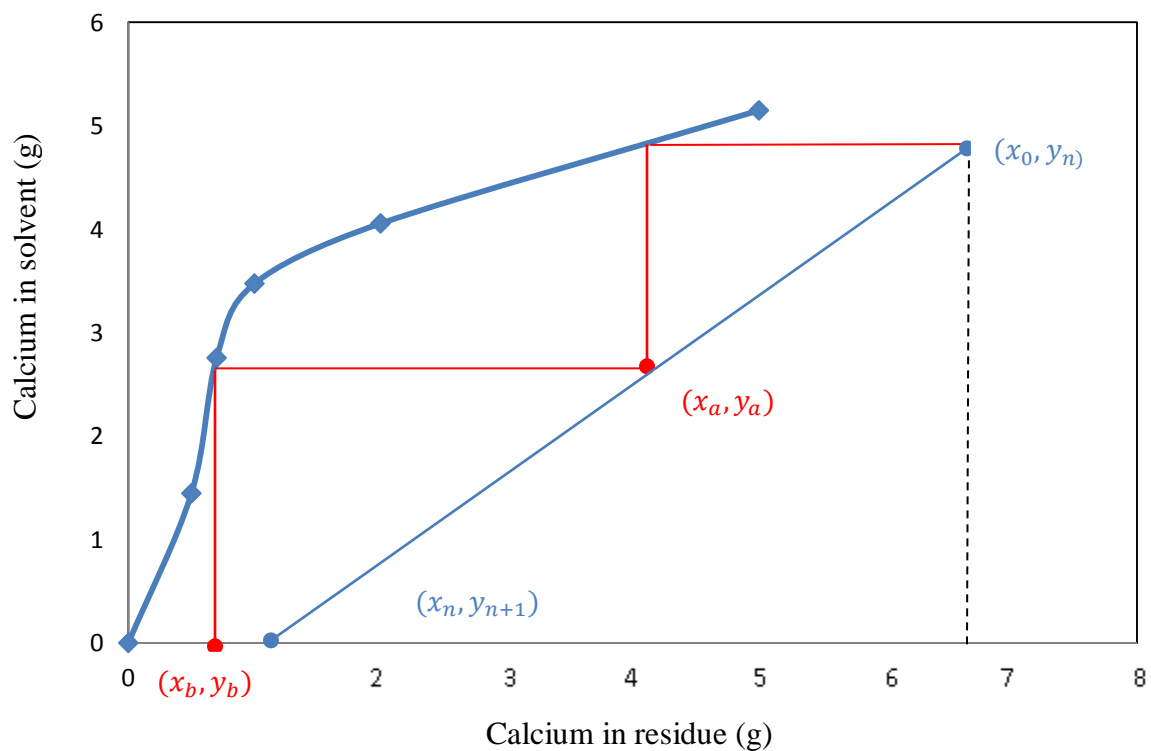
Figure 20: Mc Cabe and Thiele diagram of calcium extraction from steel slag using pure 3 M NH_4Cl solvent and a steel slag-solvent ratio (L/S) of L/S =10/1
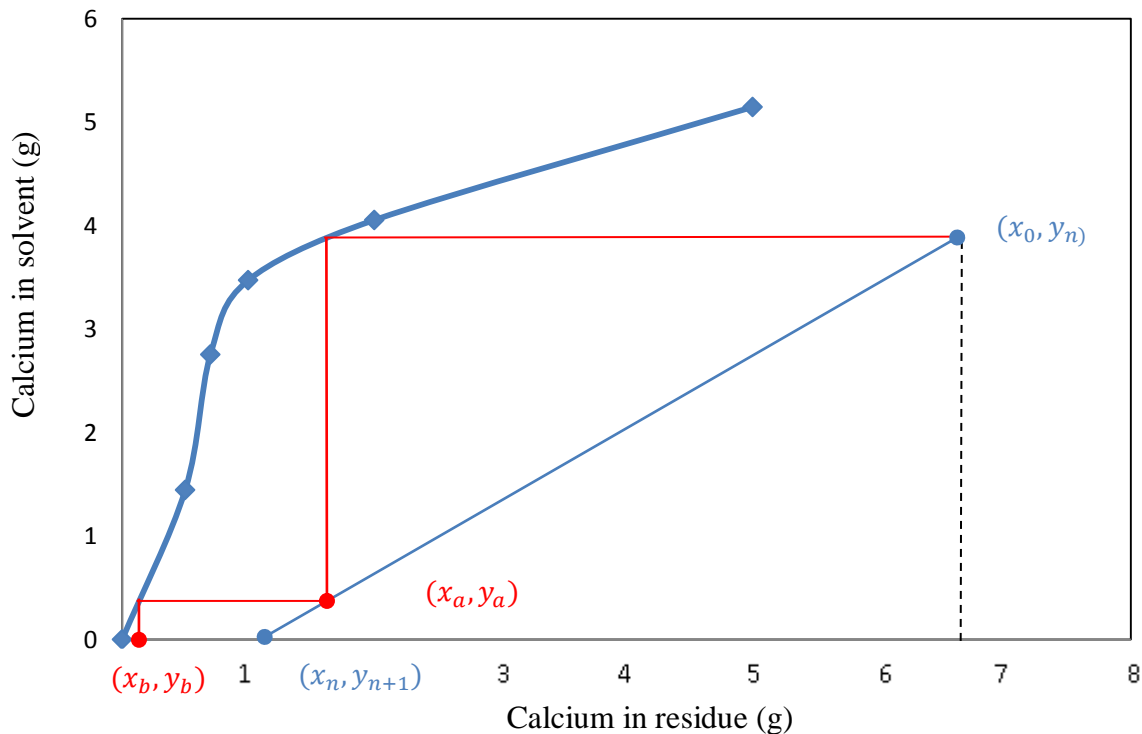
Figure 21: Mc Cabe and Thiele diagram of calcium extraction from steel slag using pure 3 M NH_4Cl solvent and a steel slag-solvent ratio (L/S) of 50/1

The possibility of the reuse of the regenerated solvents was further assessed at the end of the carbonation "step". An extraction step was found as the required extraction to achieve a calcium content of 70%. The number of extraction stages using "used" NH_4NO_3 or NH_4Cl (~Ca≤4g/l) as solvents for different L/S ratios ranging from 10/1 to 50/1 were also determined by the construction of the Mc Cabe and Thiele diagrams shown in Figures 22-25. The results show that the number of required extraction stages remained constant at 2 for both solvents and all L/S ratios between 10/1 and 50/1. Further observation of the Mc Cabe and Thiele diagrams in Figures 22- 25, showed that the residues at the end of the two stages extraction process contained less than 4% of calcium using the two different solvents.

By interpreting diagrams (Figures 18-25), it was deduced that two extraction stages are required to extract calcium from steel slag by using carbonation regenerated solvent containing at most 15% of calcium compared to calcium contained in the slag and L/S of 10/1.
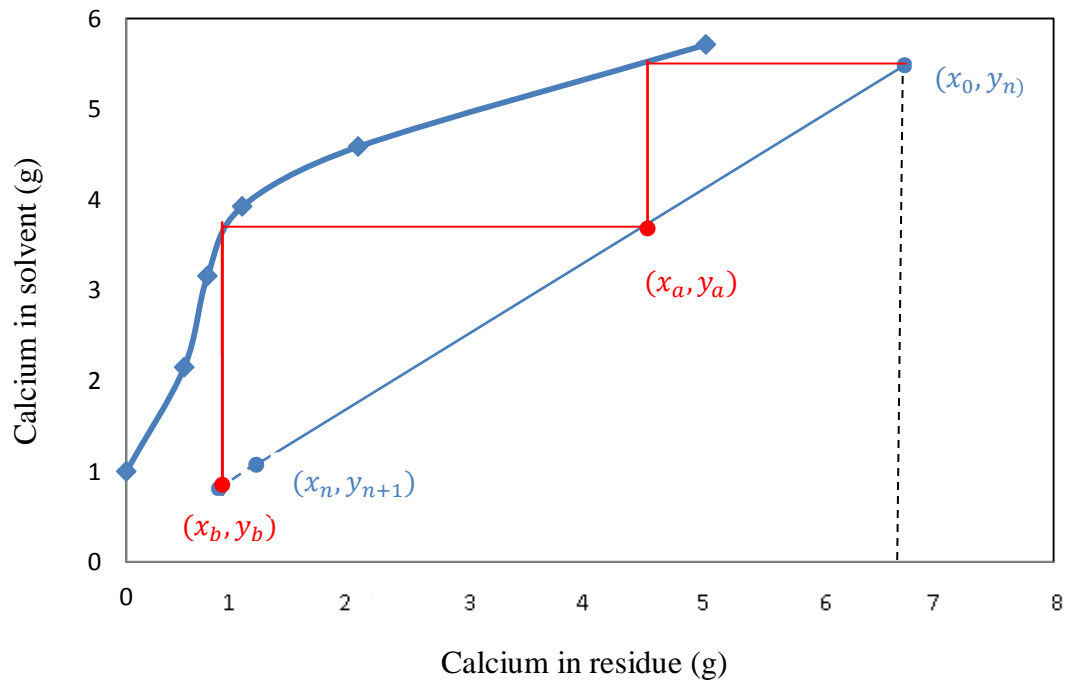
Figure 22: Mc Cabe and Thiele diagram of calcium extraction from steel slag using pure 3 M NH_4NO_3 solvent and a steel slag-solvent ratio (L/S) of 10/1
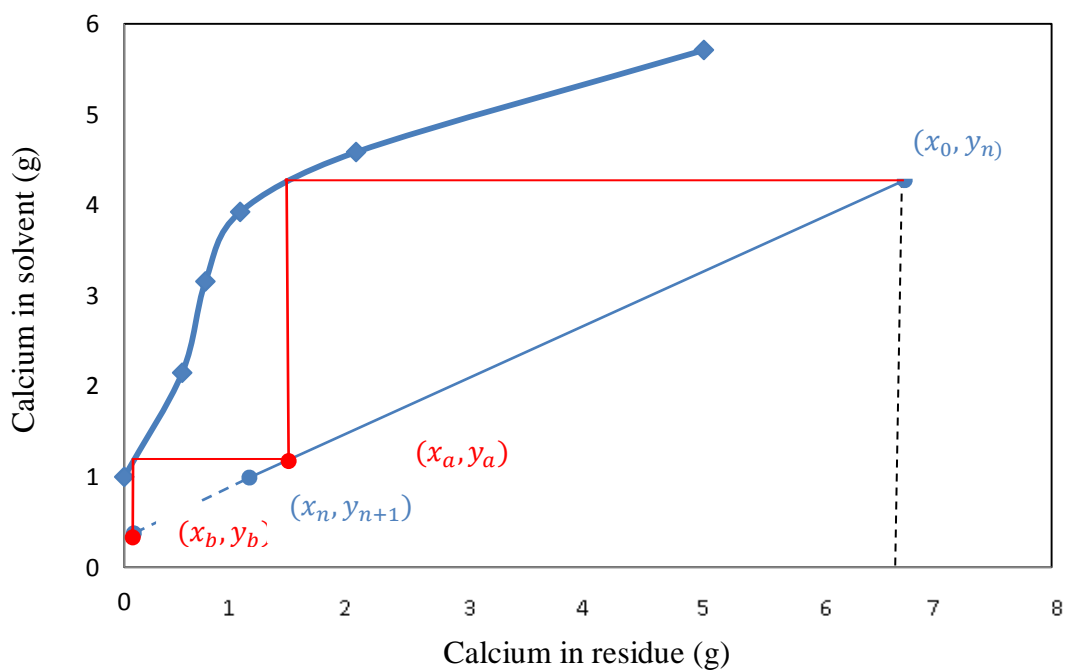
Figure 23: Mc Cabe and Thiele diagram of calcium extraction from steel slag using pure 3 M NH_4NO_3 solvent and a steel slag-solvent ratio (L/S) of 50/1
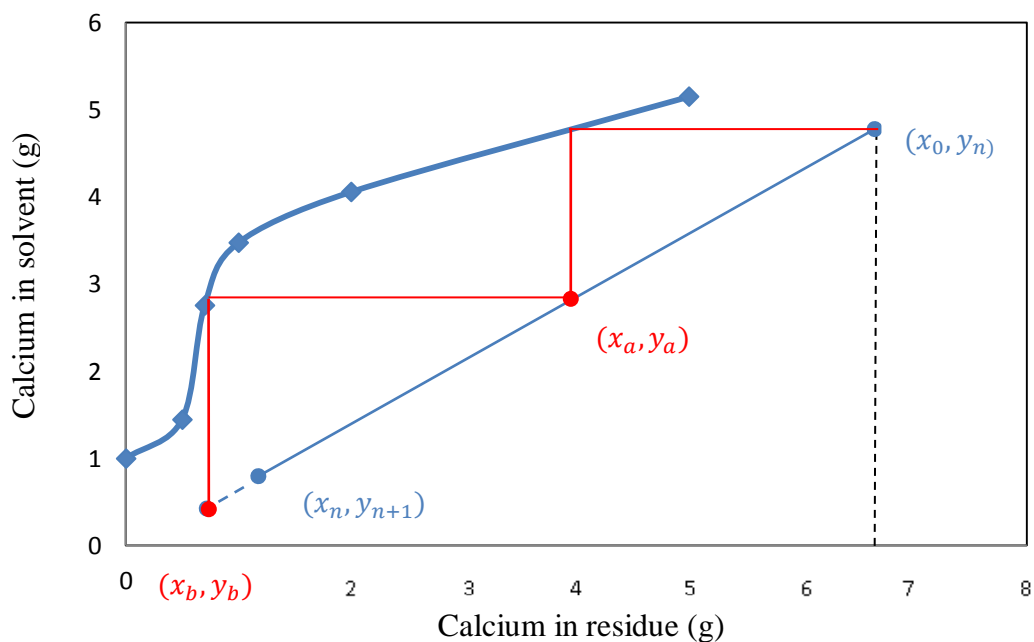
Figure 24: Mc Cabe and Thiele diagram of calcium extraction from steel slag using pure 3 M NH_4Cl solvent and a steel slag-solvent ratio (L/S) of 10/1
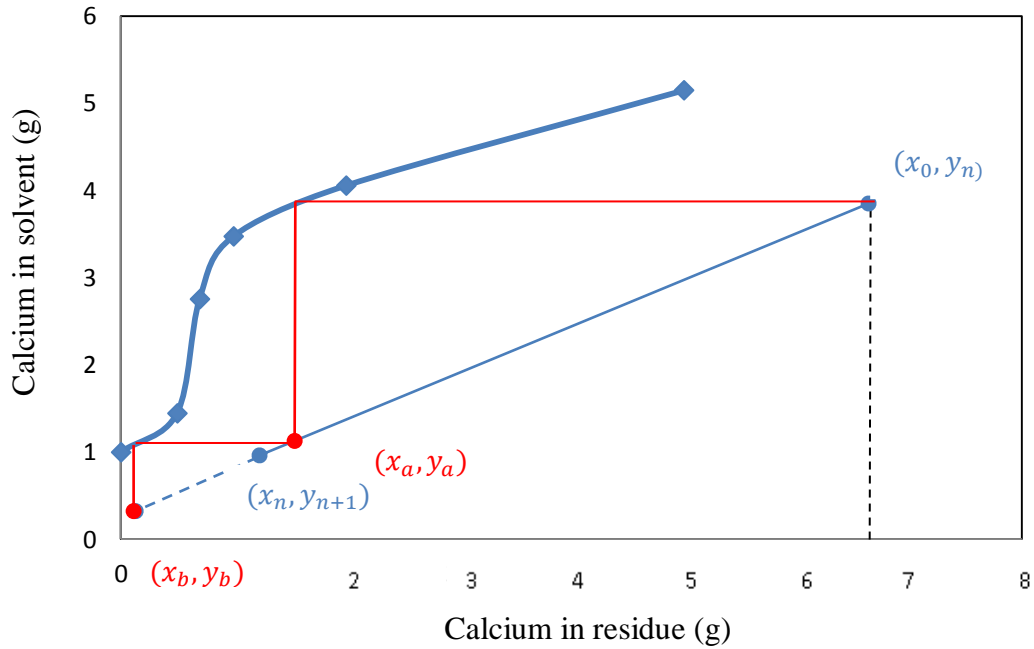
Figure 25: Mc Cabe and Thiele diagram of calcium extraction from steel slag using pure 3 mol/l NH_4Cl solvent and a steel slag-solvent ratio (L/S) of 50/1

3. CALCIUM CARBONATE PRECIPITATION

Although it has been previously demonstrated that the temperature affected calcium carbonation in the liquid phase (Mattila *et al*., 2014), in this work we have given preference to a carbonation process without heating or temperature control. The agitation of the reactive solution was done via a high-pressure injection of CO_2 gas into the reactor. The pressure was varied from 1 to 6.5 bars. Precipitates were obtained by varying the reaction times, the pressure and volume of gas injected and were filtered from the reactive solution at the end of the experiment, dried and weighted to determine the masses for the calculation of the carbonation efficiency.

Table 15 below gives the carbonation yield obtained using different solvents and ammonium hydroxide solution NH_4OH 25%. The carbonation curve reaches a peak at 15min when the extracting solution was NH_4NO_3 and 10 min when using NH_4Cl as shown on Figure 26 below.

77

In the latter case, this reduction in the time required for mineral carbonation may be due to the different abilities of the solvents to promote the formation of the necessary CO_3^{2-} ions from gaseous CO_2.

TABLE 14: CALCIUM CARBONATION EFFICIENCY VERSUS TIME USING NH_4NO_3
AND NH_4Cl SOLVENTS (Pressure = 4 bars and volume CO_2 injected = 100 cm^3)

Time (min)	Efficiency with NH_4NO_3 solvent (%)	Efficiency with NH_4Cl solvent (%)	Efficiency with NH_4NO_3 solvent and NH_4OH added (%)	Efficiency with NH_4Cl solvent and NH_4OH added (%)
5	4.68	9.18	15.03	26.71
10	7.91	10.79	25.31	31.42
15	7.15	11.41	23.19	34.68
25	6.72	10.55	19.95	28.54
40	6.13	9.43	17.22	24.02
60	6.64	9.93	18.58	21.76
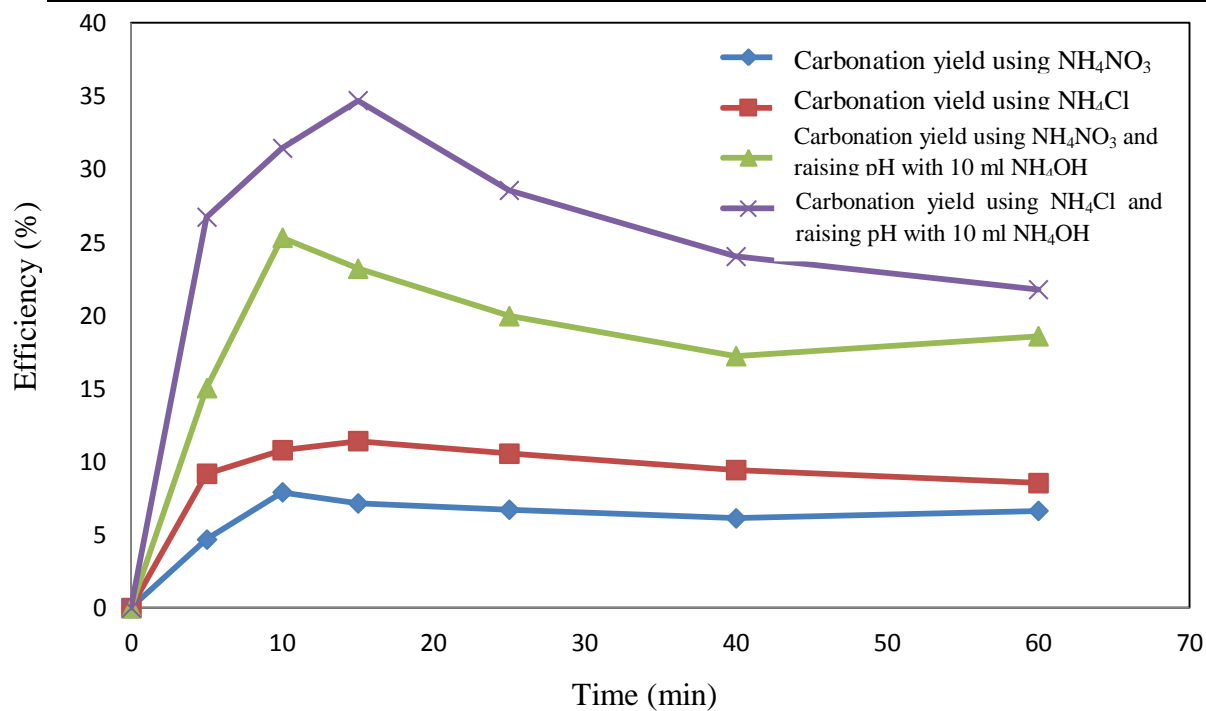
Figure 26: Calcium carbonation efficiency versus time and solvent for 100 cm^3 of CO_2 injected

NH$_4$NO$_3$ AND NH$_4$Cl SOLVENTS (volume CO$_2$ injected=100 cm^3, reaction time=15 minutes)

Injection pressure (bar)	Efficiency with NH$_4$NO$_3$ solvent (%)	Efficiency with NH$_4$Cl solvent (%)
0	0	0
1	0	0.87
2	12.11	13.48
3	18.94	19.45
4	23.19	34.68
5	36.63	41.57
6	58.04	63.65
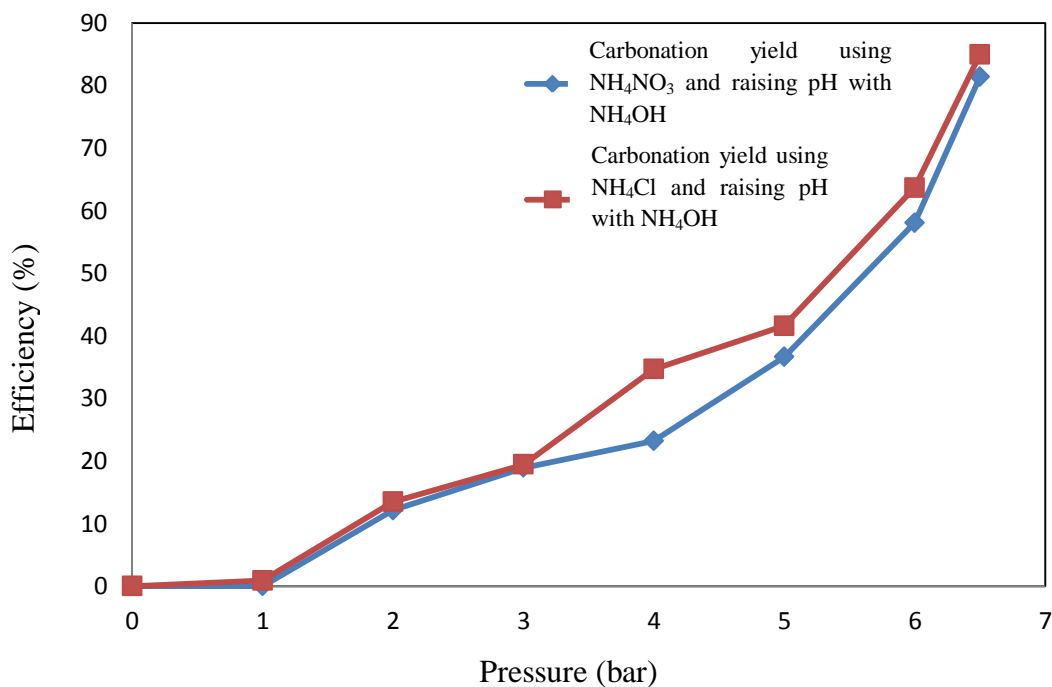
Figure 27: Calcium carbonation efficiency versus pressure for different solvents (reaction time= 15 minutes, volume of CO$_2$ injected = 100 cm^3)

Figure 26 and 27 show that the precipitation efficiency of calcium carbonate depends on pH value of the solution and increased with increasing of CO_2 injection pressure probably because it also increased the mixing and mass transfer between the gas and liquid phases. In order to increase the carbonation efficiency, the volume of CO_2 injected was increased from 50 to 150 cm^3, and this had a positive effect on the carbonation efficiency as shown in Figure 28

TABLE 16: CALCIUM CARBONATION EFFICIENCY VERSUSVOLUME CO_2 INJECTED (REACTION TIME=15MINUTES, PRESSURE= 6.5 bar, SOLVENT= NH_4OH)

Volume (cm^3)	Mass precipitate using NH_4NO_3 (g)	Mass precipitate using NH_4Cl (g)	Efficiency using NH_4NO_3 (%)	Efficiency using NH_4Cl (%)
0	0	0	0	0
50	7.01	5.03	59.66	62.48
100	8.74	6.23	74.38	77.32
125	8.96	6.50	76.26	80.71
150	9.56	6.84	81.38	84.95
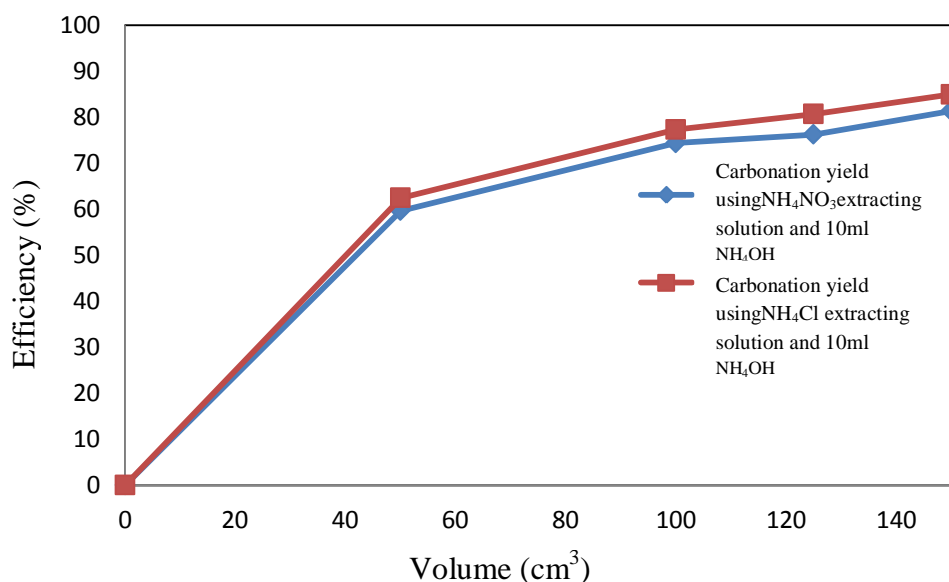
Figure 28: Calcium carbonation efficiency versus volume CO_2 injected for different solvent (reaction time=15 minutes)

The SEM photomicrograph analysis of the calcium carbonate obtained by carbonation of calcium from steel slag was conducted, the figures 29 – 40 show the morphologies and elemental distributions of the calcium carbonate produced with 150 cm^3 of CO_2 injected at different reaction times and pressures, then different observations were established mostly when carbonation time went beyond 10 min with greater pressure injection.

Figure 29: Calcium carbonate precipitate obtained by using NH_4NO_3 solvent after 5 minutes with an injected CO_2 pressure of 4 bars.

TABLE 17: COMPOSITION OF CALCIUM CARBONATE PRECIPITATE OBTAINED BY USING NH_4NO_3 SOLVENT AFTER 5 MINUTES WITH AN INJECTED CO_2 PRESSURE OF 4 BARS.

Element	Weight %	Atomic %
C	8.41	15.14
O	43.68	59.02
Ca	47.91	25.84
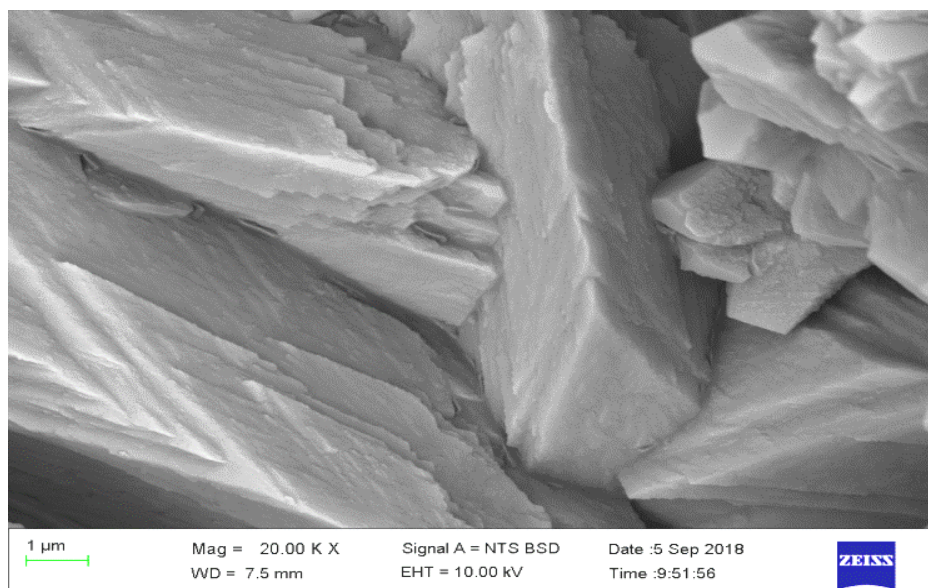
Figure 30: Calcium carbonate precipitate obtained by using NH_4NO_3 solvent after 10 minutes with an injected pressure of 4 bars.

TABLE 18: COMPOSITION OF CALCIUM CARBONATE PRECIPITATE OBTAINED BY USING NH_4NO_3 SOLVENT AFTER 10 MINUTES WITH AN INJECTED CO_2 PRESSURE OF 4 BARS.

Element	Weight %	Atomic %
C	8.47	15.22
O	43.79	59.07
Ca	47.74	25.71

Figure 31: Calcium carbonate precipitate obtained by using NH_4NO_3 solvent after 15 minutes with an injected CO_2 pressure of 4 bars.

TABLE 19: COMPOSITION OF CALCIUM CARBONATE PRECIPITATE OBTAINED BY USING NH_4NO_3 SOLVENT AFTER 15 MINUTES WITH AN INJECTED CO_2 PRESSURE OF 4 BARS.

Element	Weight %	Atomic %
C	8.62	15.63
O	42.43	57.76
Ca	48.95	26.60

Figure 32: Calcium carbonate precipitate obtained by using NH_4NO_3 solvent after 25 minutes with an injected CO_2 pressure of 4 bars.

TABLE 20: COMPOSITION OF CALCIUM CARBONATE PRECIPITATE OBTAINED BY USING NH_4NO_3 SOLVENT AFTER 25 MINUTES WITH AN INJECTED CO_2 PRESSURE OF 4 BARS.

Element	Weight %	Atomic %
C	18.27	30.02
O	40.12	49.49
Ca	41.61	20.49
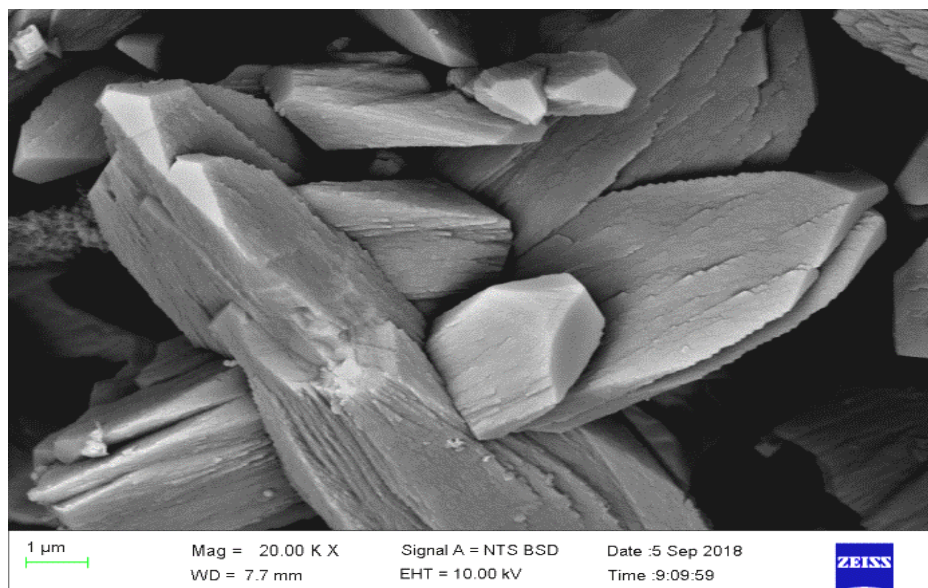
Figure 33: Calcium carbonate precipitate obtained by using NH_4NO_3 solvent after 40 minutes with an injected CO_2 pressure of 4 bars.

TABLE 21: COMPOSITION OF CALCIUM CARBONATE PRECIPITATE OBTAINED BY USING NH_4NO_3 SOLVENT AFTER 40 MINUTES WITH AN INJECTED CO_2 PRESSURE OF 4 BARS.

Element	Weight %	Atomic %
C	8.17	14.84
O	42.97	58.58
Ca	48.85	26.58
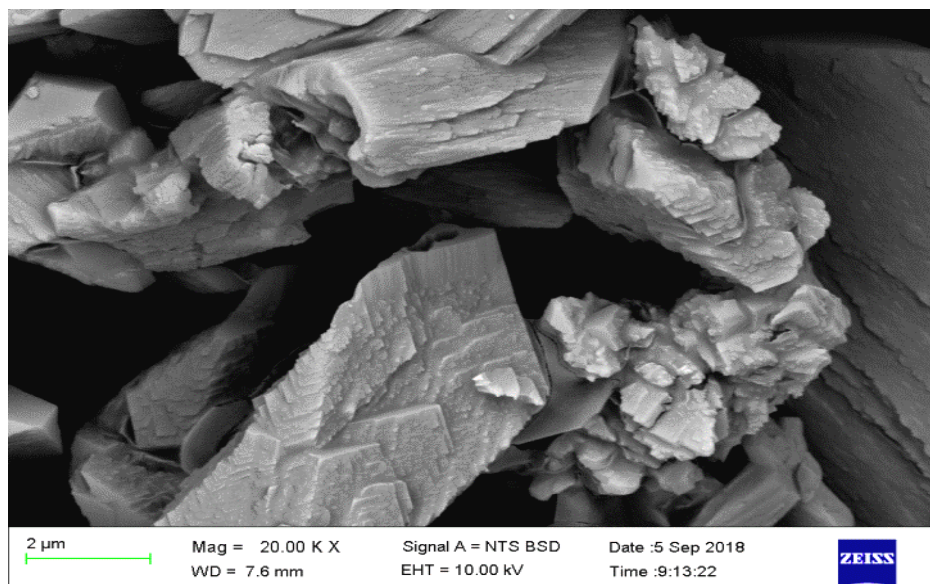
Figure 34: Calcium carbonate precipitate obtained by using NH_4NO_3 solvent after 60 minutes with an injected CO_2 pressure of 4 bars.

TABLE 22: COMPOSITION OF CALCIUM CARBONATE PRECIPITATE OBTAINED BY USING NH_4NO_3 SOLVENT AFTER 60 MINUTES WITH AN INJECTED CO_2 PRESSURE OF 4 BARS.

Element	Weight %	Atomic %
C	7.92	14.42
O	43.10	58.87
Ca	48.98	26.71
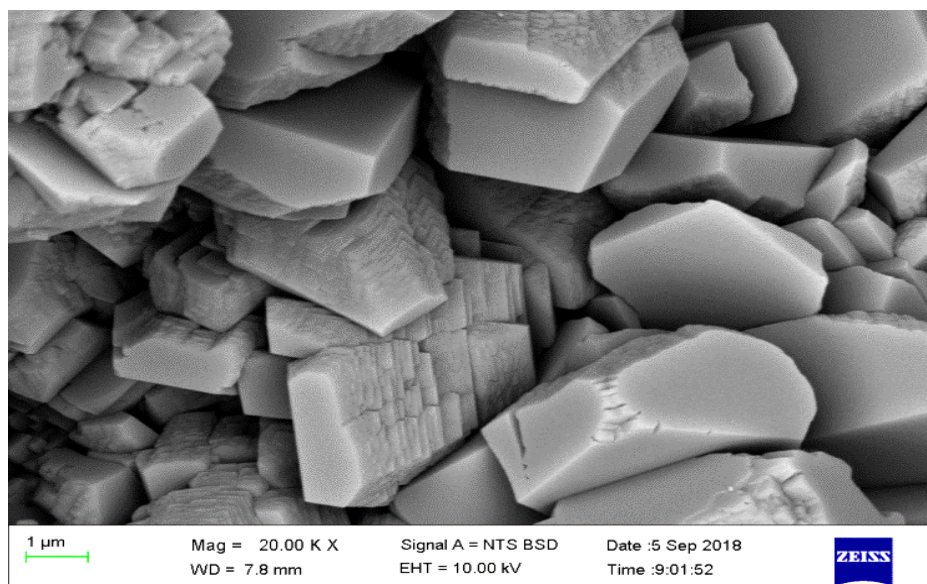
Figure 35: Calcium carbonate precipitate obtained by using NH_4NO_3 solvent after 15 minutes with an injected CO_2 pressure of 6.5 bar.

TABLE 23: COMPOSITION OF CALCIUM CARBONATE PRECIPITATE OBTAINED BY USING NH_4NO_3 SOLVENT AFTER 15 MINUTES WITH AN INJECTED CO_2 PRESSURE OF 6.5 BARS.

Element	Weight%	Atomic%
C	11.31	20.11
O	40.64	54.27
Ca	48.05	25.61
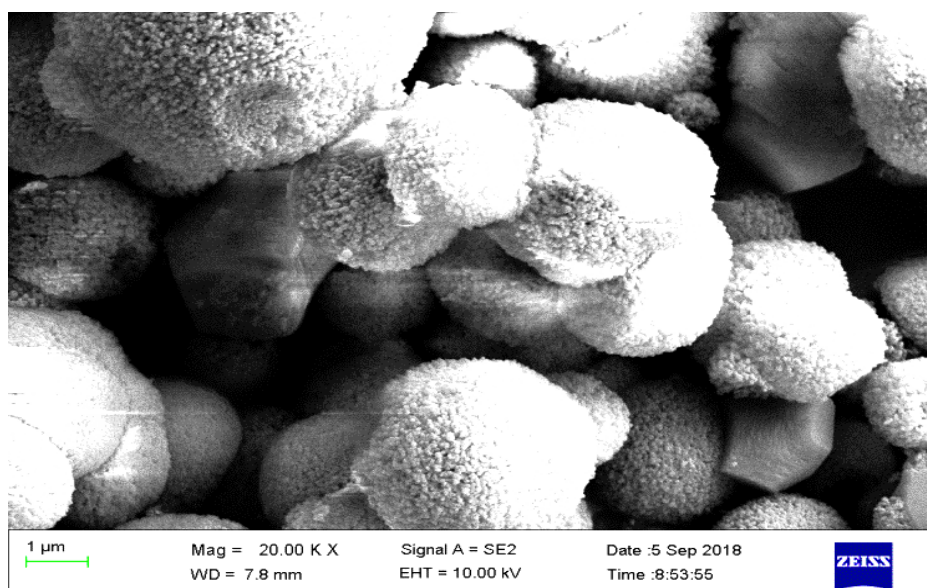
Figure 36: Calcium carbonate precipitate obtained by using NH_4NO_3 solvent after 25 minutes with an injected CO_2 pressure of 6.5 bars.

TABLE 24: COMPOSITION OF CALCIUM CARBONATE PRECIPITATE OBTAINED BY USING NH_4NO_3 SOLVENT AFTER 25 MINUTES WITH AN INJECTED CO_2 PRESSURE OF 6.5 BARS.

Element	Weight %	Atomic %
C	11.67	19.71
O	46.73	59.24
Ca	41.60	21.05
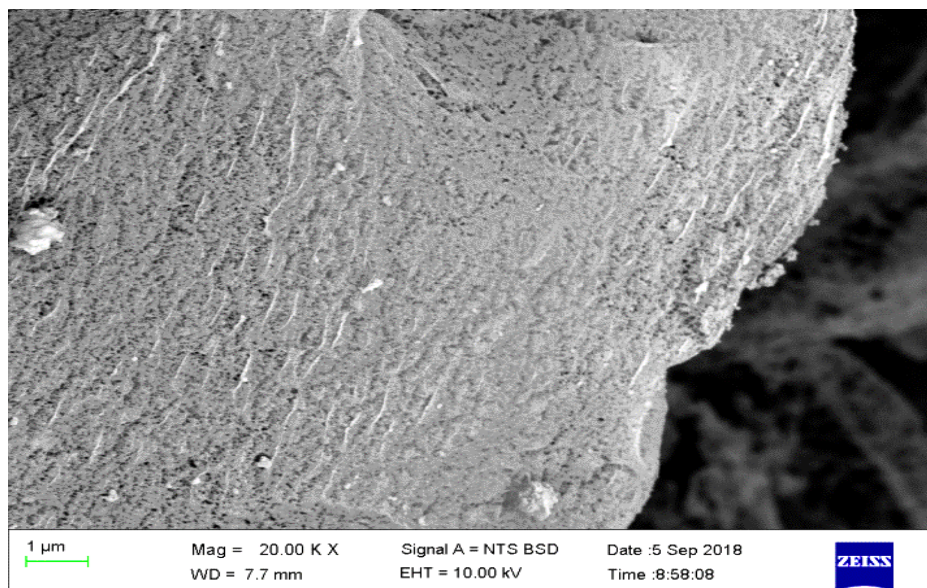
Figure 37: Calcium carbonate precipitate obtained by using NH_4NO_3 solvent after 60 minutes with an injected CO_2 pressure of 6.5 bars.

.

TABLE 25: COMPOSITION OF CALCIUM CARBONATE PRECIPITATE OBTAINED BY USING NH_4NO_3 SOLVENT AFTER 60 MINUTES WITH AN INJECTED CO_2 PRESSURE OF 6.5 BARS.

Element	Weight %	Atomic %
C	10.92	18.07
O	50.62	62.87
Ca	38.46	19.07
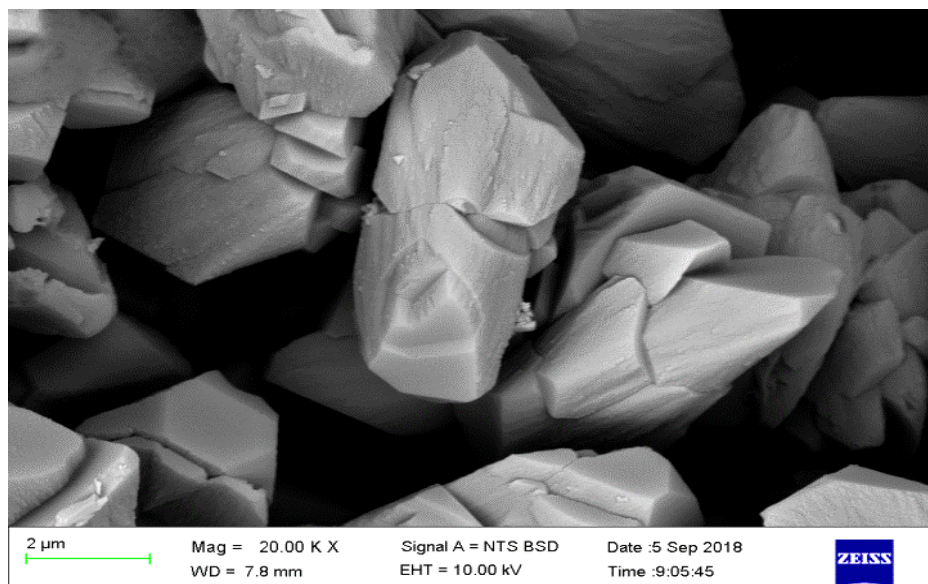
Figure 38: Calcium carbonate precipitate obtained by using NH$_4$Cl solvent after 10 minutes with an injected CO$_2$ pressure of 6.5 bars (10 ml NH$_4$OH added)

TABLE 26: COMPOSITION OF CALCIUM CARBONATE PRECIPITATE OBTAINED BY USING NH$_4$Cl SOLVENT AFTER 10 MINUTES WITH AN INJECTED CO$_2$ PRESSURE OF 6.5 BARS(10 ml NH$_4$OH ADDED).

Element	Weight%	Atomic%
C	7.48	13.62
O	43.31	59.25
Cl	3.56	2.20
Ca	45.65	24.93
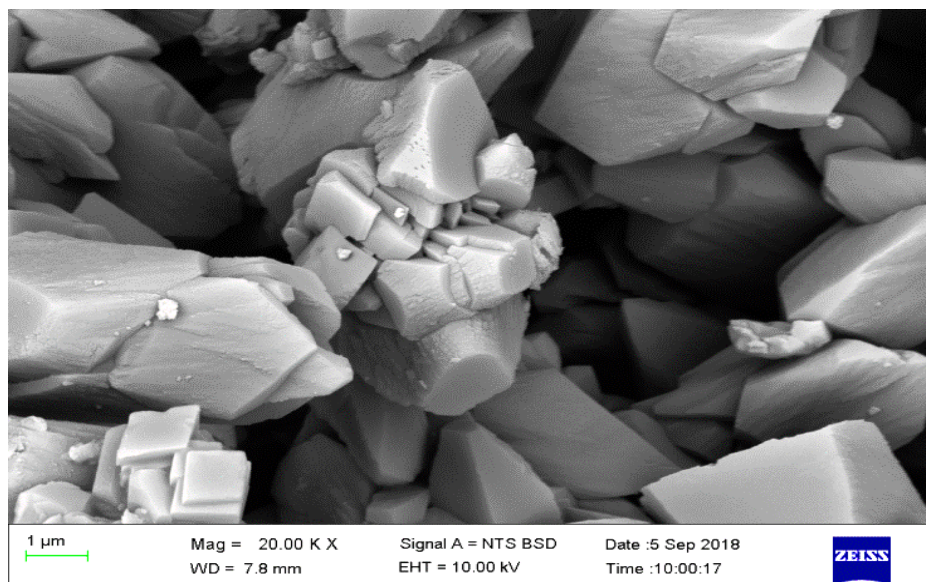
Figure 39: Calcium carbonate precipitate obtained by using NH_4NO_3 solvent after 15 minutes with an injected CO_2 pressure of 6.5 bar (10 ml NH_4OH added).

TABLE 27: COMPOSITION OF CALCIUM CARBONATE PRECIPITATE OBTAINED BY USING NH_4NO_3 SOLVENT AFTER 15 MINUTES WITH AN INJECTED CO_2 PRESSURE OF 6.5 BAR (10 ml NH_4OH ADDED).

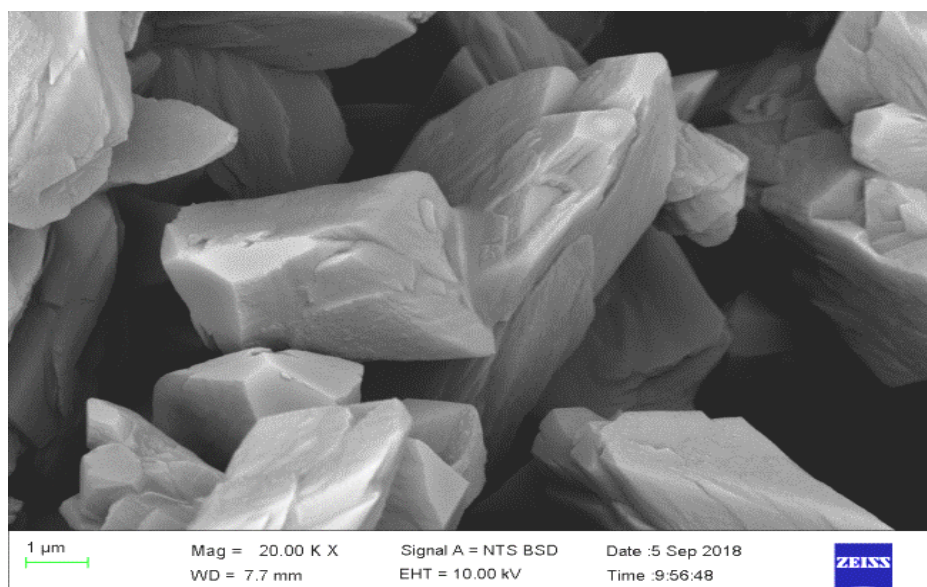| Element	Weight%	Atomic%
C	7.38	13.71
O	41.34	57.62
Ca	51.27	28.68
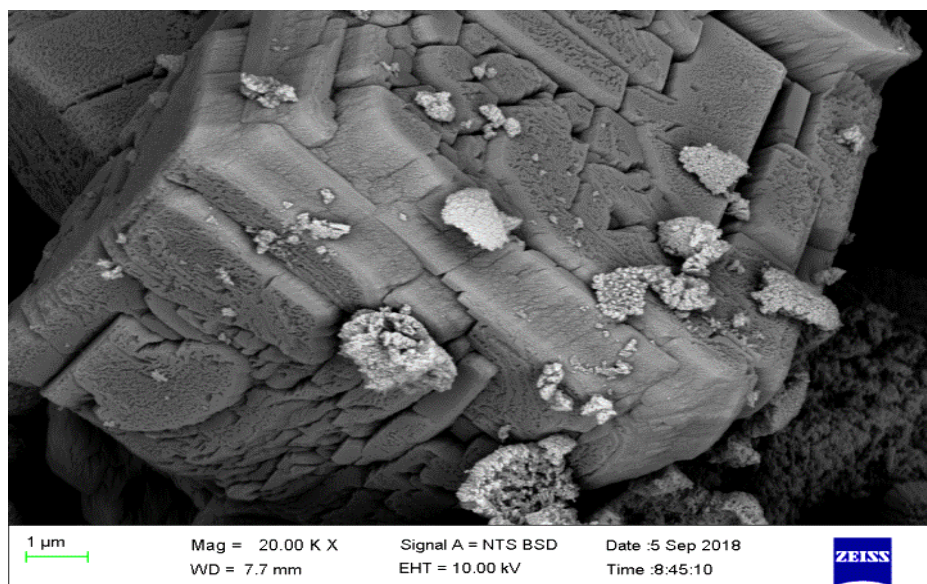
Figure 40: Calcium carbonate precipitate obtained by using NH_4NO_3 solvent after 15 minutes with an injected CO_2 pressure of 6.5 bar (10 ml EDTA and 10 ml NH_4OH added).

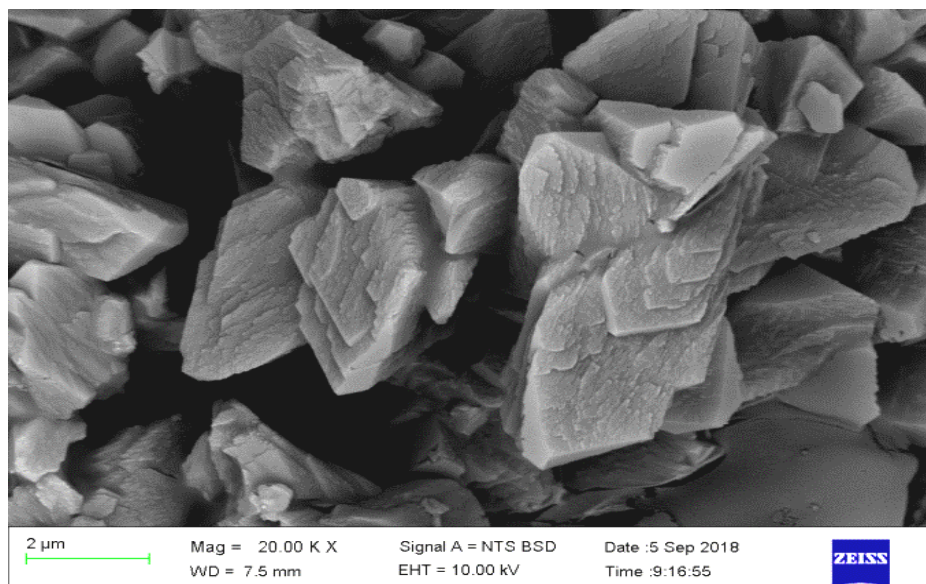TABLE 28: COMPOSITION OF CALCIUM CARBONATE PRECIPITATE OBTAINED BY USING NH_4NO_3 SOLVENT AFTER 15 MINUTES WITH AN INJECTED CO_2 PRESSURE OF 6.5 BAR (10 ml EDTA AND 10 ml NH_4OH ADDED)

Element	Weight%	Atomic%
C	7.48	13.62
O	43.31	59.25
Ca	49.21	27.13

Figures 29-40 show that the morphology of the precipitate may be closely related to the reaction time than the CO_2 injection pressure. It was noted that the distinct polymorph which is rhombic shape for calcite crystals, a needle-like shape for aragonite crystals (Figure 36), and a spherical shape for vaterite crystals (Figure 37), the expected morphologies were displayed in Figures 35, 38 and 39 (calcite). The cubic forms observed on the above images suggest a calcium carbonate with properties similar to calcite. Formation of pure calcite is obtained between 5 and 15 min of reaction times. For reaction time above 25 minutes, other forms seem to appear as shown in Figures 32-34, 36 and 37. The use of the EDTA provides a compact morphology sprinkled with other forms that blur the appearance of calcite as shown in Figure 40. An in-depth study of the different morphologies would be a recommended option in order to understand the implication of the large-scale implications for the production of calcium carbonate from steel slag.

TABLE 29: EQUILIBRIUM CONSTANTS AND HEATS OF REACTION FOR REACTIONS 29 to 38

Reaction	Parameters	k		Log(K_{eq})		ΔG (kcal)		ΔH (kcal)	
		25°C	30°C	25°C	30°C	25°C	30°C	25°C	30°C
29	K1	5.044E+032	1.387E+032	32.703	32.142	-44.610	-44.610	-46.365	-46.365
30	K2	9.200E-012	1.644E-011	-11.036	-10.784	15.055	14.957	20.870	20.833
31	K3	1.862E+005	1.494E+005	5.270	5.174	-7.189	-7.177	-7.809	-8.016
32	KW	1.020E-014	1.473E-014	-13.991	-13.832	19.086	19.184	13.338	13.092
33	K4	1.996E+008	2.173E+008	8.300	8.337	-11.322	-11.563	2.801	3.271
34	K5	9.336E-003	1.116E-002	-2.030	-1.952	2.769	2.708	6.314	6.489
35	K6	1.000E+000	1.000E+000	0.000	0.000	0.000	0.000	0.000	0.000
36	K7	1.509E-008	1.509E-008	-7.821	-7.821	10.669	10.892	-2.533	-2.706
37	K8	4.676E-011	5.135E-011	-10.330	-10.289	14.091	14.271	3.513	3.217
38	K9	1.479E+006	9.520E+005	6.170	5.979	-8.417	-8.292	-15.871	-15.798

Table 29 was compiled using HSC 5.11 Chemistry and was used to calculate the different reaction rates, which are summarized in the two primary steps below:

1) The dissolution (extraction) of calcium in the solvent

$$CaO + 2NH_4NO_3 \xrightarrow{K_{10}} Ca(NO_3)_2 + 2NH_3\,(aq) + H_2O \qquad (39)$$

$$CaO + 2NH_4Cl \xrightarrow{K_{11}} CaCl_2 + 2NH_3\,(aq) + H_2O \qquad (40)$$

$$NH_3\,(aq) + H_2O \xrightarrow{K_{12}} NH_4OH \qquad (41)$$
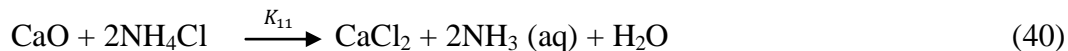
The rates of these reactions are dependent on time, temperature, solvent concentration. The experimental results show that the calcium extraction efficiency and therefore the rate of reaction are function of time and also of the steel slag particle size.

2) Carbonation of calcium extracted and regeneration of the solvent

$$Ca(NO_3)_2 + 2NH_4OH + CO_2 \xrightarrow{K_{13}} CaCO_3 + 2NH_4NO_3 + H_2O \qquad (42)$$

$$CaCl_2 + 2NH_4OH + CO_2 \xrightarrow{K_{14}} CaCO_3 + 2NH_4Cl + H_2O \qquad (43)$$
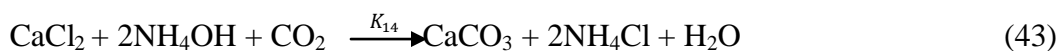
Reactions (42 - 43) show that the carbonation rate was a function of the concentration of NH_4OH and thus of the pH and the volume of CO_2 injected as it depends on the concentration of CO_3^{2-} ions present in a solution whose stability is a function of solution basicity (pH > 10.3). Carbonation experiments have also shown that pressure is a very significant parameter as shown in Figure 27.

Equilibrium constants of reactions 29 to 38 for both solvents at 25°C and 30°C respectively were calculated with HSC 5.11 and results are given in Table 29.

TABLE 30: EQUILIBRIUM CONSTANTS AND HEATS OF EXTRACTION AND CARBONATION REACTIONS CALCULATED USING HSC 5.11

Reaction	k		Log(Keq)		ΔG (kcal)		ΔH (kcal)	
	25°C	30°C	25°C	30°C	25°C	30°C	25°C	30°C
Dissolution of calcium from steel slag								
Reaction 39	1.256E+007	1.770E+007	7.099	7.248	-9.684	-10.053	12.336	12.306
Reaction 40	4.090E+001	7.491E+001	1.612	1.875	-2.199	-2.600	21.732	21.736
Calcium Carbonation								
Reaction 42	6.353E+027	1.280E+027	27.803	27.107	-37.926	-37.597	-57.510	-57.580
Reaction 43	1.951E+033	3.024E+032	33.290	32.481	-45.411	-45.050	-66.907	-67.010

The equilibrium constants and the reaction enthalpy (ΔG) in the Table 30 showed that the reaction of dissolution of calcium by the two solvents is possible but that this equilibrium is reached more quickly by using NH_4NO_3 than NH_4Cl solvent. Equilibrium constants values showed that both extraction reactions are relatively slow and that there may need to accelerate the reactions. On the other hand, carbonation rates were relatively faster and may be further accelerated by the addition of ammonia, and the increase in CO_2 concentration. Although, it may be difficult to establish exact carbonation rate values, the masses of precipitates produced showed that the carbonation rates was accelerated by using ammonia. It was also found that the extraction reaction rate is slightly faster-using NH_4NO_3 than NH_4Cl. However, the opposite was observed during carbonation experiments probably due to the values of equilibrium constants of the reactions which tend to indicate that the equilibrium of carbonation was reached more quickly when using NH_4Cl than NH_4NO_3.

A further possible reason may be that $CaCl_2$ formed at the calcium dissolution stage is less stable than $Ca(NO_3)_2$, since chlorine forms soluble ionic compounds with alkaline and alkaline earth ions, which therefore favors the presence of ions calcium in solution for precipitation (Atkins *et al*., 1998).

The results of the slag extraction residue and XRF precipitation analyses were used to calculate the calcium content in the final calcium carbonate precipitate without including losses. 11.48 g of calcium carbonate was produced using NH4NO3 and 9.85g using NH_4Cl.

Spectrophotometer AA analyses were used to determine the amount of starting steel slag calcium passing into in solution as a Ca^{2+} ion. The results showed that 75% of the initial calcium leached into solution when using NH_4NO_3 and 69% when using NH_4Cl for the same operating conditions. XRD analysis confirmed $CaCO_3$ as the main constituent of the carbonation precipitate for both solvents. However, the carbonation precipitate contained s about 4.59 g of calcium for NH_4NO_3 solvent and 3.93 g for the NH_4Cl solvent. SEM analyses were also used to deduce the morphology of the calcium carbonate produced. The overall results showed that the combined extraction and carbonation give calcium carbonate precipitates containing 68.30% and 58.48% of calcium in the starting steel slag for the fresh ammonium nitrate (3 mol/l) and ammonium chloride (3 mol/l) respectively. Whereas about 14.13% and 10.24% remain dissolved in the ammonium nitrate (3 mol/l) and ammonium chloride (3 mol/l) respectively. These results indicate that 17.57% and 31.28% of the calcium contained in the starting steel slag remain trapped in the extraction residues, meaning that the end-of-extraction residue contains at least 4% of calcium as also suggested by the Mc Cabe and Thiele analyses conducted earlier.

The main parameters for CO_2 capture were the pressure, the volume of CO_2 injected, the reaction time and the pH of the solution (NH_4OH was used to increase the pH prior to carbonation).

The impact of these different parameters on the quality of the calcium carbonate precipitate is demonstrated by the morphologies obtained in Figures 26-37. It was found that the addition of EDTA as absorber for CO_2 capture decreased the pH thus favouring the predominance of HCO_3^- ions in solution compared to CO_3^{2-} ions, resulting in an overall decrease of the carbonation efficiency that showed EDTA was not catalyst of the carbonation reaction. The efficiency of CO_2 sequestration by mineral carbonation was determined using the ratio between the amount of carbon dioxide injected into the reactor and the net amount of carbon dioxide captured by the precipitate as per the formula below:

$$CO_2 \text{ sequestration} = \sum_i^n \frac{(6.41-1.48)0.15*15}{25*293*0.082057} = 0.0184 \text{ } CO_2 \text{ g/g slag}$$

$$0.184\text{kg } CO_2/\text{kg slag}$$

The total energy consumed by the production of calcium carbonate was estimated using equation 29 which combines the energy of grinding and over grinding, and the energy contribution of filtration, pressure and agitation (Rahmani *et al.*, 2014).

$$W = 0.01 * 12.2 \left(\frac{1}{\sqrt{0.125}} - \frac{1}{\sqrt{1.24722}} \right) + \sum W_s + \sum W_F + W_p + W_{am} \text{ (kwh/t)}$$

Considering an over-grinding up to 38µm, the over-grinding energy was determined as follows:

$$W_s = 0.01 * 12.2 \left(\frac{1}{\sqrt{0.038}} - \frac{1}{\sqrt{1.24722}} \right) = 0.531\text{kwh/t}$$

Whereas the energy contribution of filtration, pressure and electric agitation were estimated using the method by Rahmani (2014)

$$W_g = 0.237 + 0.531 = 0.768 \text{ kwh/t}$$

$$W_F + W_{am} = 0.25 \text{ kwh/t}$$

$$W_p = 12.2 \text{kwh/t}$$

$$W_t = 12.2 + 0.25 + 0.768 = 13.218 \text{kwh/t}$$

The total cost of the reagents used for the carbonation process was R4767.15

(NH_4OH =129 $US/l, NH_4NO_3 = 81 $US/kg, NH_4Cl = 125 $US/kg and EDTA 5.8 $US/l as on

15th November 2018). These prices were provided by Sigma-Aldrich (Merck). A simplified and

preliminary high level diagram for the production of calcium carbonate precipitate from steel

slag is provided in Figure 41 and shows that to produce one ton of calcium carbonate precipitate

of 99.88% purity, 2.34 ton of steel slag containing 26.91 % calcium, 23.4 m^3 of NH_4NO_3 (3 M),

9.36m^3 of NH_4OH (25%) is needed. The calcium carbonate produced, therefore, has a potential

for commercial and environmental benefit as it may be used in the same steel industry or other

industries. The residues from the extraction stage can be used for construction (road) works as it

no longer contains a high proportion of calcium oxide. The beneficiation of steel slag via the

proposed route is very important because it would not only produce a commercial product

($CaCO_3$), it may also solve some of the environmental problem associated with solid industrial

waste disposal (which may contain heavy metals and acid compounds), carbon dioxide emission

and acid mines drainage waters. However, some of the challenges associated with the production

of calcium carbonate from steel slag are as follows:

- The production of rejects

- The cost of production

- The NH_3 gases emanation due to the use of ammonium products

- The management of impurities contained in the raw materials.

2.34 t STEEL SLAG FROM
ARCELOR-MITTA (26.91%Ca)

```
                                                                    RESIDUE
EXTRACTION                    LIQUID-SOLID              (4% Ca)
FIRST STAGE      ◄──────      SEPRATION      ──────►
(L/S=10)
```

23.4 m^3 SOLVENT
(NH$_4$NO$_3$/NH$_4$Cl)

```
LIQUID-SOLID                          EXTRACTION
SEPRATION         ──────►             SECOND STAGE      ◄──────
                                      (L/S=10)
```

FILTRATE EXTRACTED (20g/l Ca)   ◄────── 9.4 m^3 NH$_4$OH 25%

PRECIPITATION

```
LIQUID-SOLID
SEPRATION         ──────►      REGENERATED
                               SOLVENT (4g/l Ca)
```

DRYING

1t CALCIUM
CARBONATE
99.8%
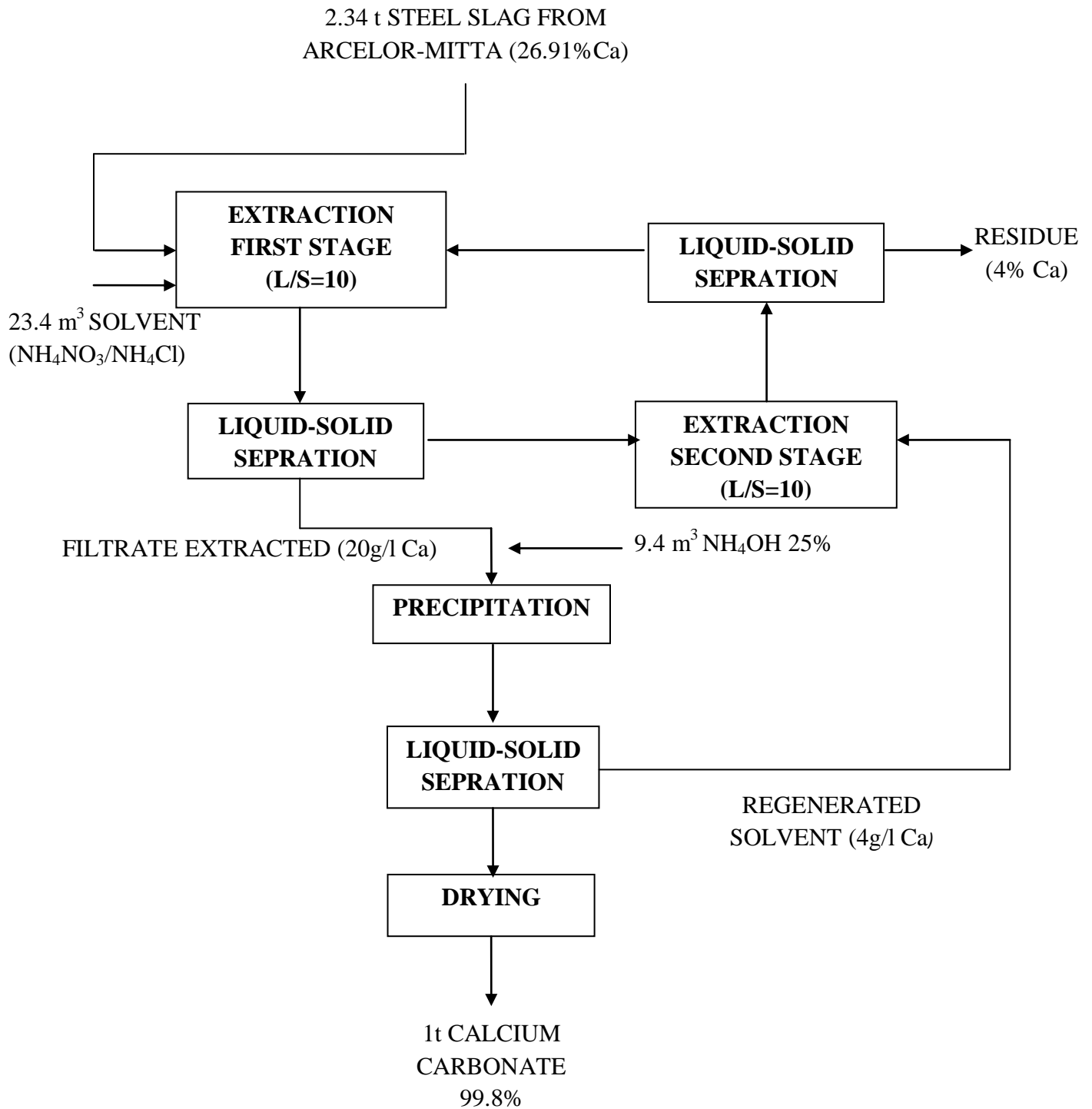
Figure 41: Mass balance for calcium carbonate production from Steel slag

4. ACID MINE DRAINAGE (AMD) TREATMENT

The most used AMD treatment method remains the conventional neutralization treatment using calcium carbonate or lime or a combination of the two (Kefeni *et al*., 2018) mainly due to his availability, low cost and ease of use. The calcium carbonate used is generally produced from natural resources and may not be sufficient considering the amount of AMD generated each year in South Africa (about 400 Megaliter of AMD are generated every day) (Mulopo, 2015). Production of calcium carbonate from other sources may be necessary for a long-term AMD neutralisation i.e.the use of calcium carbonate produced from industrial waste such as slag. The calcium carbonates produced using ammonium nitrate and ammonium chloride as solvents were tested for the neutralization of AMD and compared to commercial calcium carbonate available on the market. The purpose of this experiment was to evaluate the possibility of using calcium carbonate produced for the neutralization of AMD. The experimental neutralization procedure was as follows;

A sample of 450 g AMD collected from coal mines with composition presented in Table 31 was mixed to 0.5 g of calcium carbonate produced and commercial calcium carbonate.

- The neutralization is then monitored over some time by measuring the variation of the acidity and the pH of the mixture. For the acidity measurement, 1 g of carbonate of calcium is mixed with 900 g of AMD, and the results are presented in Figure 42.

TABLE 31: CHEMICAL COMPOSITION OF COAL MINE FEED WATER (EWRP)

Parameter	Unit	Value
pH	-	3.82
Sulphate	mg/l as SO_4	1900
Magnesium	mg/l as Mg	70
Aluminium	mg/l as Al	63
Manganese	mg/l as Mn	7.7
Iron (total)	mg/l as Fe	6.2
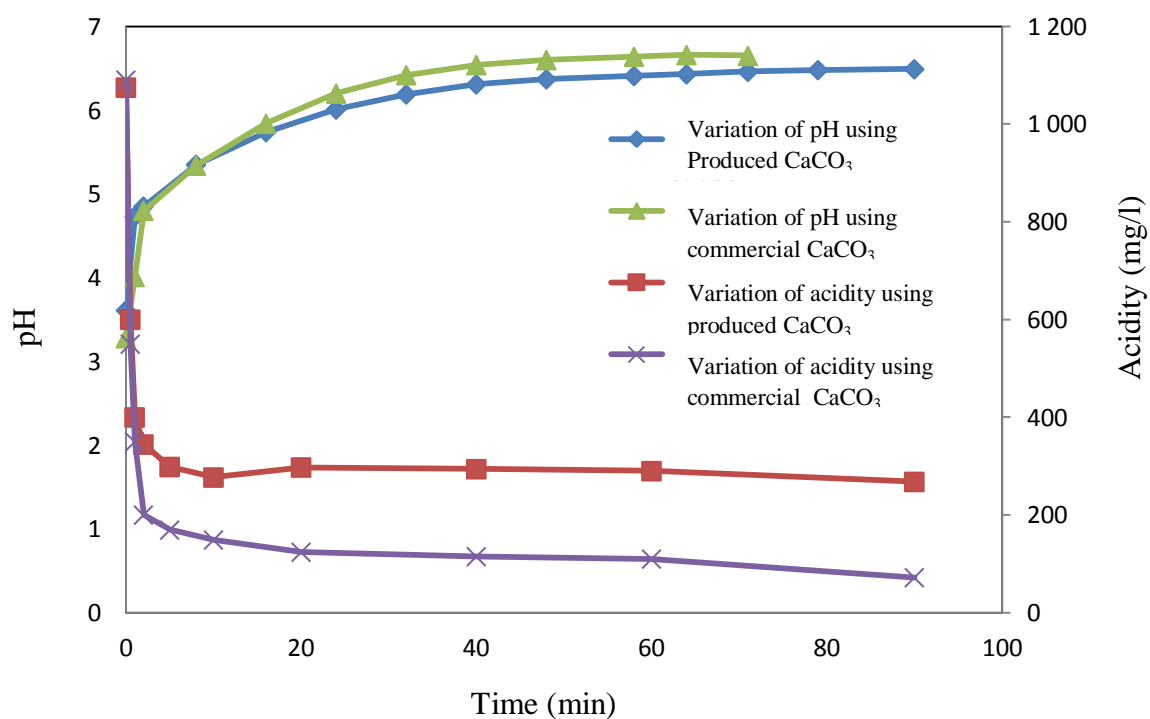
Figure 42: pH and acidity of AMD sample versus time (minutes)

AMD neutralization results show similar trends for both the produced and commercial calcium carbonate. The slight difference between the two carbonates was due to the presence of traces impurities. The presence of chlorine in the calcium carbonate produced may have slowed down the neutralization because of its high affinity with hydrogen than tends to form chloride acid. The use of NH_4NO_3 as a solvent for calcium carbonation of slag may be therefore more preferable than NH_4Cl in the case where the precipitate will be used for the neutralization of AMD. FOR neutralization of 900 g of coal mine feed water, 1 g of produced calcium carbonate was used, this showed that a ton of calcium carbonate would treat about 900 t of AMD.

TABLE 32: VARIATION OF COAL MINE FEED WATER pH AND ACIDITY   USING PRODUCED AND COMMERCIAL CALCIUM CARBONATE VERSUS TIME

Produced CaCO₃ (1 g)				Commercial PCC (1 g)			
Time (min)	pH	Time (min)	Acidity (mg/l)	Time (min)	pH	Time (min)	Acidity (mg/l)
0	3.61	0	1 075	0	3.28	0	1 091
1	4.73	0.5	600	2	4.01	0.5	550
2	4.85	1	400	3	4.80	1	350
8	5.35	2	345	5	5.34	2	200
16	5.74	5	299	13	5.84	5	169
24	6.01	10	277	22	6.20	10	149
32	6.19	20	298	30	6.42	20	124
40	6.31	40	294	38	6.54	40	115
48	6.37	60	290	46	6.60	60	110
58	6.41	90	268	58	6.64	90	72
64	6.43			74	6.66		
71	6.46			90	6.65		
79	6.48						
90	6.49						

TABLE 33: ELEMENT COMPOSITION OF CALCIUM CARBONATE

CaCO$_3$	Si %	S %	Al %	Fe %	Mg %	Ca %	Na %	K %	Cr %	Mn %
precipitate produced	0.230	0.036	0.13	0.056	0.114	41.49	0.12	0.008	0.030	0.026
Conversion factor	0.46	0.50	0.53	0.77	0.60	0.71	0.74	0.83	0.68	0.77

Table 32 showed that the pH of coal mine feed water raised up to 6.49 and the acidity decreased from 1075 mg/l to 268 mg/l in 90 min. Those results clearly demonstrated the effectiveness of neutralization capacity of the calcium carbonate precipitate produced from BOF steelmaking slag.

GENERAL CONCLUSION

Industrial waste generated from the steel industry has been recognized as a significant cause of environmental pollution. Among the most efficient approaches of ameliorating the aforementioned challenge, is the utilization of the steel slag for the production of various value-added products, thus promoting waste management and reuse. This study therefore focused on the production of calcium carbonate from steel slag for the treatment of acid mine drainage (AMD) from the Witwatersrand western basin. Steel slag samples from Arcelor Mittal steel industry, South Africa were collected. Thereafter, calcium was extracted from the obtained samples with the aid of ammonium nitrate and ammonium chloride using the Mc Cabe and Thiele plot method under varying conditions of solvent concentration, liquid/solid ratio, temperature and time. The resulting calcium-containing solution was reacted CO_2 in a closed reactor for the precipitation of calcium carbonate. The produced calcium carbonate was analysed by scanning electron microscope. The efficiency of the calcium carbonate for the neutralization of acid mine drainage was further investigated. Both solvents were found to be useful in the extraction of calcium from the steel slag at a concentration of 3 M. However, ammonium nitrate was more efficient than ammonium chloride. The enhanced extraction efficiency of both solvents was observed at a higher liquid/solid ratio of 10/1, resulting in more than 50% calcium being extracted. At room temperature, efficient calcium extraction with fewer impurities was observed at about 60 min. Effective carbonation was achieved with a solution pH of 10.4, pressure and CO_2 injection rate of 6.5 bar and 150 cm^3/min respectively, and for about 15 minutes reaction time. Beyond these operating conditions, it was found that the precipitate quality degraded. The organoleptic, chemical and microscopic analyses of the produced calcium carbonate revealed a whitish and fine rhombohedral precipitate with high purity (99.8%).

Treatment of the AMD using the obtained calcium carbonate led to treated water with a pH of 6.49 and acidity of less than 200 mg/ml after 90 minutes. Findings from this study suggest the efficacy of the produced calcium carbonate in the treatment of AMD. They further provide a rational choice of possible operating process conditions for large-scale production of calcium carbonate from steel slag.

REFERENCES

1. Adams, R.D. ed. (2005). Adhesive bonding: *Science, Technology and Applications*.

2. Afanga, K. (2014*).* Modélisation systémique des filières sidérurgiques en vue de leur optimisation énergétique et environnementale (Doctoral dissertation, Université de Lorraine).

3. Agrawal, A., & Sahu, K. K. (2009). An overview of the recovery of acid from spent acidic solutions from steel and electroplating industries. *Journal of Hazardous Materials*, 171(1-3), 61-75.

4. Ahmad, S., Assaggaf, R. A., Maslehuddin, M., Al-Amoudi, O. S. B., Adekunle, S. K., & Ali, S. I. (2017). Effects of carbonation pressure and duration on strength evolution of concrete subjected to accelerated carbonation curing. *Construction and Building Materials*, *136*, 565-573.

5. Al Omari, M. M. H., Rashid, I. S., Qinna, N. A., Jaber, A. M., & Badwan, A. A. (2016). Calcium carbonate. In *Profiles of Drug Substances, Excipients and Related Methodology* (Vol. 41, pp. 31-132). Academic Press.

6. Ali, B., Al-Wabel, N. A., Shams, S., Ahamad, A., Khan, S. A., & Anwar, F. (2015). Essential oils used in aromatherapy: A systemic review. *Asian Pacific Journal of Tropical Biomedicine*, *5*(8),

7. American Iron and Steel Institute (AISI), 1995: Steel Processing Flow Lines (Washington, DC)

8. Aminian, H., Bazin, C., Hodouin, D., & Jacob, C. (2000). Simulation of a SX–EW pilot plant. *Hydrometallurgy*, *56*(1), 13-31.601-611.

9. Amos, R. T., Blowes, D. W., Bailey, B. L., Sego, D. C., Smith, L., & Ritchie, A. I. M. (2015). Waste-rock hydrogeology and geochemistry. *Applied Geochemistry*, *57*, 140-156.

10. Anderson, F. R. (2013). *NEPA in the Courts: a Legal Analysis of the National Environmental Policy Act*. RFF Press.

11. Aprianti, E. (2017). A huge number of artificial waste material can be supplementary cementitious material (SCM) for concrete production–a review part II. *Journal of Cleaner Production*, *142*, 4178-4194.

12. Arribas, I., Santamaría, A., Ruiz, E., Ortega-López, V. and Manso, J.M. (2015). Electric arc furnace slag and its use in hydraulic concrete. *Construction and Building Materials*, *90*, pp.68-79.

13. Azdarpour, A. (2015). Direct and Indirect Aqueous Mineralization Using Red Gypsum for Carbon Dioxide Sequestration (Doctoral dissertation, Universiti Teknologi Malaysia).

14. Azdarpour, A., Asadullah, M., Junin, R., Manan, M., Hamidi, H., & Daud, A. R. M. (2014). Carbon dioxide mineral carbonation through pH-swing process: a review. *Energy Procedia*, *61*, 2783-2786.

15. Baker, I. (2018). *Fifty Materials That Make the World*. Springer.

16. Balci, N., & Demirel, C. (2018). Prediction of acid mine drainage (AMD) and metal release sources at the Küre Copper Mine Site, Kastamonu, NW Turkey. *Mine Water and the Environment*, *37*(1), 56-74.

17. Bao, W., Li, H., & Zhang, Y. (2010). Selective leaching of steelmaking slag for indirect CO_2 mineral sequestration. *Industrial & Engineering Chemistry Research*, *49*(5), 2055-2063.

18. Benzaazoua, M., Belem, T., & Bussiere, B. (2002). Chemical factors that influence the performance of mine sulphidic paste backfill. *Cement and Concrete Research*, *32*(7), 1133-1144.

19. Bertos, M. F., Li, X., Simons, S. J. R., Hills, C. D., & Carey, P. J. (2004). Investigation of accelerated carbonation for the stabilisation of MSW incinerator ashes and the sequestration of CO 2. *Green Chemistry*, *6*(8), 428-436.

20. Bezuidenhout, A., & Cock, J. (2009). Corporate power, society and the environment: a case study of ArcelorMittal South Africa. *Transformation: Critical Perspectives on Southern Africa*, *69*(1), 81-105.

21. Bobicki, E. R. (2014). Pre-treatment of ultramafic nickel ores for improved mineral carbon sequestration. *University of Alberta*

22. Bobicki, E. R., Liu, Q., Xu, Z., & Zeng, H. (2012). Carbon capture and storage using alkaline industrial wastes. *Progress in Energy and Combustion Science*, *38*(2), 302-320

23. Bodénan, F., Bourgeois, F., Petiot, C., Augé, T., Bonfils, B., Julcour-Lebigue, C., Guyot, F., Boukary, A., Tremosa, J., Lassin, A. and Gaucher, E.C. (2014). Ex situ mineral carbonation for CO_2 mitigation: Evaluation of mining waste resources, aqueous carbonation process ability and life cycle assessment (Carmex project). *Minerals Engineering*, 59, pp.52-63.

24. Bodsworth, C. (2018). The extraction and refining of metals. *Routledge*

25. Bonfils, B., Julcour-Lebigue, C., Guyot, F., Bodénan, F., Chiquet, P., & Bourgeois, F. (2012). Comprehensive analysis of direct aqueous mineral carbonation using dissolution enhancing organic additives. *International Journal of Greenhouse Gas Control*, *9*, 334-346.

26. Brady, P. V., & Gíslason, S. R. (1997). Seafloor weathering controls on atmospheric CO2 and global climate. *Geochimica et Cosmochimica Acta*, *61*(5), 965-973.

27. Braga, P., Lemos, F., dos Santos, R., Nascimento, C., & França, S. Use of Bauxite Residue (Red Mud) as CO_2 Absorbent.

28. Cabral, R. P., & Mac Dowell, N. (2017). A novel methodological approach for achieving£/MWh cost reduction of CO_2 capture and storage (CCS) processes. *Applied Energy*, *205*, 529-539.

29. Cadavid Giraldo, N. (2017). Environmental improvement of operating supply chains: a multi-objective approach for the cement industry.

30. Cai, J., Wang, S., Zeng, R., Luo, M., & Tang, X. (2018). CaO-based chemical looping gasification of biomass for the production of hydrogen-enriched gas and CO_2 negative emissions: a review. *International Journal of Energy for a Clean Environment*, *19*(3-4).

31. Chakraborty, S., & Jo, B. W. (2018). Aqueous-based carbon dioxide sequestration. In *Carbon Dioxide Sequestration in Cementitious Construction Materials* (pp. 39-64).

32. Chang, R., Kim, S., Lee, S., Choi, S., Kim, M. and Park, Y. (2017). Calcium carbonate precipitation for CO_2 storage and utilization: a review of the carbonate crystallization and polymorphism. *Frontiers in Energy Research*, 5, p.17.

33. Chen, Q., Gu, Y., Tang, Z., Wei, W., & Sun, Y. (2018). Assessment of low-carbon iron and steel production with CO_2 recycling and utilization technologies: A case study in China. *Applied Energy*, *220*, 192-207.

34. Cheng, C., Li, S. Y., & Peng, L. (2018). A quantitative method of measuring roundness of outcrop gravels and its applications in the study of carbonate slope geometry. *Carbonates and Evaporites*, 1-12.

35. Cherbański, R., & Molga, E. (2018). Sorption-enhanced steam-methane reforming with simultaneous sequestration of CO_2 on fly ashes–Proof of concept and simulations for gas-solid-solid trickle flow reactor. *Chemical Engineering and Processing: Process Intensification*, *124*, 37-49.

36. Chiang, P. C., & Pan, S. Y. (2017). Iron and Steel Slags. In *Carbon Dioxide Mineralization and Utilization* (pp. 233-252). Springer, Singapore.

37. Chiang, Y. W., Santos, R. M., Elsen, J., Meesschaert, B., Martens, J. A., & Van Gerven, T. (2014). Towards zero-waste mineral carbon sequestration via two-way valorization of iron-making slag. *Chemical Engineering Journal*, *249*, 260-269.

38. Chitaka, T. Y., von Blottnitz, H., and Cohen, B. (2018). The role of decision support frameworks in industrial policy development: A South African iron and steel scrap case study. *Sustainable Production and Consumption*, *13*, pp 113-125.

39. Clark, M. W., Johnston, M., & Reichelt-Brushett, A. J. (2015). Comparison of several different neutralisations to a bauxite refinery residue: potential effectiveness environmental ameliorants. *Applied Geochemistry*, *56*, 1-10.

40. Criado, Y. A., Arias, B., & Abanades, J. C. (2018). Effect of the Carbonation Temperature on the CO2 Carrying Capacity of CaO. *Industrial & Engineering Chemistry Research*, *57*(37), 12595-12599.

41. Cusack, P. B., Healy, M. G., Ryan, P. C., Burke, I. T., O'Donoghue, L. M., Ujaczki, É., & Courtney, R. (2018). Enhancement of bauxite residue as a low-cost adsorbent for phosphorus in aqueous solution, using seawater and gypsum treatments. *Journal of Cleaner Production*, *179*, 217-224.

42. De Beer, J., Worrell, E. and Blok, K. (1998). Future technologies for energy-efficient iron and steel making. *Annual Review of Energy and the Environment*, 23(1), pp.123-205

43. Demers, I., Mbonimpa, M., Benzaazoua, M., Bouda, M., Awoh, S., Lortie, S., & Gagnon, M. (2017). Use of acid mine drainage treatment sludge by combination with a natural soil as an oxygen barrier cover for mine waste reclamation: Laboratory column tests and intermediate scale field tests. *Minerals Engineering*, *107*, 43-52.

44. Dilmore, R. M., Howard, B. H., Soong, Y., Griffith, C., Hedges, S. W., DeGalbo, A. D., ... & Fu, J. K. (2009). Sequestration of CO_2 in mixtures of caustic byproduct and saline waste water. *Environmental Engineering Science*, 26(8), 1325-1333.

45. Droste, R. L., & Gehr, R. L. (2018). *Theory and Practice of Water and Wastewater Treatment*. John Wiley & Sons.

46. Eikeland, E., Blichfeld, A. B., Tyrsted, C., Jensen, A., & Iversen, B. B. (2015). Optimized carbonation of magnesium silicate mineral for CO_2 storage. *ACS Applied Materials & Interfaces*, *7*(9), 5258-5264.

47. Eloneva, S., Puheloinen, E. M., Kanerva, J., Ekroos, A., Zevenhoven, R., & Fogelholm, C. J. (2010). Co-utilisation of CO_2 and steelmaking slags for production of pure $CaCO_3$– legislative issues. *Journal of Cleaner Production*, *18*(18), 1833-1839.

48. Eloneva, S., Said, A., Fogelholm, C. J., & Zevenhoven, R. (2012). Preliminary assessment of a method utilizing carbon dioxide and steelmaking slags to produce precipitated calcium carbonate. *Applied Energy*, *90*(1), 329-334.

49. Eloneva, S., TEIR, S., Revitzer, H. (2009).Reduction of CO_2 emissions from steel plants by using steelmaking slags for production of marketable calcium carbonate. *Steel Research International*, vol. 80, no 6, p. 415-421.

50. Eloneva, S., Teir, S., Salminen, J., Fogelholm, C. J., & Zevenhoven, R. (2008). Fixation of CO_2 by carbonating calcium derived from blast furnace slag. *Energy*, *33*(9), 1461-1467

51. Eloneva, S., Teir, S., Salminen, J., Fogelholm, C.J., & Zevenhoven, R. (2008). Steel converter slag as a raw material for precipitation of pure calcium carbonate. *Industrial & Engineering Chemistry Research*, *47*(18), pp.7104-7111.

52. Elshkaki, A., Reck, B. K., & Graedel, T. E. (2017). Anthropogenic nickel supply, demand, and associated energy and water use. *Resources, Conservation and Recycling*, *125*, 300-307.

53. Erdogan, N. and Eken, H.A. (2017). Precipitated calcium carbonate production, synthesis and properties, *Physicochemical Problems of Mineral Processing*, 53(1), pp. 57-68.

54. Escobar, M. C., Vasquez, Y., Neculita, C. M., Arbeli, Z., & Roldan, F. (2016). Biochemical passive reactors for treatment of acid mine drainage: effect of hydraulic retention time on changes in efficiency, composition of reactive mixture, and microbial activity. *Chemosphere*, 153, 244-253.

55. Evangelou, V. P. (2018). *Pyrite oxidation and its control*. CRC press.

56. Figueroa, J. D., Fout, T., Plasynski, S., McIlvried, H., & Srivastava, R. D. (2008). Advances in CO2 capture technology—the US Department of Energy's Carbon Sequestration Program. *International Journal of Greenhouse Gas Control*, *2*(1), 9-20.

57. Friedrich, E., & Trois, C. (2013). GHG emission factors developed for the recycling and composting of municipal waste in South African municipalities. *Waste Management*, *33*(11), 2520-2531.

58. Fu, F., & Wang, Q. (2011). Removal of heavy metal ions from wastewaters: a review. *Journal of Environmental Management*, *92*(3), 407-418.

59. Galhardi, J. A., & Bonotto, D. M. (2016). Hydrogeochemical features of surface water and groundwater contaminated with acid mine drainage (AMD) in coal mining areas: a case study in southern Brazil. *Environmental Science and Pollution Research*, *23*(18), 18911-18927.

60. Gane, P. A., Buri, M., Blum, R. V., & Karth, B. (2009). *U.S. Patent No. 7,638,017*. Washington, DC: U.S. Patent and Trademark Office

61. Georgakopoulos, E., Santos, R. M., Chiang, Y. W., & Manovic, V. (2017). Two-way Valorization of Blast Furnace Slag: Synthesis of Precipitated Calcium Carbonate and Zeolitic Heavy Metal Adsorbent. *Journal of Visualized Experiments: JoVE*, (120).

62. Gerdemann, S. J., O'Connor, W. K., Dahlin, D. C., Penner, L. R., & Rush, H. (2007). Ex situ aqueous mineral carbonation. *Environmental science & technology*, *41*(7), 2587-2593.

63. Ghouleh, Z., Guthrie, R. I., & Shao, Y. (2017). Production of carbonate aggregates using steel slag and carbon dioxide for carbon-negative concrete. *Journal of CO$_2$ Utilization*, *18*, 125-138.

64. Gierer, J. (1980). Chemical aspects of kraft pulping. *Wood Science and Technology*, *14*(4), 241-266.

65. Goldberg, P., Chen, Z. Y., O'Connor, W., Walters, R., & Ziock, H. (2001). *CO₂ mineral sequestration studies in the US* (No. DOE/NETL-2001/1144). National Energy Technology Laboratory, Pittsburgh, PA (United States).

66. Grunewald, N., & Martinez-Zarzoso, I. (2016). Did the Kyoto Protocol fail? An evaluation of the effect of the Kyoto Protocol on CO2 emissions. *Environment and Development Economics*, *21*(1), 1-22.

67. Gunning, P. J., Hills, C. D., & Carey, P. J. (2010). Accelerated carbonation treatment of industrial wastes. *Waste Management*, *30*(6), 1081-1090.

68. Habashi, F. (2017). *Principles of Extractive Metallurgy*. Routledge.

69. Hall, C., Large, D. J., Adderley, B., & West, H. M. (2014). Calcium leaching from waste steelmaking slag: Significance of leachate chemistry and effects on slag grain mineralogy. *Minerals Engineering*, *65*, 156-162.

70. Han, S., Mao, H., & Dally, W. J. (2015). Deep compression: Compressing deep neural networks with pruning, trained quantization and huffman coding. *arXiv preprint arXiv:1510.00149*.

71. Han, X., Kulaots, I., Jiang, X., & Suuberg, E. M. (2014). Review of oil shale semicoke and its combustion utilization. *Fuel*, *126*, 143-161.

72. Han, Y. S., Ji, S., Lee, P. K., & Oh, C. (2017). Bauxite residue neutralization with simultaneous mineral carbonation using atmospheric CO2. *Journal of Hazardous Materials*, *326*, 87-93.

73. Hedrich, S., & Johnson, D. B. (2014). Remediation and selective recovery of metals from acidic mine waters using novel modular bioreactors. *Environmental Science & Technology*, *48*(20), 12206-12212.

74. Hitch, M., Ballantyne, S. M., & Hindle, S. R. (2010). Revaluing mine waste rock for carbon capture and storage. *International Journal of Mining, Reclamation and Environment*, *24*(1), 64-79.

75. Holt, S. P., & Berge, N. D. (2018). Life-cycle assessment of using liquid hazardous waste as an alternative energy source during Portland cement manufacturing: A United States case study. *Journal of Cleaner Production*.

76. Huijgen, W. J., Witkamp, G. J., & Comans, R. N. (2005). Mineral CO2 sequestration by steel slag carbonation. *Environmental Science & Technology*, *39*(24), 9676-9682.

77. Jallath, J. E. S., Romero, F. M., Argüelles, R. I., Macedo, A. C., & Arenas, J. G. (2018). Acid drainage neutralization and trace metals removal by a two-step system with carbonated rocks, Estado de Mexico, Mexico. *Environmental Earth Sciences*, *77*(3), 86.

78. Jewell, J., McCollum, D., Emmerling, J., Bertram, C., Gernaat, D. E., Krey, V., ... & Saadi, N. (2018). Limited emission reductions from fuel subsidy removal except in energy-exporting regions. *Nature*, *554*(7691), 229.

79. Johnson, D. B., & Hedrich, S., (2014). Remediation and selective recovery of metals from acidic mine waters using novel modular bioreactors. *Environmental Science & Technology*, 48(20), 12206-12212.

80. Judd, P., Albericio, J., Hetherington, T., Aamodt, T., Jerger, N. E., Urtasun, R., & Moshovos, A. (2015). Reduced-precision strategies for bounded memory in deep neural nets. *arXiv preprint arXiv:1511.05236*.

81. Kakizawa, M., Yamasaki, A., & Yanagisawa, Y. (2001). A new CO2 disposal process via artificial weathering of calcium silicate accelerated by acetic acid. *Energy*, *26*(4), 341-354.

82. Kanniche, M., Gros-Bonnivard, R., Jaud, P., Valle-Marcos, J., Amann, J. M., & Bouallou, C. (2010). Pre-combustion, post-combustion and oxy-combustion in thermal power plant for CO2 capture. *Applied Thermal Engineering*, *30*(1), 53-62.

83. Karve, A. (2018). Plastic waste management

84. Kefeni, K. K., Msagati, T. A., & Mamba, B. B. (2017). Acid mine drainage: prevention, treatment options, and resource recovery: a review. *Journal of cleaner production*, *151*, 475-493.

85. Kefeni, K. K., Msagati, T. A., Nkambule, T. T., & Mamba, B. B. (2018). Synthesis and application of hematite nanoparticles for acid mine drainage treatment. *Journal of Environmental Chemical Engineering*, *6*(2), 1865-1874.

86. Koukouzas, N., Ziock, H., Ziogou, F., & Typou, I. (2018). Mineral carbonation as a potential carbon dioxide storage option for the region of western macedonia, greece. *Bulletin of the Geological Society of Greece*, *40*(2), 872-883.

87. Krausmann, F., Wiedenhofer, D., Lauk, C., Haas, W., Tanikawa, H., Fishman, T., ... & Haberl, H. (2017). Global socioeconomic material stocks rise 23-fold over the 20th century and require half of annual resource use. *Proceedings of the National Academy of Sciences*, 201613773.

88. Kumar, A., Prasad, M. N. V., & Maiti, S. K. (2016). Asbestos: Resource Recovery and Its Waste Management. In *Environmental Materials and Waste* (pp. 285-305).

89. Kundak, M., Lazić, L. and Črnko, J. (2009). CO_2 emissions in the steel industry. *Metalurgija*, 48(3).

90. Lackner, K. S., Butt, D. P., & Wendt, C. H. (1997). Progress on binding CO_2 in mineral substrates. *Energy Conversion and Management*, *38*, S259-S264.

91. Larachi, F., Daldoul, I., & Beaudoin, G. (2010). Fixation of CO_2 by chrysotile in low-pressure dry and moist carbonation: Ex-situ and in-situ characterizations. *Geochimica et Cosmochimica Acta*, *74*(11), 3051-3075.

92. Leeson, D., Mac Dowell, N., Shah, N., Petit, C., & Fennell, P. S. (2017). A Techno-economic analysis and systematic review of carbon capture and storage (CCS) applied to the iron and steel, cement, oil refining and pulp and paper industries, as well as other high purity sources. *International Journal of Greenhouse Gas Control*, *61*, 71-84.

93. Lewis, H., Gertsakis, J., Grant, T., Morelli, N., & Sweatman, A. (2017). *Design+ Environment: a Global Guide to Designing Greener Goods*. Routledge

94. Li, J., & Hitch, M. (2016). Economic analysis on the application of mechanical activation in an integrated mineral carbonation process. *International Biodeterioration & Biodegradation*.

95. Li, J., Hitch, M., Power, I. M., & Pan, Y. (2018). Integrated Mineral Carbonation of Ultramafic Mine Deposits—A Review. *Minerals*, *8*(4), 147.

96. Li, J., Zhuang, X., Querol, X., Font, O., & Moreno, N. (2018). A review on the applications of coal combustion products in China. *International Geology Review*, *60*(5-6), 671-716

97. Li, Q.H., Meng, A.H. and Zhang, Y.G. (2009). Recovery status and prospect of low-grade waste energy in China. In Sustainable Power Generation and Supply, 2009. SUPERGEN'09. International Conference on (pp. 1-6). IEEE.

98. Liu, C., Huang, S., Wollants, P., Blanpain, B., & Guo, M. (2017). Valorization of BOF steel slag by reduction and phase modification: metal recovery and slag valorization. *Metallurgical and Materials Transactions B*, *48*(3), 1602-1612.

99. Liu, Q., Maroto-Valer, M. M., & Sanna, A. (2017). Mineral Carbonation Technology Overview. In *CO₂ Sequestration by Ex-Situ Mineral Carbonation* (pp. 1-15).

100. Liu, W., Su, S., Xu, K., Chen, Q., Xu, J., Sun, Z., ... & Xiang, J. (2018). CO2 sequestration by direct gas–solid carbonation of fly ash with steam addition. *Journal of Cleaner Production*, *178*, 98-107.

101. Lopez, N. S. A., Biona, J. B. M. M., & Chiu, A. S. (2018). Electricity trading and its effects on global carbon emissions: A decomposition analysis study. *Journal of Cleaner Production*.

102. Luhmann, A. J., Tutolo, B. M., Tan, C., Moskowitz, B. M., Saar, M. O., & Seyfried, W. E. (2017). Whole rock basalt alteration from CO_2-rich brine during flow-through experiments at 150° C and 150bar. *Chemical Geology*, *453*, 92-110.

103. Luptáková, A., & Andráš, P. (2018). Formation of Acid Mine Drainage in Sulphide Ore Deposits.

104. Luptakova, A., Ubaldini, S., Macingova, E., Fornari, P., & Giuliano, V. (2012). Application of physical–chemical and biological–chemical methods for heavy metals removal from acid mine drainage. *Process Biochemistry*, *47*(11), 1633-1639.

105. Mæstad, O. (2000). Data for a steel industry model.

106. Martens, J. A., Bogaerts, A., De Kimpe, N., Jacobs, P. A., Marin, G. B., Rabaey, K., ... & Verhelst, S. (2017). The chemical route to a carbon dioxide neutral world. *ChemSusChem*, *10*(6), 1039-1055.

107. Mattila, H. P. (2014). Utilization of steelmaking waste materials for production of calcium carbonate ($CaCO_3$).

108. Mattila, H. P., & Zevenhoven, R. (2014). Production of precipitated calcium carbonate from steel converter slag and other calcium-containing industrial wastes and residues. In *Advances in Inorganic Chemistry* (Vol. 66, pp. 347-384). Academic Press.

109. Mattila, H. P., Grigaliūnaitė, I., & Zevenhoven, R. (2012). Chemical kinetics modeling and process parameter sensitivity for precipitated calcium carbonate production from steelmaking slags. *Chemical Engineering Journal*, *192*, 77-89.

110. Mattila, H.P. and Zevenhoven, R. (2014). Production of precipitated calcium carbonate from steel converter slag and other calcium-containing industrial wastes and residues. *Advances in Inorganic Chemistry,* 66, pp. 347-384. Academic Press.

111. Metz, B., Davidson, O., De Coninck, H. C., Loos, M., & Meyer, L. A. (2005). IPCC, 2005: IPCC special report on carbon dioxide capture and storage. Prepared by Working Group III

of the Intergovernmental Panel on Climate Change. *Cambridge, United Kingdom and New York, NY, USA*, *442*.

112. Mo, L., Zhang, F., & Deng, M. (2016). Mechanical performance and microstructure of the calcium carbonate binders produced by carbonating steel slag paste under CO_2 curing. *Cement and Concrete Research*, *88*, 217-226.

113. Modabberi, S., Alizadegan, A., Mirnejad, H., & Esmaeilzadeh, E. (2013). Prediction of AMD generation potential in mining waste piles, in the sarcheshmeh porphyry copper deposit, Iran. *Environmental Monitoring and Assessment*, *185*(11), 9077-9087.

114. Montes-Hernandez, G., Perez-Lopez, R., Renard, F., Nieto, J. M., & Charlet, L. (2009). Mineral sequestration of CO2 by aqueous carbonation of coal combustion fly-ash. *Journal of Hazardous Materials*, *161*(2-3), 1347-1354.

115. Morfeldt, J., Nijs, W. and Silveira, S. (2015). The impact of climate targets on future steel production-an analysis based on a global energy system model. *Journal of Cleaner Production*, 103, pp.469-482.

116. Moult, E., Choi, W., Waheed, N. K., Adhi, M., Lee, B., Lu, C. D., ... & Fujimoto, J. G. (2014). Ultrahigh-speed swept-source OCT angiography in exudative AMD. *Ophthalmic Surgery, Lasers and Imaging Retina*, *45*(6), 496-505.

117. Mudd, G. M. (2010). Global trends and environmental issues in nickel mining: Sulfides versus laterites. *Ore Geology Reviews*, *38*(1-2), 9-26.

118. Mulopo, J. (2015). Continuous pilot scale assessment of the alkaline barium calcium desalination process for acid mine drainage treatment. *Journal of Environmental Chemical Engineering*, *3*(2), 1295-1302.

119. Mulopo, J., Mashego, M., et Zvimba, J. N. (2012) Recovery of calcium carbonate from steelmaking slag and utilization for acid mine drainage pre-treatment. *Water Science* and *Technology*, , vol. 65, no 12, p. 2236-2241.

120. Mun, M., Cho, H., Kwon, J., Kim, K., & Kim, R. (2017). Investigation of the CO2 Sequestration by Indirect Aqueous Carbonation of Waste Cement. *American Journal of Climate Change*, *6*(01), 132

121. Nancucheo, I., Bitencourt, J. A., Sahoo, P. K., Alves, J. O., Siqueira, J. O., & Oliveira, G. (2017). Recent developments for remediating acidic mine waters using sulfidogenic bacteria. *BioMed Research International*, *2017*.

122. Ndlovu, S. (2017). Acid Mine DrainageTreatment Technologies. *Management and Mitigation of Acid Mine Drainage in South Africa: Input for Mineral Beneficiation in Africa*, 216.

123. Norgate, T. E., Jahanshahi, S., & Rankin, W. J. (2007). Assessing the environmental impact of metal production processes. *Journal of Cleaner Production*, 15(8-9), 838-848

124. Nurmesniemi, H., Pöykiö, R., Perämäki, P., & Kuokkanen, T. (2008). Extractability of trace elements in precipitated calcium carbonate (PCC) waste from an integrated pulp and paper mill complex. *Chemosphere*, *70*(7), 1161-1167.

125. Oelkers, E. H., Gislason, S. R., & Matter, J. (2008). Mineral carbonation of CO_2. *Elements*, *4*(5), 333-337.

126. Olajire, A.A. (2013). A review of mineral carbonation technology in sequestration of CO_2. *Journal of Petroleum Science and Engineering*, *109*, pp.364-392.

127. Ong, S. K., Mo, K. H., Alengaram, U. J., Jumaat, M. Z., & Ling, T. C. (2018). Valorization of wastes from power plant, steel-making and palm oil industries as partial sand substitute in concrete. *Waste and Biomass Valorization*, *9*(9), 1645-1654.

128. Özbay, E., Erdemir, M., & Durmuş, H. İ. (2016). Utilization and efficiency of ground granulated blast furnace slag on concrete properties–A review. *Construction and Building Materials*, *105*, 423-434.

129. Pan, S. Y., Chang, E. E., & Chiang, P. C. (2012). CO2 capture by accelerated carbonation of alkaline wastes: a review on its principles and applications. *Aerosol Air Qual Res*, *12*(5), 770-791.

130. Pan, S. Y., Chen, Y. H., Chen, C. D., Shen, A. L., Lin, M., & Chiang, P. C. (2015). High-gravity carbonation process for enhancing CO_2 fixation and utilization exemplified by the steelmaking industry. Environmental science & technology, 49(20), 12380-12387.

131. Pan, S. Y., Chiang, P. C., Pan, W., & Kim, H. (2018). Advances in state-of-art valorization technologies for captured CO_2 toward sustainable carbon cycle. *Critical Reviews in Environmental Science and Technology*, 1-64.

132. Pan, S. Y., Shah, K. J., Chen, Y. H., Wang, M. H., & Chiang, P. C. (2017). Deployment of accelerated carbonation using alkaline solid wastes for carbon mineralization and utilization toward a circular economy. *ACS Sustainable Chemistry & Engineering*, *5*(8), 6429-6437

133. Percival, R. V., Schroeder, C. H., Miller, A. S., & Leape, J. P. (2017). *Environmental regulation: Law, Science, and Policy*. Wolters Kluwer Law & Business.

134. Perez-Lopez, R., Montes-Hernandez, G., Nieto, J. M., Renard, F., & Charlet, L. (2008). Carbonation of alkaline paper mill waste to reduce CO_2 greenhouse gas emissions into the atmosphere. *Applied Geochemistry*, *23*(8), 2292-2300.

135. Portier, C. J., Thigpen, T. K., Carter, S. R., Dilworth, C. H., Grambsch, A. E., Gohlke, J., ... & Maslak, T. (2017). *A Human Health Perspective on Climate Change: A report outlining the research needs on the human health effects of climate change*. Environmental Health Perspectives/National Institute of Environmental Health Sciences.

136. Power, I. M., Dipple, G. M., & Southam, G. (2009). Bioleaching of ultramafic tailings by Acidithiobacillus spp. for CO_2 sequestration. *Environmental Science & Technology*, *44*(1), 456-462.

137. Prokopec, T., & Rigopoulos, G. (2018). Functional renormalization group for stochastic inflation. *Journal of Cosmology and Astroparticle Physics*, 2018(08), 013.

138. Rahman, F. A., Aziz, M. M. A., Saidur, R., Bakar, W. A. W. A., Hainin, M. R., Putrajaya, R., & Hassan, N. A. (2017). Pollution to solution: Capture and sequestration of carbon dioxide (CO_2) and its utilization as a renewable energy source for a sustainable future. *Renewable and Sustainable Energy Reviews*, *71*, 112-126.

139. Rahmani, O. (2018). CO2 sequestration by indirect mineral carbonation of industrial waste red gypsum. *Journal of CO_2 Utilization*, *27*, 374-380.

140. Reddy, S., Panwar, L. K., Panigrahi, B. K., & Kumar, R. (2017). Modeling of carbon capture technology attributes for unit commitment in emission-constrained environment. *IEEE Transactions on Power Systems*, *32*(1), 662-671.

141. Rey, C., Combes, C., Drouet, C., Grossin, D., Bertrand, G., & Soulié, J. (2017). 1.11 Bioactive Calcium Phosphate Compounds: Physical Chemistry. *Comprehensive Biomaterials II*, 244.

142. Ritcey, G. M., & Lucas, B. H. (1974). Some aspects of extraction of metal from acidic solutions by kelex-100. *Cim Bulletin*, 67(742), 87-92.

143. Said, A. (2017). CO_2 sequestration by steelmaking slags for the production of precipitated calcium carbonate-From laboratory to demonstration stage

144. Said, A., Laukkanen, T., & Järvinen, M. (2016). Pilot-scale experimental work on carbon dioxide sequestration using steelmaking slag. *Applied Energy*, *177*, 602-611.

145. Said, A., Mattila, H. P., Järvinen, M., & Zevenhoven, R. (2013). Production of precipitated calcium carbonate (PCC) from steelmaking slag for fixation of CO_2. *Applied Energy*, *112*, 765-771.

146. Samadi, J., & Garbolino, E. (2018). *Future of CO_2 Capture, Transport and Storage Projects: Analysis Using a Systemic Risk Management Approach*. Springer.

147. Sanna, A. (2015). Reduction of CO_2 Emissions Through Waste Materials Recycling by Mineral Carbonation. *Handbook of Clean Energy Systems*, 1-13.

148. Sanna, A., Uibu, M., Caramanna, G., Kuusik, R. and Maroto-Valer, M.M. (2014). A review of mineral carbonation technologies to sequester CO_2. *Chemical Society Reviews,* 43(23), pp.8049-8080.

149. Santos, R. M., Chiang, Y. W., Elsen, J., & Van Gerven, T. (2014). Distinguishing between carbonate and non-carbonate precipitates from the carbonation of calcium-containing organic acid leachates. *Hydrometallurgy*, *147*, 90-94.

150. Sas, W., Głuchowski, A., Radziemska, M., Dzięcioł, J. and Szymański, A. (2015). Environmental and geotechnical assessment of the steel slags as a material for road structure. *Materials*, 8(8), pp.4857-4875.

151. Setién, J., Hernández, D. and González, J.J. (2009). Characterization of ladle furnace basic slag for use as a construction material. *Construction and Building Materials*, *23*(5), pp.1788-1794.

152. Strunz, T., Grassmann, F., Gayán, J., Nahkuri, S., Souza-Costa, D., Maugeais, C., & Weber, B. H. (2018). A mega-analysis of expression quantitative trait loci (eQTL) provides insight into the regulatory architecture of gene expression variation in liver. *Scientific Reports*, 8(1), 5865.

153. Strydom, H.A. and King, N.D. eds. (2009). *Environmental Management in South Africa*. Juta and Company Ltd.

154. Sufriadin, S., Widodo, S., Ito, A., Otake, T., & Sanematsu, K. (2018). Geochemical study of ultramafic rocks from Latowu area of North Kolaka, Southeast Sulawesi and its implication for CO_2 sequestration. *Journal of Degraded and Mining Lands Management*, *5*(4), 1403-1408.

155. Sutar, H., Mishra, S. C., Sahoo, S. K., & Maharana, H. S. (2014). Progress of red mud utilization: an overview.

156. Takeshi, M., Hiroyuki, T., Keiji, W. (2018). Iron and steel slag products and new effective utilization technologies. *JFE Technical Report*, 23.

157. Teir, S., Eloneva, S., Fogelholm, C. J., & Zevenhoven, R. (2007). Dissolution of steelmaking slags in acetic acid for precipitated calcium carbonate production. *Energy*, *32*(4), 528-539.

158. Teir, S., Eloneva, S., Fogelholm, C. J., & Zevenhoven, R. (2009). Fixation of carbon dioxide by producing hydromagnesite from serpentinite. *Applied Energy*, *86*(2), 214-218.

159. Tolonen, E. T., Sarpola, A., Hu, T., Rämö, J., & Lassi, U. (2014). Acid mine drainage treatment using by-products from quicklime manufacturing as neutralization chemicals. *Chemosphere*, *117*, 419-424.

160. Uibu, M., Somelar, P., Raado, L. M., Irha, N., Koroljova, A., & Kuusik, R. (2015, June). Utilization of oil shale ash as a concrete constituent and carbon sink. In *5th International Conference on Accelerated Carbonation for Environmental and Materials Engineering* (pp. 21-24).

161. Uibu, M., Viires, R., & Kuusik, R. (2017). MC Technologies Developed for Waste Materials. In *CO_2 Sequestration by Ex-Situ Mineral Carbonation* (pp. 91-131).

162. Ukwattage, N. L., Ranjith, P. G., Yellishetty, M., Bui, H. H., & Xu, T. (2015). A laboratory-scale study of the aqueous mineral carbonation of coal fly ash for CO2 sequestration. *Journal of Cleaner Production*, *103*, 665-674.

163. Vaněk, O., Jakob, M., Hrstka, O., & Pěchouček, M. (2013). Agent-based model of maritime traffic in piracy-affected waters. *Transportation Research Part C: Emerging Technologies*, *36*, 157-176.

164. Vasquez, Y., Escobar, M. C., Neculita, C. M., Arbeli, Z., & Roldan, F. (2016). Biochemical passive reactors for treatment of acid mine drainage: effect of hydraulic retention time on changes in efficiency, composition of reactive mixture, and microbial activity. *Chemosphere*, *153*, 244-253.

165. Voormeij, D. A., & Simandl, G. J. (2004). Geological, ocean, and mineral CO_2 sequestration options: a technical review. *Geoscience Canada*, *31*(1).

166. Wang, C. Y., Bao, W. J., Guo, Z. C., & Li, H. Q. (2018). Carbon Dioxide Sequestration via Steelmaking Slag Carbonation in Alkali Solutions: Experimental Investigation and Process Evaluation. *Acta Metallurgica Sinica (English Letters)*, *31*(7), 771-784.

167. Wang, L., Jin, Y., & Nie, Y. (2010). Investigation of accelerated and natural carbonation of MSWI fly ash with a high content of Ca. *Journal of Hazardous Materials*, *174*(1-3), 334-343.

168. Wei, Y., Li, J., Shi, D., Liu, G., Zhao, Y., & Shimaoka, T. (2017). Environmental challenges impeding the composting of biodegradable municipal solid waste: A critical review. *Resources, Conservation and Recycling*, *122*, 51-65.

169. Xu, B., & Lin, B. (2017). Assessing CO_2 emissions in China's iron and steel industry: A nonparametric additive regression approach. *Renewable and Sustainable Energy Reviews*, *72*, 325-337.

170. Xu, R., Li, R., Ma, J., He, D., & Jiang, P. (2017). Effect of mineral dissolution/precipitation and CO_2 exsolution on CO_2 transport in geological carbon storage. *Accounts of chemical research*, *50*(9), 2056-2066.

171. Xylia, M., Silveira, S., Duerinck, J., & Meinke-Hubeny, F. (2018). Weighing regional scrap availability in global pathways for steel production processes. *Energy Efficiency*, *11*(5), 1135-1159.

172. Yadav, H. L., & Jamal, A. (2015). Impact of Mining on Water Resources in India. *International Journal of Advanced Research*, *3*(10), 1009-1015.

173. Yang, H., Xu, Z., Fan, M., Gupta, R., Slimane, R. B., Bland, A. E., & Wright, I. (2008). Progress in carbon dioxide separation and capture: A review. *Journal of Environmental Sciences*, *20*(1), 14-27.

174. Yi, H., Xu, G., Cheng, H., Wang, J., Wan, Y. and Chen, H. (2012). An overview of utilization of steel slag. *Procedia Environmental Sciences*, 16, pp.791-801.

175. Yu, Q. (2018). *Metal Recovery from Steelmaking Slag* (Doctoral dissertation).

176. Yu, Z. G., Orsetti, S., Haderlein, S. B., & Knorr, K. H. (2016). Electron transfer between sulfide and humic acid: electrochemical evaluation of the reactivity of Sigma-Aldrich humic acid toward sulfide. *Aquatic geochemistry*, *22*(2), 117-130.

177. Zhang, X., Shen, J., Wang, Y., Qi, Y., Liao, W., Shui, W., ... & Yu, X. (2017). An environmental sustainability assessment of China's cement industry based on emergy. *Ecological Indicators*, *72*, 452-458.

178. Zheng, Y., Zhang, W., Li, Y., Chen, J., Yu, B., Wang, J., ... & Zhang, J. (2017). Energy related CO_2 conversion and utilization: advanced materials/nanomaterials, reaction mechanisms and technologies. *Nano Energy*, *40*, 512-539.

179. Zhu, J., Zhang, P., Yuan, S., Liao, P., Qian, A., Liu, X., ... & Li, L. (2017). Production of Hydroxyl radicals from oxygenation of simulated AMD due to $CaCO_3$-induced pH increase. *Water Research*, *111*, 118-126.